Odoribacter splanchnicus mitigates pathogen-induced gut inflammation and its associated pathogenesis via its secreted bacteriocin

Dipasree Hajra[1], Debapriya Mukherjee [1#], Rhea Vij [1#], Raju S Rajmani [2], Venkatareddy Dadireddy[3], Deepakash Das[4], Tanweer Hussain[4], Mahipal Ganji[3], Utpal Tatu [3], Chakravortty D [1,5 *]

[1]Department of Microbiology and Cell Biology, Indian Institute of Science

[2]Centre of Infectious Disease Research, Indian Institute of Science, Bangalore, India

[3]Department of Biochemistry, Indian Institute of Science, Bangalore, India

[4]Department of Developmental Biology and Genetics, Indian Institute of Science, Bangalore, India

[5]Adjunct Faculty, School of Biology, Indian Institute of Science Education and Research, Thiruvananthapuram

*Corresponding author: Prof. Dipshikha Chakravortty

#Equal Contribution

Email: dipa@iisc.ac.in

Tel. No. 0091 80 22932842

Abstract

Foodborne pathogens pose a major global health hazard, worsened by drug-resistant strains. Therefore, designing novel therapeutic strategies is crucial. Here, we identified the protective role of gut-commensal *Odoribacter splanchnicus* (OS) against *Salmonella* in mice by promoting colonization resistance, preserving gut barrier integrity, and preventing acute inflammation and biofilm formation. *In vitro,* both live *O. splanchnicus* (OS) and their culture supernatant inhibited *Salmonella* biofilm formation, intracellular proliferation in human intestinal cells, and virulence gene expression. Further, our results depicted that OS's protective role acts over a broad spectrum as it confers protection against Gram-positive, *Listeria*

monocytogenes and Gram-negative, *Salmonella* Typhimurium. Notably, OS conferred protection even when administered post-infection in mice, highlighting its therapeutic potential. Using several biochemical and proteomics approaches, we characterized key OS-secreted molecules that limit intracellular *Salmonella* and *Listeria* replication in human intestinal epithelial cells by regulating key virulence effectors and flagella. Collectively, our study establishes OS as the broad-spectrum protective agent against *Salmonella* and *Listeria* infections, with promising therapeutic potential.

Keywords: *Salmonella* pathogenesis, **Gut vascular barrier permeability**, **inflammation**, **inter-species bacterial regulation**, ***Listeria***, ***Odoribacter splanchnicus***, **gut commensal**, **biofilm, flagella**

Author Summary

Foodborne pathogens such as *Salmonella* and *Listeria* continue to threaten global health, especially with the rise of antibiotic resistance. In this study, we identify the gut commensal bacterium *Odoribacter splanchnicus* (OS) as a potent protectant against these pathogens. Using a mouse model, we show that OS enhances colonization resistance, maintains gut barrier integrity, and prevents both inflammation and biofilm formation during infection. Remarkably, OS also limits pathogen proliferation and virulence gene expression in human intestinal cells. These protective effects are mediated by both live OS and its secreted molecules within culture supernatant**.** Importantly, OS administration post-infection also conferred protection, indicating strong therapeutic potential. Biochemical and proteomic analyses revealed OS-secreted factors that suppress key virulence and motility pathways in pathogens. Our findings establish *Odoribacter splanchnicus* as a promising broad-spectrum biotherapeutic agent against major foodborne infections.

54 **INTRODUCTION**

55 The existence of the gut vascular barrier (GVB) acts as a protective barrier against the entry of
56 microorganisms into systemic blood circulation (1, 2). Enteric pathogens such as *Salmonella*
57 *enterica* can cross the mucus and intestinal epithelial barrier, ultimately leading to GVB
58 damage and systemic dissemination (1). The gut microbiota aids in the maintenance of the
59 intestinal epithelial barrier by the production of several metabolites such as Short-chain fatty
60 acids (SCFAs), indoles, and polyphenol metabolites that contribute to epithelial barrier
61 integrity and turnover by regulating the expression of Tight-junction (TJ) genes (3).
62 Additionally, these SCFAs have the potential to exert anti-inflammatory properties by
63 regulating cytokine production, mucosal immune cell migration, and secretion of antimicrobial
64 peptides (AMPs) by intestinal epithelial cells and macrophages (4-6).

65 *Salmonella* enters the body through the ingestion of contaminated food and water, resisting the
66 acidic stomach pH with acid tolerance response (ATR) genes, and finally reaches the lumen of
67 the small intestine(7). The pathogen gains entry into the non-phagocytic epithelial cells via
68 *Salmonella* Pathogenicity Island-1 (SPI-1) effectors to breach the intestinal barrier (8). Once
69 traversing through the mucosal lining of the gut epithelium, it reaches the lamina propria (8).
70 In the lamina propria, *Salmonella* encounters various host immune cells like neutrophils,
71 macrophages, and dendritic cells. Macrophages, dendritic cells, and neutrophils are responsible
72 for successful dissemination throughout the body through the reticulo-endothelial system
73 (RES) to the secondary organs such as Mesenteric Lymph Node (MLN), liver, and spleen(8).
74 *Salmonella* relies on the SPI-2 secretion for its intracellular and intravacuolar life by injecting
75 various virulence factors into the host cell cytosol (9, 10).

76 *Odoribacter splanchnicus* (OS, belonging to the order Bacteroidales, is a common member of
77 the human intestinal microbiota. *Bacteroidetes* is one of the major commensal phyla
78 dominating the healthy mouse as well as the human gut (11). A decrease in *Odoribacter*

abundance has been linked to different microbiota-associated diseases, such as non-alcoholic fatty liver disease, cystic fibrosis, and inflammatory bowel disease (IBD)(12). A recent report indicated the ability of OS and its effectors transported in Outer membrane vesicles (OMVs) to exhibit anti-inflammatory effects on the gut epithelium(12). Further, OS has been implicated in conferring resistance against colitis and colorectal cancer(13). This led us to hypothesize that *O. splanchnicus* might ameliorate the inflammatory disease conditions associated with *Salmonella* infection and dissemination. Here, in the present study, we aim to understand whether colonization with the gut commensal, *Odoribacter splanchnicus* (OS) could ameliorate *Salmonella*-induced inflammation and pathogenic dissemination.

Our study shows that OS colonization promotes colonization resistance of *Salmonella*, and systemic dissemination. OS ameliorates acute *Salmonella*-induced inflammation and its associated pathogenesis by promoting colonization resistance, resulting in decreased *Salmonella* invasion of gut tissue, the preservation of tight junctions, and GVB maintenance. Further, we demonstrate that not only live OS but its culture supernatant inhibits *Salmonella in vitro* biofilm formation, intracellular proliferation in human intestinal cells, and virulence gene expression. Subsequently, our results depict that the specific protective role of OS acts over a broad spectrum as it confers protection against both flagellated Gram-positive, *Listeria monocytogenes* and Gram-negative, *Salmonella* Typhimurium. Furthermore, OS conferred protection even after its administration to mice post-establishment of infection highlighting its therapeutic potential. Subsequently, we identified the key OS-secreted bacteriocin protein responsible for limiting intracellular *Salmonella* and *Listeria* replication in human intestinal cells by regulating virulence genes such as flagella. Overall, our study implicates the broad-spectrum protective role of OS in mitigating foodborne infections caused by *Salmonella* and *Listeria* pathogenesis.

MATERIALS AND METHODS

Bacterial Strains and Culture Conditions

Salmonella enterica serovar Typhimurium (STM) strain ATCC 14028S, STM ATCC 14028S constitutively expressing mCherry (pFPV25.1-mCherry-Amp^R, RFP), laboratory stock of *Enterococcus faecalis* MTCC 439 (Ef), *Listeria monocytogenes* MTCC 657 (LM) expressing mCherry and *Odoribacter splanchnicus* (OS) strain NCTC 10825 [1651/6] from ATCC were used in this study. 4% paraformaldehyde-fixed-OS was used as killed bacteria control. The STM, LM, and Ef bacterial strain was grown overnight in LB broth at 37 ^{0}C under 160 rpm shaking conditions. OS was cultured in anaerobic condition in tryptic soy broth at 37ºC for 48-72h after its revival from glycerol stock.

Preparation of Cell-free Bacterial Culture Supernatant

The overnight grown OS culture in tryptic soy broth was centrifuged at 10,000rpm for 10 min and the supernatant was harvested. The collected supernatant was further subjected to another two rounds to centrifugation to remove any residual cells. The supernatant was subsequently filtered using a 0.2 µm filter and stored at − 20˚C.

Animal Experiments

The animal experiments were conducted in accordance with the approved guidelines of the institutional animal ethics committee at the Indian Institute of Science, Bangalore, India (Registration No: 48/GO/ReRcBiBt-S/Re-L/99/CPCSEA). All procedures involving the use of animals were performed according to the Institutional Animal Ethics Committee (IAEC)-approved protocol (CAF/Ethics/853/2021). 6–8 weeks old adult C57BL/6 male mice were used in this study (bred, housed, and provided (purchased) by Central Animal Facility, Indian Institute of Science, Bangalore). After one day of OS colonization (10^5 CFU/mice via oral gavage), the mice were infected with 10^6 (organ burden) CFU or 10^8 CFU (for assessing

127 survival) of *S.* Typhimurium, and 10^8 (organ burden) or 10^9 (survival) CFU of *L.*
128 *monocytogenes* via oral gavage. The colonization of *O. splanchnicus* was confirmed via RT-
129 qPCR mediated quantitation of OS 16S rRNA from the mice fecal (3 fecal pellets harvested
130 from the intestine and resuspended in Trizol) and ileal samples at 6th day post-OS colonization.
131 For post-infection OS administration studies, OS was orally administered (10^5 CFU/ mice) post
132 1 or 3dpi. 5-day post-infection, mice were euthanized, dissected out, and blood and organs
133 were harvested. The bacterial organ load was enumerated by plating the tissue homogenates on
134 *Salmonella-Shigella* (SS) agar plates for *Salmonella* or LB plates containing 50µg/ml of
135 Ampicillin for LM. The harvested tissues and the fecal samples were collected in protein lysis
136 buffer and TRIzol (Takara) for protein and RNA extraction respectively and were stored at -
137 80ºC. For calculating percentage survival, the infected mice cohorts were monitored till fatality
138 and fatalities were reported.

139 **Blood collection and serum preparation**

140 Blood collection was performed on the 5th day post-infection via cardiac puncture post-
141 euthanization of the mouse. The collected blood was allowed to clot by incubating the vials at
142 room temperature for 45 minutes. After allowing the standing time of 45 mins, centrifugation
143 was performed at 2000g for 15 minutes in a refrigerated centrifuge. Following the
144 centrifugation, the clear, yellowish supernatant was transferred to an autoclaved microfuge tube
145 and stored at -80ºC till further downstream processing.

146 **ELISA**

147 Cytokines in mice serum were quantified according to the manufacturer's instructions(10, 14).
148 Briefly, 96-well ELISA plates of IL-6 ELISA kit (BD Bioscience- Cat No-555240) were coated
149 overnight with capture antibody at 4°C. Following day, plates were washed with 0.1% Tween-
150 20 containing PBS and blocked with 10% FBS for 1 h. Following blocking, wells were washed

151 and incubated with 50µl of serum samples in duplicates for 2 h at room temperature.
152 Subsequently, plates were washed and incubated with detection antibody and enzyme reagent
153 for 1 h at room temperature (BD Bioscience). TMB (Sigma) was used as a substrate and
154 reactions were stopped with 2 N H_2SO_4.

155 For the estimation of IL-1β, pre-coated ELISA (SARD Biosciences-Cat:SB-EKM1085) plates
156 of IL-1β ELISA kit were used, and ELISA was performed as per the manufacturer's protocol.
157 The ileal tissues were harvested in phosphate-buffered saline solution and homogenized using
158 gentleMACS homogenizer. The homogenized tissue samples were centrifuged to collect cell-
159 free supernatant and the cell-free supernatant was subjected to ELISA for cytokine estimation.

160 Absorbance was measured at 450 nm wavelength in Tecan Plate reader and the concentration
161 of cytokines were interpolated from a standard curve.

162 **Quantitative Real Time PCR**

163 Total RNA was isolated from the ileal section of the intestinal tissues or feces harvested in
164 TRIzol (Takara) as per manufacturer's protocol. RNA was quantified using Nano Drop
165 (Thermo-Fischer scientific). Integrity of isolated RNA was detected by performing 2% agarose
166 gel electrophoresis. 3 µg of total isolated RNA was subjected to DNaseI (Thermo Fischer
167 Scientific) treatment at 37°C for 1 hr followed by heat inactivation at 75°C in the presence of
168 5mM concentration of EDTA for 10 mins. The mRNA was reverse transcribed to cDNA using
169 oligo $(dT)_{18}$ primer, random hexamer primer, buffer, dNTPs and reverse transcriptase (Takara)
170 as per manufacturer's protocol. The expression profile of target gene was evaluated using
171 specific primers (Table-S2) by using SYBR green RT-PCR master mix (Takara) in Applied
172 Biosystems (Quantstudio 5) or BioRad Real time PCR instrument. β-actin was used as an
173 internal control for mammalian genes and for bacterial genes 16S rRNA was used. All the
174 reaction was setup in 384 well plate with three replicates for each sample.

175 **Western blotting**

176

177 The harvested tissue samples were lysed in ice-cold RIPA buffer (50 mM Tris-Cl, pH 8.0, 150
178 mM NaCl, 5mM EDTA, 1% NP-40, 1 % Sodium deoyxycholate, 1% SDS) containing protease
179 inhibitor cocktail (Roche). Total protein was estimated using Bradford reagent (BioRad).
180 Protein samples were denatured in **Laemmli SDS loading buffer** at 95ºC for 10 min and then
181 subjected to separation on 12% SDS-PAGE gels followed by transfer onto activated 0.45µm
182 PVDF membrane. Finally, the membrane was blocked with 5% skimmed milk in TBST (Tris
183 Buffered Saline containing 0.1% Tween-20) and probed with appropriate primary (Table-S3)
184 and secondary HRP-conjugated antibodies. The blots were developed using ECL substrate
185 (Bio-Rad) using a Chemidoc (BioRad). All densitometric analysis was performed using
186 ImageJ software.

187 **Immunohistochemistry**

188 The harvested tissues were fixed in 4% paraformaldehyde, embedded in paraffin and 5 µm
189 thick paraffin sections were collected on poly-lysine coated glass slides. The sectioned tissue
190 samples were deparaffinized using standard protocol. Briefly, the slides containing the
191 paraffinized tissues were immersed in xylene for 10 minutes and this step was repeated twice.
192 After the xylene treatment, the tissues were subjected to absolute alcohol treatment for 5
193 minutes twice, followed by 95% and 70% alcohol treatment for 5 minutes. The slides were
194 rinsed in water followed by boiling step in water for 2 minutes and then dried. Primary antibody
195 staining of the deparaffinized sections was performed with specific primary antibody in the
196 presence of a permeabilizing agent, 0.01% saponin (Sigma) dissolved in 2.5% BSA containing
197 PBS at 4°C for overnight. Following wash with PBS, sections were stained with appropriate
198 secondary antibody tagged with fluorochrome for 1 hr at RT. This was followed by DAPI
199 staining and mounting. For in vivo estimation of biofilm, deparaffinized tissue samples were
200 stained with Calcofluor White (Sigma) stain for 20 min at RT. All immunofluorescence images

201 were obtained using Zeiss multi-photon 880 microscope and were analyzed using ZEN black
202 2012 software.

203 **Haematoxylin and Eosin Staining**

204 The harvested ileal tissues were collected and fixed using 3.5% paraformaldehyde. The fixed
205 liver was then dehydrated using a gradually increasing concentration of ethanol and embedded
206 in paraffin. 5µm sections were collected on coated plates. Sections were further rehydrated and
207 then stained with hematoxylin and eosin. Images were collected in a Leica microscope.

208 The scoring of the pathological changes is graded as 0-4; for each of the pathological lesions
209 (Severe/ marked -4; Moderate -3; mild -2; Minor/minimum -1; No pathology -0) considering
210 the intestinal inflammation and associated villi injury as described previously (15, 16).

211 **Cell Culture**

212 Human colorectal adenocarcinoma cell line Caco-2 were maintained in Dulbecco's Modified
213 Eagle's Media (DMEM) (Lonza) and supplemented with 10% FCS (Fetal calf serum, Gibco)
214 and 1% non-essential amino acid solution (Sigma Aldrich) at 37ºC temperature in the presence
215 of 5% CO_2 in humidified incubator. Prior to each experiment, cells were seeded into 24 well
216 or 6 well plate as per requirement at a confluency of 60%.

217 **Intracellular proliferation or gentamicin protection assay**

218 Caco-2 epithelial were infected with 3 to 4 h old log phase *S*. Typhimurium (STM) or *Listeria*
219 *monocytogenes* (LM) or *S.* Typhi (STY) bacterial culture, STM (or LM or STY) with *O.*
220 *splanchnicus*, STM (or LM or STY) in presence of *O. splanchnicus* supernatant and STM along
221 with PFA-fixed OS at an MOI of 10. For attachment of bacteria to the cells, tissue culture plates
222 were subjected to centrifugation at 600xg for 5 min and incubated at 37 ^{0}C humified incubator
223 with 5% CO_2 for 25 min. Following infection of the cells with STM at an MOI of 10, cells were

224 treated with DMEM (Sigma) + 10% FBS (Gibco) containing 100 µg/ml gentamicin for 1 hr.
225 Subsequently, the gentamicin concentration was reduced to 25 µg/ml and maintained until the
226 specified time point. Post 2hr and 16hr post-infection, cells were lysed in 0.1% triton-X-100.
227 Lysed cells were serially diluted and plated on *Salmonella-Shigella* (SS) or LB agar to obtain
228 colony-forming units (CFU). Percent invasion was determined using the following formula
229 (17, 18):

230 **Percent invasion= [CFU at 2 h]/ [CFU of pre-inoculum] X 100**

231 Fold proliferation was calculated as CFU at 16hr divided by CFU at 2hr.

232 **Fold Proliferation= [CFU at 16h] / [CFU at 2h]**

233 **Immunofluorescence confocal microscopic studies**

234 At the specified time points post infection with mCherry-tagged STM, or GFP-tagged OS or
235 with both mCherry-STM and GFP-OS, cells were fixed with 3.5% paraformaldehyde for 15
236 min. Primary antibody staining was performed with specific primary antibody in the presence
237 of a permeabilizing agent, 0.01% saponin (Sigma) dissolved in 2.5% BSA containing PBS at
238 4°C for overnight or for 6hr at room temperature (RT). Following this, cells were washed with
239 PBS stained with appropriate secondary antibody tagged with fluorochrome for 1 hr at RT. This
240 was followed by DAPI staining and mounting of the coverslip onto a clean glass slide using
241 the mounting media containing the anti-fade agent. The coverslip sides were sealed with a
242 transparent nail paint. All immunofluorescence images were obtained using Zeiss Multiphoton
243 880 and were analyzed using ZEN black 2012 software.

244 **Growth Curve analysis**

245 For *in vitro* growth curve experiments a single colony of STM and OS was inoculated in 5mL
246 of LB broth singly or in co-culture and grown overnight at 37ºC in anaerobic jar. In another

247 set, STM was inoculated in 5mL of LB in presence of OS supernatant. Overnight-grown
248 stationary phase bacteria were sub-cultured at a ratio of 1: 100 in freshly prepared LB in
249 presence or absence of OS supernatant and kept at 37ºC. At different time intervals, aliquots
250 were taken for measurement of [OD]600nm by TECAN 96 well microplate reader and were
251 plated for CFU enumeration.

252 **Biofilm-inducing growth media and conditions**

253 LB medium lacking NaCl and containing 1% casein enzyme hydrolysate (Hi-Media, India) and
254 0.5% yeast extract (Hi-Media, India)) was used as biofilm media as per previous literature (19).
255 Overnight grown culture was subcultured in 2 ml biofilm medium at the dilution of 1:100 in a
256 flat-bottom 24-well plate (Tarsons, India) and incubated at 28˚C for 72 h without shaking.

257 **Biofilm inoculation with OS culture supernatant**

258 20 µl of STM overnight culture and indicated volume (1% v/v or as indicated) of the OS culture
259 supernatants were added to 2 ml of biofilm media and incubated under biofilm-promoting
260 conditions(19). For co-culture experiments, the overnight cultures of the STM and OS or STM
261 and PFA-fixed OS were added in a 1:1 ratio to 2 ml of biofilm media and incubated under
262 biofilm-inducing conditions.

263 **Crystal Violet Staining**

264 Post 72 h of biofilm induction, the media was discarded, and the plates were thoroughly washed
265 in water. The plates were dried, and 2 ml of 1% Crystal Violet (CV) was added to each well
266 and incubated for 15 min. Post 15 min incubation, the CV stain was removed, and the plate was
267 thoroughly rinsed in water to remove excess stain. The stained biofilm was destained with 70%
268 ethanol, and the intensity of the colour of the destained solution was quantified at OD_{595} in the
269 Tecan plate reader (Infinite Pro 200) (19).

270 **Glass bead assay**

271 1 mm glass beads were added onto the pellicle to assess the strength of the pellicle at the air-
272 liquid interface. The initial weight of the glass beads was noted. The glass beads were added
273 until the pellicle collapsed, and the final weight was noted down and plotted.

274 **Gut Permeability Assay**

275 The infected mice cohorts were orally administered with FITC Dextran (25mg/kg,FD-4-
276 100MG, Sigma) 4h before euthanization. The blood plasma was collected post-euthanization
277 by cardiac puncture followed by centrifugation. The blood plasma was evaluated for mean
278 fluorescence via plate reader (TECAN) and flow cytometry(CytoFlex, Beckman).

279 **MTT Assay**

280 Post-16h treatment of pre-seeded Caco-2 cells with 10µg/ml of bacteriocin, MTT staining
281 solution (0.5mg/ml) was added to each well followed by incubation at 37ºC CO_2incubator for
282 4h. 50µl of DMSO was added per well for solubilizing the formazan crystals. Absorbance was
283 measured at 570nm using a plate reader (TECAN).

284 **Transmission electron microscopy**

285 Overnight STM or LM-grown cultures (in the presence or absence of OS supernatant or
286 bacteriocin) were subcultured into fresh media (1:10) ratio and incubated at 37ºC for 6 hours
287 under shaking conditions. These samples were centrifugated at 1000rpm for 10 min to obtain
288 the bacterial pellet. The bacterial pellet was subjected to PBS wash twice via centrifugation at
289 1000 rpm for 10 min.5 µl of the finally resuspended cell suspension was added on a glow-
290 discharged copper-grid, air dried, stained with 1% uranyl acetate for 30 s, and visualized under
291 a transmission electron microscope (JEM-100 CX II; JEOL).

292 **Supernatant Treatment**

293 The supernatant was treated with 7.5 mM concentrations of EDTA and incubated at 65 °C for
294 1 h. 10 µl of proteinase-K (NEB, stock 20 mg/ml) was added to the 200 µl supernatant and
295 incubated at 37 °C for 1 h. The proteinase was inactivated with 0.5 mM PMSF and incubated
296 at 28 °C for 1 h. The supernatant was subjected to heating at 37˚C (60 min), 65˚C (15 min) or
297 95˚C (15 min) and immediately frozen at − 20˚C (19). Post-treatment, the supernatants were
298 used to inoculate the biofilm to test the nature of the biofilm inhibitory molecules.

299 **Supernatant concentration and molecular weight-based separation**

300 4 ml of the supernatants were transferred to the 3k MWCO or 10k MWCO Amicon ultra filter
301 centrifugal device (Amicon® Ultra-4 centrifugal filter device, 3k MWCO, UFC800324;
302 Amicon® Ultra-4 Centrifugal filter Unit, 10k MWCO, UFC801024) and centrifuged at 4000 g
303 for 30 min in a swing bucket rotor(19). The concentrated solute from the bottom of the filter
304 device and the flowthrough were collected and subjected to biofilm inoculation.

305 **Size Exclusion Chromatography**

306 The bacterial supernatant was concentrated to 0.5ml using 3k MWCO-Amicon-Ultra-4-
307 centrifugal unit and loaded onto the Superdex 200pg size exclusion column (XK16/60, 124mL;
308 Cytiva, USA), pre-equilibrated Tris-Cl buffer (pH-8) containing 100mM NaCl and 20mM Tris-
309 Cl. The sample was eluted with the same buffer at a flow rate of 0.8mL/min, and 1mL fractions
310 were collected. The fractions corresponding to the elution peaks were analyzed for biofilm
311 inhibition activity and subjected to mass spectrometry.

312 **LC/MS analysis of the supernatant fractions**

313 The concentrated gel filtration fractions of supernatants were subjected to in-solution trypsin
314 digestion for LC Q-TOF MS analysis. Briefly, 100 µg of total protein was resuspended in

315 100 µl of 7-8M of urea buffer. To this, 5 µl 200mM DTT was added and incubated at room
316 temperature for 1 hr, followed by alkylation with 20µl of 200 mM iodoacetamide and
317 incubation at room temperature for 1h in the dark. This was followed by the addition of 1mM
318 of Calcium chloride and incubation at RT for 10 min. For protein digestion, trypsin solution
319 was added to the sample to a final trypsin to protein ratio of 1:30 (w/w) and incubated at 37˚C
320 for 16 h, with frequent shaking. The reaction was stopped by adding 0.1% formic acid to adjust
321 the pH to 3-4. The digested protein samples were desalted using a reverse phase C-18 column
322 (Acclaim prep EASY-Spray (C18-RP)) using mobile phase solvent A-2% acetonitrile and
323 solvent B- 80% acetonitrile. The sample injection volume was 10µl. All the samples were
324 analyzed using Thermo Scientific SII for Xcalibur method. The MS scan was acquired using
325 Orbitrap detector with 60000 resolution in the positive polarity and scan range (*m/z*) 350-2000.
326 The ion source type was NSI with static voltage; positive ion (V)- 2200V and negative ion (V)-
327 600 along with temperature settings at 275ºC. This was followed by $ddMS^2$ IT HCD with 30%
328 fragmentation HCD collision energy using ion trap detector. The raw data was analyzed using
329 Proteome Discoverer 2.5 against the *O. splanchnicus* proteome available in UniProt (Proteome
330 ID: UP000006657).

331 **Purification of bacteriocin**

332 *O. splanchnicus* culture supernatant was concentrated within the range of >3kDa and <10kDa
333 using the Amicon Ultra-4 Centrifugal filter units of 10MWCO and 3MWCO. The concentrated
334 cell-free supernatant containing the bacteriocin (~7kDa) was precipitated by ammonium
335 sulphate (80% to 98%). The precipitate was collected by centrifugation at 12000rpm for 30
336 min and dissolved in 1X PBS. The dissolved precipitate was again filtrated using the 3KDa
337 cutoff Amicon centrifugal filter units. This concentrated fraction was further subjected to Fast
338 Performance Liquid Chromatography using Superdex 75 Increase 10/300 GL- 24ml volume

339 (GE Healthcare) column. The column was equilibrated with 1X Phosphate Buffered Saline
340 buffer and 0.5ml of concentrated sample (23.6 mg/ml) was injected into the column. Based on
341 the increase in Absorbance units at 280nm from baseline, 0.3ml fractions were collected at a
342 retention volume of 13.3ml to 21.8ml (Fig. S9). The fractions were analyzed by 20% SDS-
343 PAGE electrophoresis and stained with Coomassie staining solution.

344 ***In vitro* swim motility assay**

345 2 µl ($2*10^6$ CFU/ml) of treated or untreated stationary phase bacterial samples were spotted on
346 the 0.3% agar (LB-STM, BHI-LM) plates supplemented with 0.5% yeast extract, 1% casein
347 enzyme hydrolysate, 0.5% NaCl, and 0.5% glucose. The plates were incubated at 37˚C and
348 images were taken every 6 h (STM) or 24h (LM) using the camera of Biorad illuminator.

349 **Statistical analysis**

350 Data were analyzed and graphed using the GraphPad Prism 8 software (San Diego, CA).
351 Statistical significance was determined by Student's t-test or One-way ANOVA followed by
352 Dunnett's Multiple Comparisons test to obtain p values. ANOVA was used during comparison
353 among three or more groups whereas Student's t-test was used to compare the difference
354 between two groups. Mann Whitney t-test was used as a non-parametric counterpart of Student
355 t-test when variances differed. The log-rank test also known as Mantel-Cox test is used to
356 compare the survival percentages of the mice groups. Adjusted p-values below 0.05 are
357 considered statistically significant (****$p<0.0001$, *** $p < 0.001$, ** $p<0.01$, * $p<0.05$). The
358 results are expressed as mean ± SD or SEM of three independent experiments.

359

360 **RESULTS**

361 ***O. splanchnicus* hinders *Salmonella* burden and its systemic dissemination**

362 To denote the role of OS in *Salmonella* pathogenesis, we colonized C57BL/6 mice with 10^5
363 CFU of OS 1 day prior to *Salmonella* infection via the oral route and validated the colonization
364 by undertaking OS 16S rRNA qPCR analysis (Fig 1, A-B). OS pre-colonized mice showed
365 decreased susceptibility to *Salmonella* infection in comparison to the non-colonized mice
366 cohort which succumbed to death by day 9 post-infection (p.i.). Contrastingly, 100% of the OS
367 colonized mice were alive even at day 11 post *Salmonella* infection (Fig 1, C). *Salmonella*
368 colonization of the feces and intestinal tissue and dissemination to the MLN, blood, and liver
369 were reduced upon OS pre-colonization (Fig 1, D-K). OS non-colonized mice exhibited
370 increased weight loss percentage upon *Salmonella* infection and OS pre-colonization prevented
371 weight loss (Fig 1, H). Our result suggests OS could prevent *Salmonella* colonization, organ
372 burden and dissemination (Fig 1).

373 ***O. splanchnicus* colonization ameliorate the acute *Salmonella-induced* inflammation and**
374 **its associated pathogenesis**

375 Heightened inflammatory responses facilitate *Salmonella* dissemination in mice(20). Thus, we
376 hypothesized that OS gut colonization might ameliorate the *Salmonella*-induced inflammation.
377 ELISA-mediated IL-6 serum quantification revealed reduced IL-6 production upon *S.*
378 Typhimurium (STM) infection in the OS colonized mice group to the non-colonized cohort
379 (Fig 2, A). To combat the enteric pathogen challenge, the host employs one of its major defence
380 arsenals, that is, the production of antimicrobial peptides (AMPs)(21, 22). STM infection
381 induces enhanced mRNA expression of AMPs in mice with respect to the uninfected control
382 as per previous literature findings (17). We found that OS colonization in mice resulted in the
383 downregulation of several AMP genes such as Lysozyme-C1 precursor, Angiogenin-4
384 precursor, CCL20, Beta-defensin-4 and Regenerating-islet-derived 3 beta-precursor (Fig 2, B).
385 Mucus lining serves as another crucial barrier against the entry of enteric pathogens(23).
386 However, enteric pathogens adopt several strategies to circumvent this barrier to reach the

387 underlying epithelium(24). To assess the mucin layer dynamics upon the *Salmonella* challenge,
388 we assessed MUC2 expression in the ileal tissues of OS colonized versus non-colonized mice
389 groups. Our result depicted enriched MUC2 expression in the OS non-colonized mice cohort
390 compared to the colonized cohort (Fig.2, C). The increase in the mucus lining upon *Salmonella*
391 infection could be one of the host defense mechanisms to bolster the barrier and exclude
392 pathogens(25). As per previous literature, the rate of mucin production is modulated by several
393 stimuli including inflammatory cytokines (26), vasoactive antimicrobial peptides, and other
394 innate and adaptive immune responses (23). Germ-free mice depict a reduced number of goblet
395 cells, and mucin storage granules(27) as well as reduced expression of AMPs(28). The
396 haematoxylin eosin-stained intestinal sections suggested increased intestinal tissue damage
397 with irregularly organized villi, necrotic submucosa layer, and detached intestinal cells in all
398 the STM-infected non-OS-colonized cohorts. However, OS pre-colonization restored the
399 intestinal tissue architecture in all the mice cohorts (Fig 2, D).

400 ***O. splanchnicus* restricts *Salmonella*-mediated GVB damage and promotes tight junction**
401 **gene expression**

402 *Salmonella* breaches the gut vascular barrier (GVB) by inducing tight junction disruption.
403 *Salmonella* like other food-borne antigens enters into the Mesenteric Lymph Node (MLN) by
404 accessing the lymphatics and subsequently gains entry into the liver via the bloodstream(29).
405 The translocation of the pathogen across the blood endothelial cells is governed by the integrity
406 of the GVB(1). The GVB refers to the endothelial barrier and the microvasculature
407 characterized by the elaborate framework of the junctional complexes (1). The GVB
408 architecture is maintained by several tight junctions and adherens junction proteins that control
409 paracellular trafficking(30, 31). Other cell types associated with the microvasculature of the
410 GVB forming a vascular unit includes pericytes and fibroblasts(32). PV-1 (plasmalemma-
411 vesicle associated protein-1) expression is a marker of GVB damage and heightened PV-1

412 expression denotes EC permeability(33, 34). Our data show reduced PV-1 marker expression,
413 alongside enhanced tight junction protein mRNA expression, such as Tjp1 and Claudin5, upon
414 OS colonization during *Salmonella* infection in comparison to the non-OS-colonized cohorts.
415 (Fig. 3, A-B). CD34, an endothelial marker lining the blood vessels (35, 36), is induced upon
416 OS colonization in *Salmonella*-infected mice intestines in comparison to the non-colonized
417 mice cohorts indicative of intact vasculature (Fig.S1, A). On the contrary, OS mice cohorts
418 exhibited reduced CD34 expression in secondary sites of dissemination such as the liver,
419 suggesting reduced vasculature (Fig.S1, B). Angiogenesis is one of the processes that facilitate
420 bacterial dissemination. Previous studies in *Mycobacterium marinum* have shown that
421 transcriptional induction of pro-angiogenic markers like *Vegfa* contributes to increased
422 bacterial burden and dissemination(37). In our study, OS pre-colonization in the gut resulted in
423 reduced expression of the pro-angiogenic *Vegfa* in the infected liver tissues, which coincided
424 with the reduced *S.* Typhimurium burden in the bloodstream and liver (Fig S1, C). Previous
425 literature suggested reduced expression of *Axin2,* a β catenin target gene, upon wildtype
426 *Salmonella* infection, even after Wnt3a stimulation suggesting that *Salmonella* affects the GVB
427 by inhibiting canonical Wnt signalling (1). Here, our results suggest that OS pre-colonization
428 restores the *Salmonella*-triggered attenuated Wnt signalling response with increased Axin2
429 expression in the *Salmonella*-infected intestinal tissues (Fig. S1, D). The integrity of the
430 infected mice gut was estimated by the gut permeability assay using FITC-Dextran (Fig. 3, C).
431 Our results indicate increased gut vascular permeability upon *Salmonella* challenge which
432 declined upon OS pre-colonisation, implicating the ability of OS to prevent gut barrier
433 disruption.

434 ***O. splanchnicus* culture supernatant restricts *Salmonella* biofilm formation and**
435 **intracellular proliferation in human intestinal cells**

436 To delineate the mechanism behind the protective role of OS against *Salmonella* pathogenesis,
437 we performed *Salmonella* infection studies in human intestinal epithelial cell line Caco-2 in
438 the presence of OS. The intracellular survival assay suggested decreased STM invasion and
439 subsequently attenuated intracellular replication within the infected Caco-2 cells upon co-
440 infection with live OS and in the presence of OS culture supernatant (Fig 4, A-B). However,
441 STM co-infection with fixed OS showed percent invasion and intracellular replication like that
442 of STM infection (Fig 4, A-B). Together, these results hinted at the presence of some secreted
443 inhibitory components in the OS culture supernatant that has the propensity to limit STM
444 infection. The reduced invasion and proliferation of STM within Caco-2 cells in presence of
445 OS was subsequently validated in immunofluorescence studies, wherein STM showed a
446 significant reduction in invasion at 2hr p.i. and intracellular proliferation at 16hr p.i. in case of
447 OS co-infection (Fig 4, C-D). Similar results were obtained upon infection with the human-
448 restricted serovar *S.* Typhi (STY) to the Caco-2 cells wherein OS and its supernatant attenuated
449 STY invasion and intracellular replication (Fig. 4, E-F). Further, we assessed the *in vitro* growth
450 of the STM in co-culture conditions with OS or in the presence of OS culture supernatant in
451 anaerobic conditions to mimic the microaerophilic or hypoxic environment of the gut or in
452 aerobic culture conditions. We observed no significant delay *in vitro* growth of STM at its
453 initial lag to log phase of its growth in the presence of OS supernatant or with live OS under
454 anaerobic culture conditions (Fig S2, A-B). In aerobic growth conditions as well, *Salmonella*
455 growth remained unperturbed even in the presence of OS or its culture supernatant (Fig S2, C-
456 D). Several previous studies have corroborated the ability of commensal bacterial culture
457 supernatants to inhibit colonization and the biofilm formation of several pathogens. For
458 instance, a commensal bacterium, *Staphylococcus epidermis*, could inhibit biofilm formation
459 and nasal colonization of its pathogenic counterpart, *Staphylococcus aureus* (38). Moreover,
460 biofilm formation is also regulated at the interspecies level. Indole is an inter-species biofilm

461 regulator that decreases *E. coli* biofilm formation and facilitates biofilm formation of
462 pseudomonads (39). STM forms biofilm to colonize the host, evade host defence arsenals and
463 antibiotics, persist during chronic infections, and transmit to new hosts (40, 41). We, therefore,
464 examined the biofilm pellicle strength and biofilm formation of STM via crystal violet staining
465 on the solid-liquid interface in the presence or absence of live, PFA-fixed-OS or OS culture
466 supernatant by inoculating STM in biofilm-inducing media with low salinity. STM exhibited
467 biofilm formation defect in the presence of live OS or OS supernatant (Fig 4, G). However, the
468 STM biofilm inhibitory property of OS was diminished upon treatment with paraformaldehyde
469 (PFA)-fixed OS (Fig 4, G). Further, qPCR-mediated gene expression studies of *Salmonella*
470 biofilm genes revealed decreased expression of genes regulating biofilm (*csgD*, *csgA*, *bapA*)
471 under treatment with live OS or its culture supernatant (Fig.4, H-J). Flagella-mediated
472 attachment and several virulence factors such as SPI-1 and SPI-2 genes are responsible for
473 *Salmonella* pathogenesis and its biofilm formation (19, 42, 43). Therefore, we evaluated a few
474 of the *Salmonella* flagellar and SPI-1 and SPI-2 gene expression in the presence or absence of
475 OS or its culture supernatant via quantitative real-time PCR. Our results depicted attenuated
476 expression of flagellar gene (*fliC*), SPI-1 (*sipC*) and SPI-2 (*pipB2*) genes both in the presence
477 of live OS and its spent media but not in presence of PFA fixed-OS (Fig. 4, K-M). The loss in
478 *Salmonella* flagellar motility was further validated via TEM imaging wherein OS or its
479 supernatant reduced the flagella formation of *Salmonella* considerably (Fig.4, N). Together,
480 our results implicate the ability of OS to inhibit STM biofilm formation via active secretion of
481 certain inhibitory molecules in the supernatant.

482 ***O. splanchnicus* inhibitory effect on *Salmonella* is specific as *Enterococcus faecalis*,**
483 **another gut resident microbe, fail to inhibit *Salmonella* intracellular proliferation or**
484 **biofilm formation**

485 The resident gut microbes provide colonization resistance against invading pathogens by
486 deploying several mechanisms, including the production of inhibitory molecules, nutrient
487 competition, maintenance of the intestinal epithelial integrity, immune activation, and via the
488 deployment of bacteriophages (44, 45). To understand whether our observed inhibitory trait of
489 OS against *Salmonella* is due to a common colonization restriction phenomenon of gut
490 microbes via competitive inhibition, or it is a specific phenomenon, we evaluated the role of
491 another gut resident microbe, *Enterococcus faecalis* on *Salmonella* intracellular replication in
492 human intestinal epithelial cells and *Salmonella* biofilm formation. *Enterococcus sp.* belong to
493 the phylum of Firmicutes in the family Enterococcaceae. Approximately, 10^6-10^7 *Enterococcus*
494 *sp*. reside in the human intestine with major abundance of *E. faecalis* (10^5-10^7 CFU/gm feces)
495 and *E. faecium* (10^4-10^5/gm feces) (46). *E. faecalis*, *E. faecium*, *Bifidobacterium sp*.
496 *Lactobacillus sp.,* and *E. coli* colonize the gut of healthy breastfed infants during the initial 7-
497 10 days post birth (47). Our intracellular survival assay data showed no defect in *Salmonella*
498 invasion or intracellular replication capability in Caco-2 cells in presence or absence of *E.*
499 *faecalis*, its culture supernatant or PFA-fixed *E. faecalis* (Fig. S3, A-B). Moreover, *E. faecalis*
500 or its *E. faecalis* supernatant did not inhibit *Salmonella* biofilm formation (Fig. S3, C).
501 Together, our results suggest the inability of *E. faecalis* to inhibit *Salmonella* invasion,
502 intracellular proliferation or its *in vitro* biofilm formation, thereby highlighting the specificity
503 of OS in restricting *Salmonella* pathogenesis.

504 ***O. splanchnicus* confers protection against another foodborne pathogen *Listeria***
505 ***monocytogenes***

506 To understand whether OS exerts a common broad-spectrum protection or colonization
507 resistance against other foodborne pathogens such as *Listeria monocytogenes*, we orally
508 infected 6-8-week-old C57Bl/6 mice with 10^8 CFU of *L. monocytogenes* (LM) 1 day post
509 colonization with 10^5 CFU of *O. splanchnicus* for organ burden evaluation via oral gavage. For

510 survival study, mice were orally gavaged with 10^9 CFU of *L. monocytogenes*. OS-colonized
511 mice exhibited increased survival rates upon LM challenge compared to the non-colonized
512 mice cohort (Fig. 5, A). In line with the survival data, the increased bacterial burden was
513 observed in the blood, feces, intestinal tissue, MLN, spleen and liver alongside enhanced
514 percent loss in mice body weight in the case of *Listeria* infection in non-colonized mice group
515 with respect to OS-precolonized- mice group (Fig. 5, B-J). In a similar line to *Salmonella*
516 infection, OS mitigated host antimicrobial response with reduced expression of antimicrobial
517 peptide transcripts and Muc2 production during LM infection amounting to reduced intestinal
518 tissue damage. Further, OS promoted tight junction functions during *Listeria* infection with
519 reduced expression of GVB damage marker, *PV-1* and angiogenesis marker, *Vegf* expression
520 (Fig. S4, A-E). Moreover, OS colonization could restrict the *in vivo Salmonella* and *Listeria*
521 biofilm within the spleens of the infected mice cohorts as opposed to the non-colonized mice
522 cohorts (Fig.S4, F-G). We estimated the biofilm or the communities of bacterial cells within
523 the spleen tissue via Calcofluor white staining (48). Calcofluor white stains the biofilm matrix
524 or extracellular polymeric substances (EPS) comprised of cellulose (48, 49) and
525 exopolysaccharides that help in the adherence of the bacterial cells. This is the first study
526 demonstrating biofilm-like bacterial colonies of *Salmonella* or *Listeria* secreting EPS in
527 spleens. Like *Salmonella*, *in vitro* culture of *Listeria* with OS or its culture supernatant led to a
528 loss in flagella as evidenced via the TEM imaging (Fig.S4, H). Since flagella is one of the
529 factors facilitating biofilm formation and invasion, OS could inhibit both *Salmonella* and
530 *Listeria* colonisation and biofilm formation. Similar to *Salmonella* infection, OS colonization
531 enhanced CD34 expression in *Listeria*-infected mice intestines and reduced CD34 expression
532 in the *Listeria*-infected liver (Fig. S4, I-J). Further, LM exhibited attenuated intracellular
533 proliferation within human intestinal Caco-2 cells upon live OS or OS supernatant treatment

534 (Fig. 6). Altogether, this result hints at the potency of OS to act broadly against Gram-positive
535 and Gram-negative bacteria.

536 **The protective role of *O. splanchnicus* against *Salmonella* Typhimurium and *Listeria***
537 ***monocytogenes* persists even on administration post-establishment of infection**

538 Next, we sought to examine whether the protective role of OS against *Salmonella* and *Listeria*
539 is sustained when the infection has been fully developed and whether it can serve as a treatment
540 regimen against foodborne diseases. Our results indicate the protective ability of OS against
541 both foodborne pathogens in their intestinal phase of infection when administered at 1-day
542 post-infection (dpi) as depicted by lower pathogen loads in all the organs and blood along with
543 reduced percent weight loss at 5th-day post-*Salmonella* or *Listeria* challenge in the OS-
544 administered (1-dpi) cohort when compared to the untreated cohorts (Fig. 7,A-K, Fig. S5, A-
545 C). Although the protective ability of OS persists even upon establishment of infection when
546 administered at 3rd-day post-*Salmonella* or *Listeria* challenge as indicated by reduced organ
547 loads and percent weight loss in the OS-colonized cohorts, the extent of protection is lower
548 compared to its administration at 1-dpi (Fig. 7, L-W, Fig. S5, D-S), Further, the OS challenge
549 at 1-dpi reduced the mice's susceptibility to the *Salmonella* and *Listeria* challenge(Fig. 7, L,R).
550 However, administration of OS at 3-dpi delayed the death of the *Salmonella* and *Listeria*-
551 infected mice cohorts by 1 day (Fig. 7, L,R). In line with the survival and organ burden data,
552 OS treatment at both 1st and 3rd dpi reduced both *Salmonella* and *Listeria*-induced GVB
553 damage with reduced PV-1 expression, mucin, AMPs, and *Vegf* expression, alongside
554 promoting tight junction protein (*Tjp1* and *Claudin5*) and *Axin2* expression (Fig. S5, D-M).
555 However, OS administration at 3-dpi conferred less protection than at 1-dpi as indicated by the
556 protein expression profiles of Muc2, PV-1, and tight junction protein ZO-1 (Fig. S5, R-S).
557 Additionally, OS colonization mitigated gut vascular permeability during *Salmonella* and
558 *Listeria* challenges as indicated by reduced FITC-dextran fluorescence units in the plasma both

559 upon pre or post-OS colonization (Fig. S5, T). Moreover, the hematoxylin- eosin-stained
560 intestinal sections revealed reduced intestinal tissue damage with restoration in the villi
561 architecture in the 1- and 3-dpi OS-administered mice cohorts compared to the non-OS-treated
562 groups (Fig.S5, U).

563 Moreover, OS colonization could restrict the *in vivo Salmonella* and *Listeria* biofilm within the
564 spleens of the infected mice cohorts as opposed to the non-colonized mice cohorts both when
565 administered at 1-day and 3-day post-pathogen challenge. (Fig.S5, V-W). Furthermore, OS
566 alleviated *Salmonella*-induced intestinal inflammation with reduced IL-1β production in the
567 infected intestinal tissues both upon pre-colonization and post-colonization at 1-dpi (Fig. S6).

568 **Characterization of the inhibitory active molecule within *O. splanchnicus* culture**
569 **supernatant**

570 Our results suggested that not only live OS but also its spent culture supernatant could inhibit
571 *Salmonella* invasion and intracellular proliferation in intestinal human epithelial cells.
572 Moreover, the OS and its supernatant could inhibit STM biofilm formation *in vitro.* This
573 inhibitory effect disappeared upon co-culture with paraformaldehyde-fixed-OS indicating the
574 presumable role of certain inhibitory microbial products secreted by metabolically live OS. To
575 delineate the nature of the secreted molecule/s, we subjected the supernatant to various
576 conditions such as high temperature, divalent cationic chelator, EDTA, and protease (proteinase
577 K), and subsequently assessed the biofilm formation (Fig. 8, A-C). Our biofilm assay suggested
578 that the active molecule is resistant to EDTA treatment and is stable at higher temperatures
579 (Fig. 8, A-B). Nevertheless, the active molecules within the fraction were sensitive to the
580 proteinase K treatment, suggesting the possibility of being protein in nature (Fig. 8, C). SDS-
581 PAGE of the OS supernatant revealed the size of the differential proteins with respect to the
582 media control ranged below 65kDa. (Fig. 8, D). Concentration-dependent estimation of the

583 biofilm activity of the supernatant revealed that the active molecules retain their activity at a
584 minimal concentration of 0.4% v/v (Fig. 8, E). We further fractionated the supernatant using
585 an Amicon 3k MWCO and 10k MWCO ultra filter device (Fig. 8, F-G). We found that the
586 active molecule/s is/ are higher than 3kDa cut-off range eliminating the role of small molecules
587 and ions (Fig. 8, F-G). A summary of the conditions tested for active molecule characterisation
588 and their effective outcome has been summarized in Fig. 8, H. Subsequently, we subjected the
589 culture supernatant to gel filtration chromatography (Fig. S7, A). Out of all the fractions tested,
590 around 24 fractions showed a biofilm inhibitory role. These 24 fractions were further subjected
591 to a titration experiment to zero down upon the three fractions with the highest inhibitory
592 activity (A82,A83,A84) (S7, B-D). The gel filtration standard curve run suggested that the
593 active molecules fall in the size range of <60kDa and >3kDa (Fig. S7, A). These three fractions
594 along with the total concentrated supernatant (serving as positive control) and fractions with
595 no or least inhibitory activity (serving as negative control-A31,B12) were ultimately subjected
596 to Reverse Phase LC-MS mass spectrometry. Upon analysis of the proteomics dataset (Fig. S7,
597 E), we obtained 364 proteins showing enrichment in the positive fractions. Among the 364
598 proteins, 74 proteins exhibited known or predicted function as per UniProt and STRING
599 database and 11 proteins were linked to antibacterial, bacteriostatic, flagella, and biofilm
600 regulation based on data curation and literature survey (Table-S1). We selected bacteriocin
601 proteins exhibiting direct association with antibacterial activity for further analysis. These
602 proteins include bacteriocins (A0A412WSU3 and A0A412WSS0) which are antimicrobial
603 peptides that can kill or inhibit closely related or unrelated bacterial strains(50, 51). We purified
604 the bacteriocins via ammonium sulphate precipitation followed by gel filtration
605 chromatography to obtain a single fraction comprising of bacteriocins with close-range
606 molecular weight (6.6 kDa and 7.156kDa, respectively) (Fig. S8).

607 ***O. splanchnicus*-derived purified peptide, bacteriocin, limits both *Salmonella* and *Listeria***
608 **pathogenesis *in vitro***

609 Treatment of the Caco-2 cells with the purified bacteriocin inhibited STM, STY, and LM
610 invasion and fold proliferation without compromising host-cell viability (Fig. 9, A-D).
611 Additionally, the purified bacteriocin treatment inhibited STM biofilm formation in a dose-
612 dependent manner alongside reduced transcript level expression of *Salmonella* biofilm
613 regulatory genes (Fig. S9, A-D). Moreover, bacteriocin treatment (10µg/ml) attenuated
614 *Salmonella* virulence gene expression such as SPI-1 gene- *sipC*, SPI-2 gene-*pipB2,* and
615 flagellar gene *fliC* (Fig. S9, E-G). Subsequently, TEM imaging revealed a complete loss of
616 *Listeria* flagella upon treatment with the OS-derived bacteriocin in contrast to *Salmonella*
617 which retained few flagella even on bacteriocin treatment (Fig. 9, E-H). Furthermore, the
618 motility assay demonstrated a significant swimming defect of *Listeria* and *Salmonella* upon
619 treatment with either OS supernatant or bacteriocin to the untreated control (Fig. 9, I-J).
620 Overall, our study depicts the novel role of OS-derived bacteriocin in limiting *Salmonella* and
621 *Listeria* invasion and pathogenesis by regulating virulence effectors such as SPI-1, SPI-2
622 genes, biofilm regulatory genes, and flagella.

623 **DISCUSSION**

624 *Salmonella* gains access to the systemic sites by traversing the gut intestinal barrier via utilizing
625 several routes. Its primary site of entry is the distal ileum wherein it induces the SPI-1 Type
626 Three Secretion System (T3SS) effector proteins to facilitate its uptake. After its initial entry
627 into the enterocytes and M-cells overlying the Peyer's patches, *Salmonella* colonizes the
628 draining MLN and eventually disseminates to the liver and spleen via the circulating
629 lymphatics and the bloodstream (52). *Salmonella* uptake by M cells facilitates its stealthy entry
630 via avoidance of the mucus barrier. Additionally, the presence of flagella allows them to propel

631 through the viscous mucus and activate the immune responses(23). The onset of systemic
632 dissemination coincides with GVB disruption and loss of tight-junction protein expression (1).
633 Several reports have suggested the protective role of gut commensals in maintaining gut
634 epithelial health against food-borne pathogen insults. *E. coli* provide colonization resistance
635 against STM in the presence of a specific microbial consortium by limiting galactitol wherein
636 *Lachnospiraceae* consume the free sugar, conferring colonization resistance (53). Moreover,
637 *E. coli* contribute to colonization resistance by competing with *S.* Enteritidis for aerobic
638 respiration (54). Similarly, the commensal *Klebsiella michiganensis* retention or transmission
639 provided colonization resistance to Enterobacteriaceae by exhibiting nutrient competition (55).

640 Previous literature hinted toward the beneficial effects of OS in healthy human gut wherein
641 reduced OS abundance have been linked to obese gut signature (56). Furthermore, OS
642 colonization in mice have been shown to enhance $Foxp3^{+}$/$ROR\gamma t^{+}$ regulatory T cells,
643 interleukin IL-10 and short chain fatty acids production, limiting colitis in mouse models (57).
644 OS have been depicted to confer protection against colitis and colorectal cancer in mice by
645 inducing intestinal Th17 development(13).

646 In this study, we report the broad-spectrum protective role of the gut commensal of
647 bacteroidales order *O. splanchnicus* that limits *Salmonella* and *Listeria* invasion, pathogenesis,
648 and systemic dissemination by promoting colonization resistance and regulating virulence
649 effectors such as SPI-1, SPI-2, flagella, and biofilm regulatory genes. Additionally, not only
650 OS but its culture supernatant could exert its inhibitory effect on *Salmonella* invasion and
651 intracellular proliferation in intestinal human epithelial cells. Moreover, the OS and its
652 supernatant could inhibit STM biofilm formation by regulating flagella formation. This STM
653 biofilm inhibitory effect was however lost upon co-culture with paraformaldehyde-fixed-OS
654 indicating the presumable role of certain inhibitory microbial products secreted by
655 metabolically live OS. Further, our studies identified OS-produced bacteriocins responsible for

656 restricting intracellular replication of *Salmonella* and *Listeria* in intestinal epithelial cells by
657 regulating bacterial virulence arsenals such as biofilm regulatory genes, SPI-1, SPI-2 genes,
658 and flagellar machinery. However, the presence of flagella on *Salmonella* post bacteriocin
659 treatment suggests the potential involvement of additional secreted accessory molecules within
660 the OS supernatant and indicates that bacteriocins might exert their effects through multiple
661 mechanism of actions, warranting future research. Due to the proteinaceous nature of the
662 bacteriocin, oral administration experiments in mice were aborted. Previous studies have
663 suggested that bacteriocin expression by commensal bacteria can influence gut niche
664 competition and bacteriocin delivery can serve as an effective therapeutic strategy to eliminate
665 colonization of multi-drug resistant bacteria in the gastrointestinal tract without disrupting the
666 indigenous microbiota (58, 59). Several studies have highlighted the role of commensal-
667 produced bacteriocins. Bacteriocin-producing *Streptococcus salivarius* has been shown to
668 effectively target the CRC-causing pathogen *Fusobacterium nucleatum* in a model of the
669 human distal colon(60). *Lactobacillus plantarum* bacteriocin has been linked to intestinal and
670 systemic improvements in diet-induced obese mice and confers epithelial barrier integrity (61).
671 Further studies show that a class IIa bacteriocin, Pediocin PA-1, has an anti-bacterial effect
672 against *L. monocytogenes* (62).

673 This study provides evidence about inter-species regulation of gut colonization in maintaining
674 gut homeostasis and protecting against several invading foodborne pathogens. Moreover, the
675 long-term protective ability conferred by OS during pre-or post-infection colonization to mice
676 against broad-spectrum foodborne pathogens such as *Salmonella* and *Listeria* highlights its
677 therapeutic potential as a prebiotic for prophylaxis or post-infection treatment option, paving
678 the way for future therapeutic interventions to thwart food-borne infections.

679

ACKNOWLEDGEMENTS

We thank Nikhita Kirthivasan for her support during the commencement of the project.

We also thank our Divisional Mass Spectrometry facility, TEM facility, Departmental Confocal Facility, Divisional Flowcytometry Facility and Central Animal Facility at IISc.

FUNDING

This work was supported by the DAE SRC fellowship (DAE00195) and DBT-IISc partnership umbrella program for advanced research in biological sciences and Bioengineering to DC.

Infrastructure support from ICMR (Centre for Advanced Study in Molecular Medicine), DST (FIST), UGC (special assistance) and TATA fellowship is highly acknowledged.

DH sincerely acknowledges the CSIR- SPM fellowship for her financial support.

DM and RV are supported by MHRD-GATE and CSIR fellowships respectively.

The funders had no role in study design, data collection and analysis, decision to publish, or preparation of the manuscript.

AUTHOR CONTRIBUTION

Conceptualization: DH, DC

Methodology: DH, DM, RV, VD (Gel Filtration Chromatography), DD (Fast Performance Liquid Chromatography)

Investigation: DH, DM, RV, VD (Gel Filtration Chromatography), DD (Size exclusion chromatography for bacteriocin purification), RSR (Scoring of haemoxylin and eosin-stained samples)

Visualization: DH, DM, RV

Formal analysis: DH

Funding acquisition: DC

Project administration: DH, DC

Supervision: DC, UT (Proteomics), TH (Size Exclusion Chromatography), MG (Size Exclusion Chromatography)

Writing – original draft: DH

Writing – review & editing: DH, DM, RV, RSR, VD, DD, TH, MG, UT, DC

COMPETING INTERESTS Authors declare that they have no competing interests.

DATA AND MATERIALS AVAILABILITY

All data are available in the main text or the supplementary materials.

The article has been submitted to the preprint server (63).

REFERENCES

1. Spadoni I, Zagato E, Bertocchi A, Paolinelli R, Hot E, Di Sabatino A, et al. A gut-vascular barrier controls the systemic dissemination of bacteria. Science (New York, NY). 2015;350(6262):830-4.

2. Brescia P, Rescigno M. The gut vascular barrier: a new player in the gut–liver–brain axis. Trends in Molecular Medicine. 2021;27(9):844-55.

3. Ghosh S, Whitley CS, Haribabu B, Jala VR. Regulation of Intestinal Barrier Function by Microbial Metabolites. Cellular and Molecular Gastroenterology and Hepatology. 2021;11(5):1463-82.

720 4. Zhao Y, Chen F, Wu W, Sun M, Bilotta AJ, Yao S, et al. GPR43 mediates microbiota metabolite
721 SCFA regulation of antimicrobial peptide expression in intestinal epithelial cells via activation of
722 mTOR and STAT3. Mucosal immunology. 2018;11(3):752-62.
723 5. Schulthess J, Pandey S, Capitani M, Rue-Albrecht KC, Arnold I, Franchini F, et al. The short
724 chain fatty acid butyrate imprints an antimicrobial program in macrophages. Immunity.
725 2019;50(2):432-45. e7.
726 6. Hajra D, Kirthivasan N, Chakravortty D. Symbiotic Synergy from Sponges to Humans:
727 Microflora-Host Harmony Is Crucial for Ensuring Survival and Shielding against Invading Pathogens.
728 ACS infectious diseases. 2024;10(2):317-36.
729 7. Garcia-del Portillo F, Foster JW, Finlay BB. Role of acid tolerance response genes in
730 Salmonella typhimurium virulence. Infection and immunity. 1993;61(10):4489-92.
731 8. Haraga A, Ohlson MB, Miller SI. Salmonellae interplay with host cells. Nat Rev Microbiol.
732 2008;6(1):53-66.
733 9. Hensel M. Evolution of pathogenicity islands of Salmonella enterica. International journal of
734 medical microbiology : IJMM. 2004;294(2-3):95-102.
735 10. Hajra D. Understanding the mechanism of host deacetylase SIRT1 and SIRT3 in the
736 modulation of Salmonella pathogenesis. 2024.
737 11. Wang J, Lang T, Shen J, Dai J, Tian L, Wang X. Core Gut Bacteria Analysis of Healthy Mice.
738 Frontiers in microbiology. 2019;10:887.
739 12. Hiippala K, Barreto G, Burrello C, Diaz-Basabe A, Suutarinen M, Kainulainen V, et al. Novel
740 Odoribacter splanchnicus Strain and Its Outer Membrane Vesicles Exert Immunoregulatory Effects in
741 vitro. Frontiers in microbiology. 2020;11:575455.
742 13. Xing C, Wang M, Ajibade AA, Tan P, Fu C, Chen L, et al. Microbiota regulate innate immune
743 signaling and protective immunity against cancer. Cell host & microbe. 2021;29(6):959-74.e7.
744 14. Gogoi M, Chandra K, Sarikhani M, Ramani R, Sundaresan NR, Chakravortty D. Salmonella
745 escapes adaptive immune response via SIRT2 mediated modulation of innate immune response in
746 dendritic cells. PLoS pathogens. 2018;14(11):e1007437.
747 15. Schaefer JS, Montufar-Solis D, Nakra N, Vigneswaran N, Klein JR. Small intestine inflammation
748 in Roquin-mutant and Roquin-deficient mice. PloS one. 2013;8(2):e56436.
749 16. Erben U, Loddenkemper C, Doerfel K, Spieckermann S, Haller D, Heimesaat MM, et al. A
750 guide to histomorphological evaluation of intestinal inflammation in mouse models. International
751 journal of clinical and experimental pathology. 2014;7(8):4557-76.
752 17. Hajra D, Nair AV, Roy Chowdhury A, Mukherjee S, Chatterjee R, Chakravortty D. Salmonella
753 Typhimurium U32 peptidase, YdcP, promotes bacterial survival by conferring protection against in
754 vitro and in vivo oxidative stress. Microbial pathogenesis. 2022;173(Pt B):105862.
755 18. Roy Chowdhury A, Hajra D, Mukherjee D, Nair AV, Chakravortty D. Functional OmpA of
756 Salmonella Typhimurium provides protection from lysosomal degradation and inhibits autophagic
757 processes in macrophages. The Journal of infectious diseases. 2024.
758 19. Chandra K, Nair AV, Chatterjee R, Muralidhara P, Singh A, Kamanna S, et al. Absence of
759 proline-peptide transporter YjiY in Salmonella Typhimurium leads to secretion of factors which
760 inhibits intra-species biofilm formation. Microbiological research. 2023;273:127411.
761 20. Hajra D, Rajmani RS, Chaudhary AD, Gupta SK, Chakravortty D. Salmonella-induced SIRT1 and
762 SIRT3 are crucial for maintaining the metabolic switch in bacteria and host for successful
763 pathogenesis. eLife Sciences Publications, Ltd; 2024.
764 21. Balakrishnan A, Schnare M, Chakravortty D. Of men not mice: bactericidal/permeability-
765 increasing protein expressed in human macrophages acts as a phagocytic receptor and modulates
766 entry and replication of Gram-negative bacteria. Frontiers in immunology. 2016;7:455.
767 22. Chatterjee R, Chowdhury AR, Nair AV, Hajra D, Kar A, Datey A, et al. Salmonella Typhimurium
768 PgtE is an essential arsenal to defend against the host resident antimicrobial peptides.
769 Microbiological research. 2023;271:127351.

23. McGuckin MA, Lindén SK, Sutton P, Florin TH. Mucin dynamics and enteric pathogens. Nature reviews Microbiology. 2011;9(4):265-78.
24. Estimates of the global, regional, and national morbidity, mortality, and aetiologies of lower respiratory infections in 195 countries, 1990-2016: a systematic analysis for the Global Burden of Disease Study 2016. The Lancet Infectious diseases. 2018;18(11):1191-210.
25. Davis CW, Dickey BF. Regulated airway goblet cell mucin secretion. Annual review of physiology. 2008;70:487-512.
26. Enss ML, Cornberg M, Wagner S, Gebert A, Henrichs M, Eisenblätter R, et al. Proinflammatory cytokines trigger MUC gene expression and mucin release in the intestinal cancer cell line LS180. Inflammation research : official journal of the European Histamine Research Society [et al]. 2000;49(4):162-9.
27. Hill RR, Cowley HM, Andremont A. Influence of colonizing micro-flora on the mucin histochemistry of the neonatal mouse colon. The Histochemical journal. 1990;22(2):102-5.
28. Cash HL, Whitham CV, Behrendt CL, Hooper LV. Symbiotic bacteria direct expression of an intestinal bactericidal lectin. Science (New York, NY). 2006;313(5790):1126-30.
29. Goubier A, Dubois B, Gheit H, Joubert G, Villard-Truc F, Asselin-Paturel C, et al. Plasmacytoid Dendritic Cells Mediate Oral Tolerance. Immunity. 2008;29(3):464-75.
30. Müller-Redetzky HC, Suttorp N, Witzenrath M. Dynamics of pulmonary endothelial barrier function in acute inflammation: mechanisms and therapeutic perspectives. Cell and tissue research. 2014;355(3):657-73.
31. Daneman R, Rescigno M. The gut immune barrier and the blood-brain barrier: are they so different? Immunity. 2009;31(5):722-35.
32. Yuan SY, Rigor RR. Integrated Systems Physiology: From Molecule to Function to Disease. Regulation of Endothelial Barrier Function. San Rafael (CA): Morgan & Claypool Life Sciences

Copyright © 2011 by Morgan & Claypool Life Sciences.; 2010.
33. Wang Y, Rattner A, Zhou Y, Williams J, Smallwood PM, Nathans J. Norrin/Frizzled4 signaling in retinal vascular development and blood brain barrier plasticity. Cell. 2012;151(6):1332-44.
34. Liebner S, Corada M, Bangsow T, Babbage J, Taddei A, Czupalla CJ, et al. Wnt/beta-catenin signaling controls development of the blood-brain barrier. The Journal of cell biology. 2008;183(3):409-17.
35. Simmons DL, Satterthwaite AB, Tenen DG, Seed B. Molecular cloning of a cDNA encoding CD34, a sialomucin of human hematopoietic stem cells. Journal of immunology (Baltimore, Md : 1950). 1992;148(1):267-71.
36. Pusztaszeri MP, Seelentag W, Bosman FT. Immunohistochemical expression of endothelial markers CD31, CD34, von Willebrand factor, and Fli-1 in normal human tissues. The journal of histochemistry and cytochemistry : official journal of the Histochemistry Society. 2006;54(4):385-95.
37. Oehlers SH, Cronan MR, Scott NR, Thomas MI, Okuda KS, Walton EM, et al. Interception of host angiogenic signalling limits mycobacterial growth. Nature. 2015;517(7536):612-5.
38. Iwase T, Uehara Y, Shinji H, Tajima A, Seo H, Takada K, et al. Staphylococcus epidermidis Esp inhibits Staphylococcus aureus biofilm formation and nasal colonization. Nature. 2010;465(7296):346-9.
39. Lee J, Jayaraman A, Wood TK. Indole is an inter-species biofilm signal mediated by SdiA. BMC microbiology. 2007;7(1):1-15.
40. Fux CA, Costerton JW, Stewart PS, Stoodley P. Survival strategies of infectious biofilms. Trends in microbiology. 2005;13(1):34-40.
41. Costerton JW, Stewart PS, Greenberg EP. Bacterial biofilms: a common cause of persistent infections. Science (New York, NY). 1999;284(5418):1318-22.
42. Hajra D, Nair AV, Chakravortty D. An elegant nano-injection machinery for sabotaging the host: Role of Type III secretion system in virulence of different human and animal pathogenic bacteria. Physics of life reviews. 2021;38:25-54.

43. Jennings ME, Quick LN, Ubol N, Shrom S, Dollahon N, Wilson JW. Characterization of Salmonella type III secretion hyper-activity which results in biofilm-like cell aggregation. PloS one. 2012;7(3):e33080.
44. Ducarmon QR, Zwittink RD, Hornung BVH, van Schaik W, Young VB, Kuijper EJ. Gut Microbiota and Colonization Resistance against Bacterial Enteric Infection. Microbiology and molecular biology reviews : MMBR. 2019;83(3).
45. Caballero-Flores G, Pickard JM, Núñez G. Microbiota-mediated colonization resistance: mechanisms and regulation. Nature Reviews Microbiology. 2023;21(6):347-60.
46. Qin J, Li R, Raes J, Arumugam M, Burgdorf KS, Manichanh C, et al. A human gut microbial gene catalogue established by metagenomic sequencing. Nature. 2010;464(7285):59-65.
47. Gewolb IH, Schwalbe RS, Taciak VL, Harrison TS, Panigrahi P. Stool microflora in extremely low birthweight infants. Archives of disease in childhood Fetal and neonatal edition. 1999;80(3):F167-73.
48. Chakraborty P, Bajeli S, Kaushal D, Radotra BD, Kumar A. Biofilm formation in the lung contributes to virulence and drug tolerance of Mycobacterium tuberculosis. Nature communications. 2021;12(1):1606.
49. Yamamoto K, Tsujimura Y, Ato M. Catheter-associated Mycobacterium intracellulare biofilm infection in C3HeB/FeJ mice. Sci Rep. 2023;13(1):17148.
50. Heilbronner S, Krismer B, Brötz-Oesterhelt H, Peschel A. The microbiome-shaping roles of bacteriocins. Nature reviews Microbiology. 2021;19(11):726-39.
51. Cotter PD, Ross RP, Hill C. Bacteriocins - a viable alternative to antibiotics? Nature reviews Microbiology. 2013;11(2):95-105.
52. Watson KG, Holden DW. Dynamics of growth and dissemination of Salmonella in vivo. Cellular microbiology. 2010;12(10):1389-97.
53. Eberl C, Weiss AS, Jochum LM, Durai Raj AC, Ring D, Hussain S, et al. E. coli enhance colonization resistance against Salmonella Typhimurium by competing for galactitol, a context-dependent limiting carbon source. Cell host & microbe. 2021;29(11):1680-92.e7.
54. Litvak Y, Mon KKZ, Nguyen H, Chanthavixay G, Liou M, Velazquez EM, et al. Commensal Enterobacteriaceae Protect against Salmonella Colonization through Oxygen Competition. Cell host & microbe. 2019;25(1):128-39.e5.
55. Oliveira RA, Ng KM, Correia MB, Cabral V, Shi H, Sonnenburg JL, et al. Klebsiella michiganensis transmission enhances resistance to Enterobacteriaceae gut invasion by nutrition competition. Nat Microbiol. 2020;5(4):630-41.
56. Chanda D, De D. Meta-analysis reveals obesity associated gut microbial alteration patterns and reproducible contributors of functional shift. Gut Microbes. 2024;16(1):2304900.
57. Lima SF, Gogokhia L, Viladomiu M, Chou L, Putzel G, Jin WB, et al. Transferable Immunoglobulin A-Coated Odoribacter splanchnicus in Responders to Fecal Microbiota Transplantation for Ulcerative Colitis Limits Colonic Inflammation. Gastroenterology. 2022;162(1):166-78.
58. Kommineni S, Bretl DJ, Lam V, Chakraborty R, Hayward M, Simpson P, et al. Bacteriocin production augments niche competition by enterococci in the mammalian gastrointestinal tract. Nature. 2015;526(7575):719-22.
59. Kommineni S, Kristich CJ, Salzman NH. Harnessing bacteriocin biology as targeted therapy in the GI tract. Gut Microbes. 2016;7(6):512-7.
60. Lawrence GW, McCarthy N, Walsh CJ, Kunyoshi TM, Lawton EM, O'Connor PM, et al. Effect of a bacteriocin-producing Streptococcus salivarius on the pathogen Fusobacterium nucleatum in a model of the human distal colon. Gut Microbes. 2022;14(1):2100203.
61. Heeney DD, Zhai Z, Bendiks Z, Barouei J, Martinic A, Slupsky C, et al. Lactobacillus plantarum bacteriocin is associated with intestinal and systemic improvements in diet-induced obese mice and maintains epithelial barrier integrity in vitro. Gut Microbes. 2019;10(3):382-97.

62. Kuniyoshi TM, O'Connor PM, Lawton E, Thapa D, Mesa-Pereira B, Abulu S, et al. An oxidation resistant pediocin PA-1 derivative and penocin A display effective anti-Listeria activity in a model human gut environment. Gut Microbes. 2022;14(1):2004071.

63. Hajra D, Mukherjee D, Vij R, Rajmani RS, Dadireddy V, Das D, et al. Odoribacter splanchnicus mitigates Salmonella-induced gut inflammation and its associated pathogenesis via its secreted bacteriocin. bioRxiv. 2024:2024.08.23.609322.

MAIN FIGURES AND LEGENDS

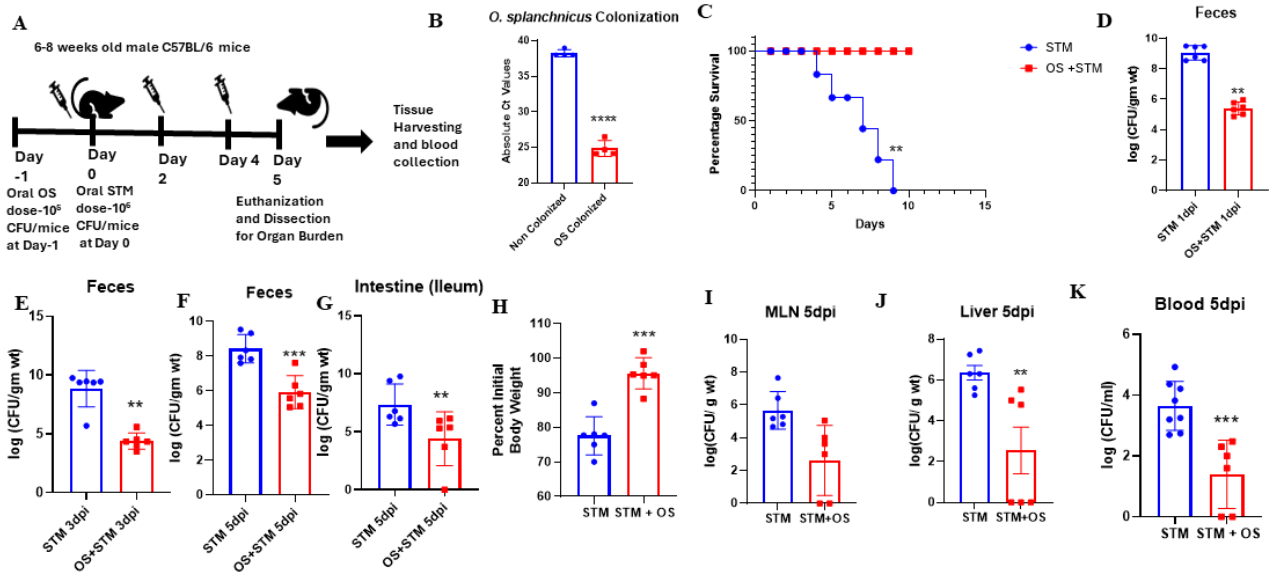

Figure 1. *Odoribacter splanchnicus* colonization protects mice from *Salmonella* colonization and dissemination

A-Schematic representation showing animal experimental strategy of infection.

B-OS colonization validation via qPCR quantification of *O. splanchnicus* 16S rRNA from fecal samples of mice at 6th day post-OS colonization .

C-Survival percentage of non-colonized-STM-infected mice versus OS-colonized-STM-infected mice cohorts. Data is representative of N=3, n=5 where N denotes number of biological replicates and n denotes the number of mice per group. Mantel Cox or the log-rank test was used to determine the p values.

889 **D-G**- STM organ loads in feces at 1st day post-infection (D), 3rd day post-infection (E), 5th
890 post-infection (F) and in ileal tissues (contents and wall) at 5th day post-infection (G) in OS
891 colonized and non-colonized mice cohorts. Data is representative of N=2, n=6 where N
892 denotes number of biological replicates and n denotes the number of mice per group. Mann
893 Whitney Test was performed to obtain p-values.

894 **H**-Percent of initial weight (at Day 0) exhibited by OS colonized and non-colonized mice upon
895 STM infection at 5th day post-infection. Data is representative of N=3,n=6 where N denotes
896 number of biological replicates and n denotes the number of mice per group.

897 **I-K**- STM organ loads in MLN (I), liver (J) and blood (K) at 5th post-infection in OS colonized
898 and non-colonized mice cohorts. Data is representative of N=3, n=6 where N denotes number
899 of biological replicates and n denotes the number of mice per group. Mann Whitney Test was
900 performed to obtain p-values.

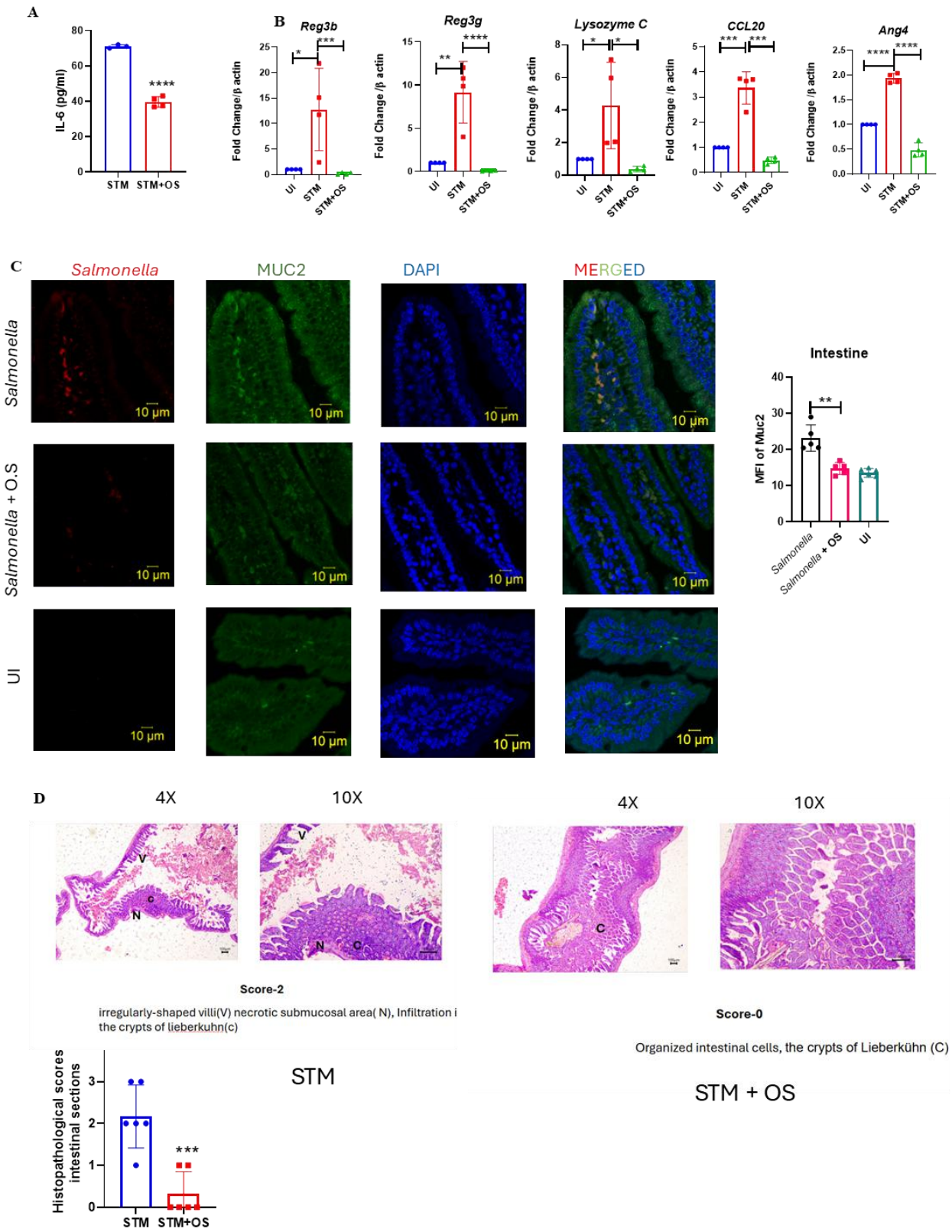
A
IL-6 (pg/ml)
STM
STM+OS
B
Reg3b
Reg3g
Lysozyme C
CCL20
Ang4
Fold Change/β actin
UI
STM
STM+OS
C
Salmonella
MUC2
DAPI
MERGED
Salmonella
Salmonella + O.S
UI
10 µm
Intestine
MFI of Muc2
Salmonella
Salmonella + OS
UI
D
4X
10X
V
C
N
Score-2
irregularly-shaped villi(V) necrotic submucosal area(N), Infiltration i
the crypts of lieberkuhn(c)
Score-0
Organized intestinal cells, the crypts of Lieberkühn (C)
STM
STM + OS
Histopathological scores
intestinal sections
STM
STM+OS

901

902

903

904

905 **Figure 2. *O. splanchnicus* reduces *Salmonella*-induced inflammation and intestinal**
906 **damage**

907 **A**-Estimation of serum IL-6 production via ELISA upon STM infection in OS non-colonized
908 and colonized mice cohorts at 5th day post-*Salmonella* infection. Unpaired t-test is performed
909 to obtain the p-values. Data is representative of N=3, n=3.

910 **B**-Quantitative gene expression data of several antimicrobial peptides (AMPs) precursor genes
911 in uninfected and STM-infected mice intestinal tissues harvested at 5th dpi from OS colonized
912 or non-colonized cohorts. Unpaired t-test is performed to obtain the p-values. Data is
913 representative of N=3, n=4.

914 **C**- Immunostaining representing Muc2 protein expression in intestinal ileal tissues of OS non-
915 colonized and colonized mice cohorts upon STM infection. Unpaired t-test is performed to
916 obtain the p-values. Data is representative of N=3, n=5.

917 **D**-Haematoxylin-eosin-stained intestinal sections harvested from STM-infected OS non-
918 colonized or colonized mice cohorts at 5th dpi. 0-represents normal pathology, 1- represents-
919 mild pathology, 2-3-represents severe pathology.

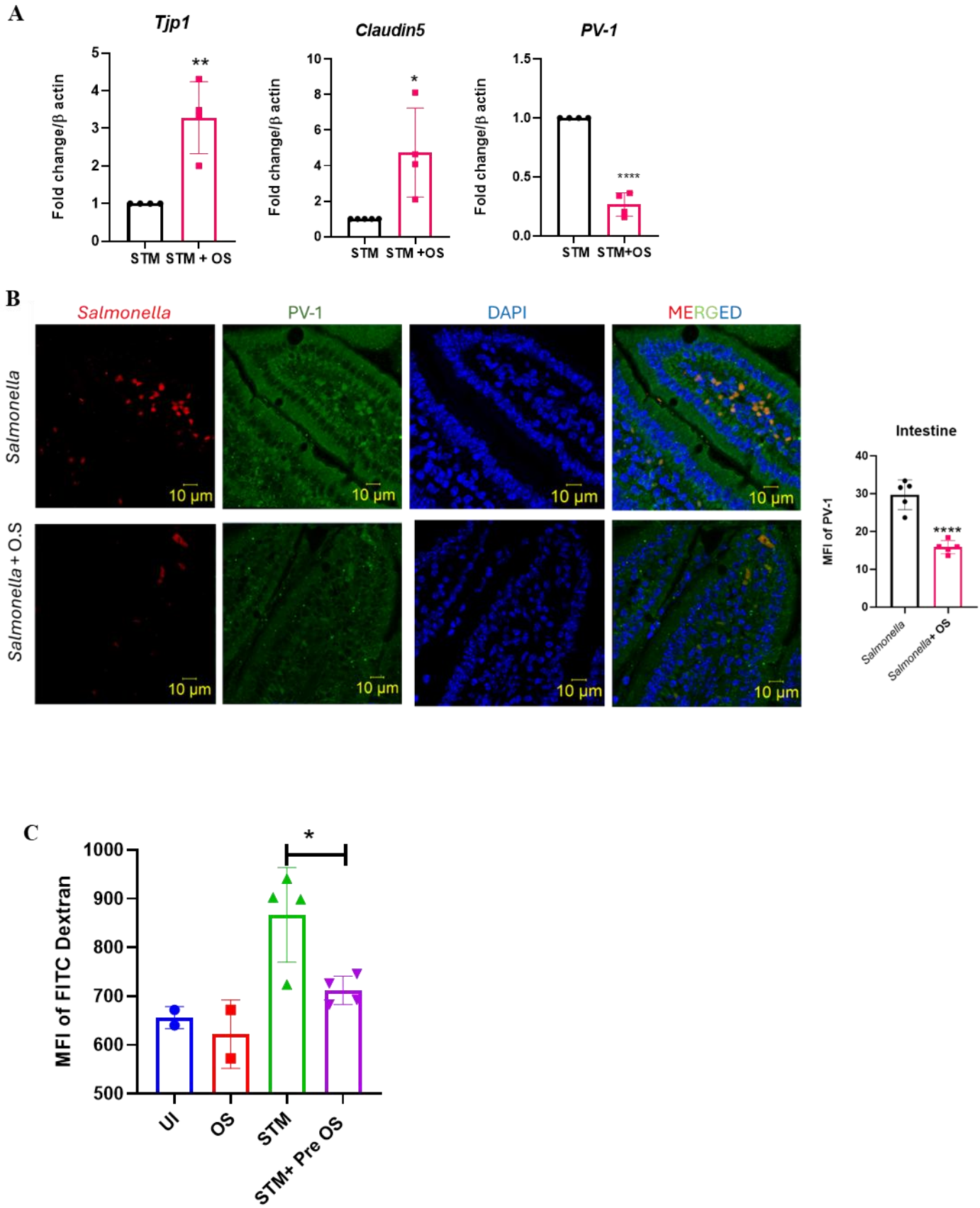
A
Tjp1
Claudin5
PV-1
Fold change/β actin
STM
STM + OS
STM +OS
STM+OS
B
Salmonella
PV-1
DAPI
MERGED
Salmonella
Salmonella + O.S
10 µm
Intestine
MFI of PV-1
Salmonella
Salmonella+ OS
C
MFI of FITC Dextran
UI
OS
STM
STM+ Pre OS

920

921

922 **Fig 3. *Odoribacter splanchnicus* gut colonization prevents *Salmonella*-induced GVB**
923 **damage and promotes tight junction gene expression.**

924 **A**-Quantitative gene expression studies of tight junction protein complexes (*Tjp1*, *Claudin5*)
925 and PV-1 gene (marker of GVB damage) in STM-infected mice intestinal (ileal) tissue in
926 presence or absence of OS gut colonization at 5th day post-infection. Un-paired t-test was used
927 to obtain the p-values. Data is representative of N=3, n=4.

928 **B**- Immunofluorescence image demonstrating PV-1 protein expression in intestinal (ileal)
929 tissues of OS non-colonized and colonized mice cohorts upon STM infection. Data is
930 representative of N=2, n=5 (tissue samples). Un-paired t-test was used to obtain the p-values.

931 **C**- Estimation of FITC fluorescence in mice plasma via gut permeability assay in infected mice
932 cohorts upon oral administration of FITC Dextran (25mg/kg) 4h before euthanization at 5th day
933 post *Salmonella* infection. Un-paired t-test was used to obtain the p-values. Data is
934 representative of N=2, n>2.

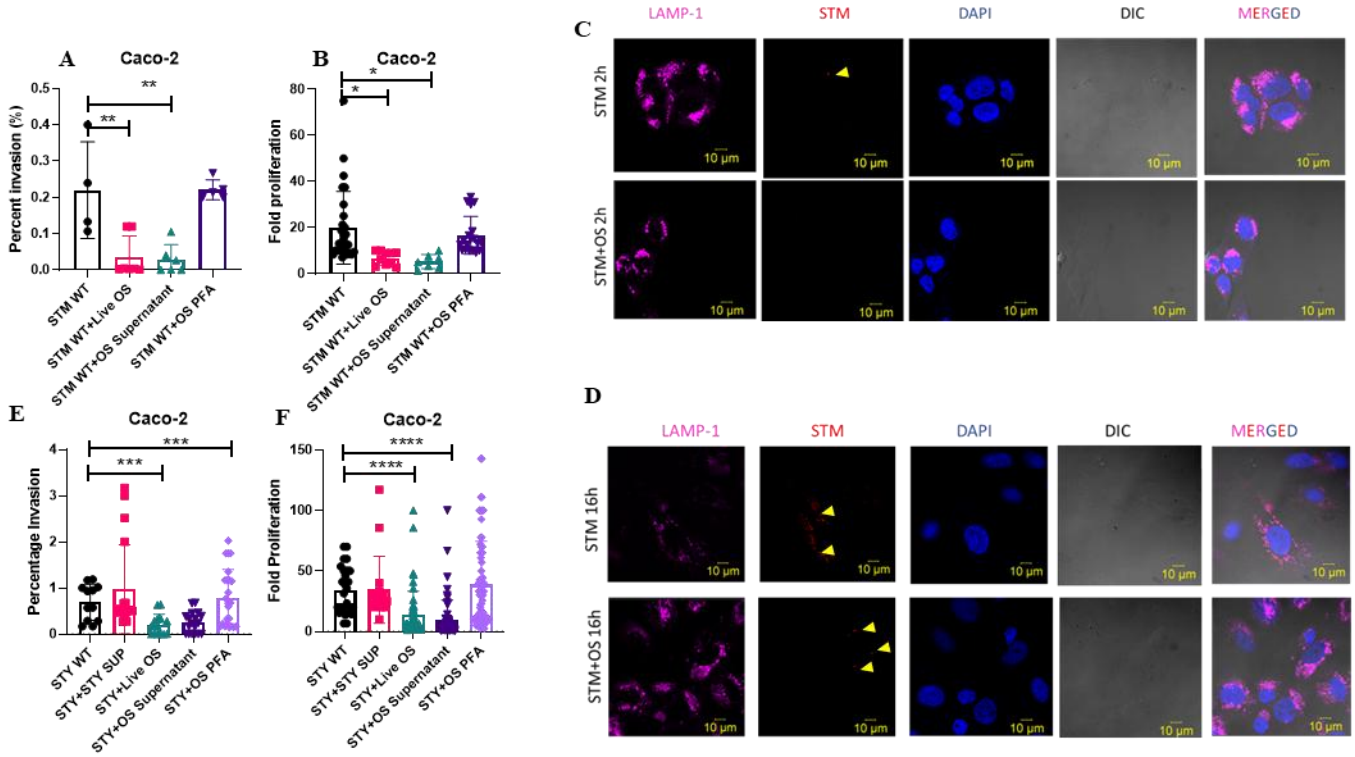

935

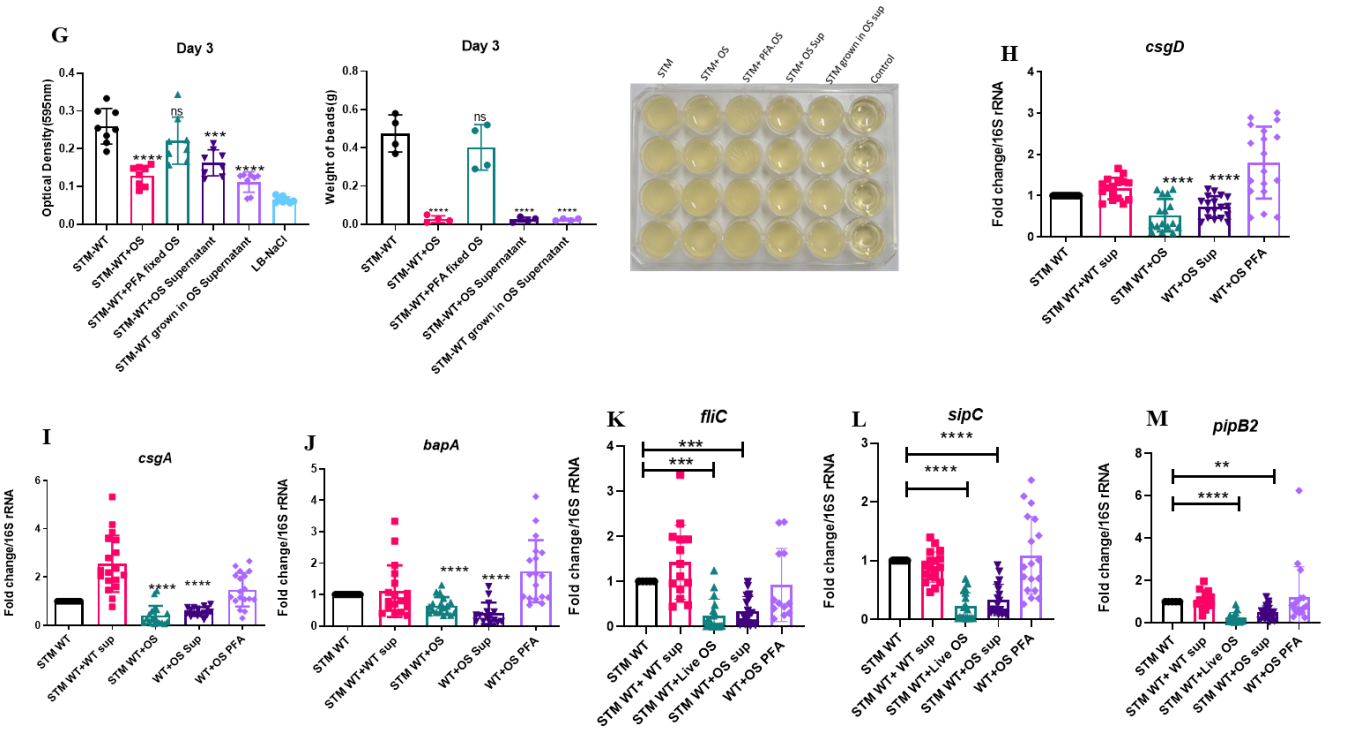

936

937

938

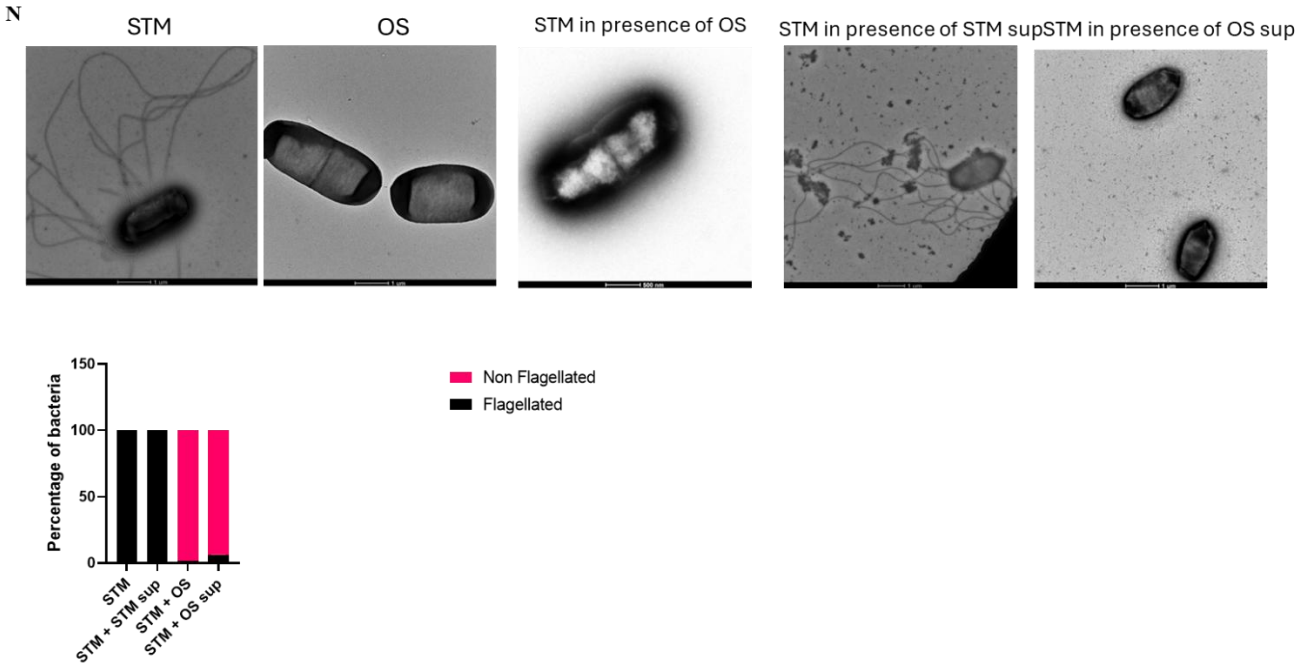

Fig 4. *O. splanchnicus* exhibits its inhibitory effect on *Salmonella* biofilm formation and inhibits invasion and intracellular replication in human intestinal cells

A-Percent invasion of STM in human Caco-2 human intestinal cells in presence or absence of live OS, OS culture supernatant, PFA-fixed-OS. Data is representative of N=3, n=4. One-way ANOVA was used to determine the p-values.

B-Intracellular proliferation of STM Caco-2 cells in presence or absence of live OS, OS culture supernatant, PFA-fixed-OS. Data is representative of N=3, n=4. One-way ANOVA was used to determine the p-values.

C- Representative immunofluorescence images depicting STM invasion into Caco-2 cells in the presence or absence of OS at 2hr post-infection. Data is representative of N=3, n=100.

952 **D**- Representative immunofluorescence images depicting STM invasion into Caco-2 cells in
953 presence or absence of OS at 2hr post-infection. Data is representative of N=3, n=100.

954 **E**-Percent invasion of STY in Caco-2 human cells in presence or absence of OS, OS culture
955 supernatant, PFA-fixed OS. Data is representative of N=3, n≥9. One-way ANOVA was used to
956 determine the p-values.

957 **F**-Intracellular proliferation of STY in Caco-2 cells in presence or absence of live OS, OS
958 culture supernatant, PFA-fixed-OS. Data is representative of N=3, n≥9. One-way ANOVA was
959 used to determine the p-values.

960 **G**- Biofilm assay showing the biofilm formation ability of STM-WT or STM-WT grown in OS
961 supernatant after 72h of inoculation in presence or absence of live OS, OS culture supernatant,
962 PFA-fixed-OS. Data is representative of N=4, n=4.One-way ANOVA was used to determine
963 the p-values. Image of the STM biofilm-formed plate in the above stated conditions has been
964 shown.

965 **H-M-** RT-qPCR mediated gene expression of STM biofilm regulatory genes (*csgD*) (H), *csgA*
966 (I), *bapA* (J), along with flagellar gene (*fliC*) (K), SPI-1 (*sipC*) (L) and SPI-2 (*pipB2*) (M)
967 genes in presence or absence of live OS or its spent media or PFA-fixed-OS. Data is
968 representative of N=4, n=4. One-way ANOVA was used to determine the p-values.

969 **N-** Transmission Electron Microscopic (TEM) images of STM in presence or absence of
970 *Salmonella* WT supernatant, OS and its supernatant to assess the possession of flagella. The
971 quantification plot exhibits the percentage of bacterial flagellated or non-flagellated cells
972 (number of cells quantified n≥ 100)

973

974

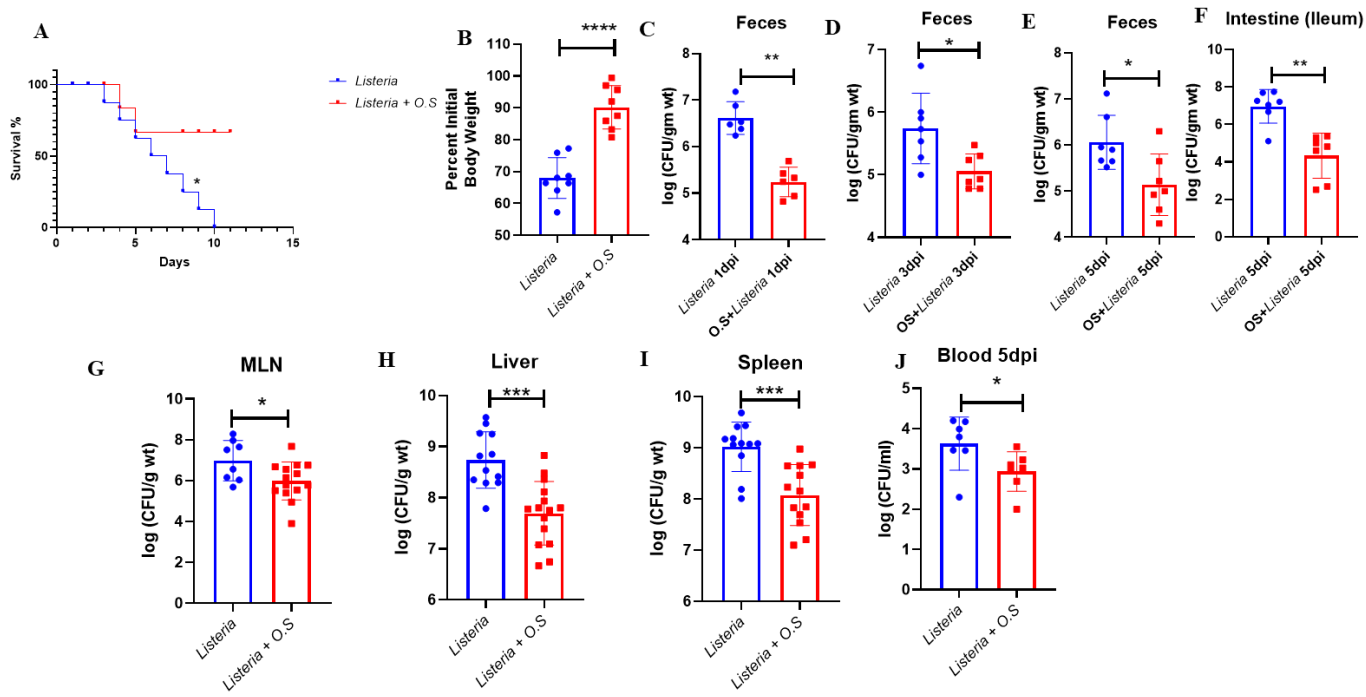

Fig 5. *Odoribacter splanchnicus* exerts its protective role against *Listeria monocytogenes* in mice

A- Survival percentage of non-colonized LM-infected mice versus OS-colonized *Listeria*-infected mice cohorts. Data is represantative of N=2, n=8, where N denotes number of biological replicates and n denotes the number of mice per group. Mantel Cox or the log-rank test was used to determine the p values.

B-Percent of initial weight (at Day 0) exhibited by OS colonized and non-colonized mice upon LM infection at 5th dpi. Data is representative of N=2,n=8, where N denotes number of biological replicates and n denotes the number of mice per group. Mann Whitney Test was performed to obtain p-values.

C-F- LM organ loads in feces at 1st day post-infection (C), 3rd day post-infection (D), 5th post-infection (E) and in ileal tissues (contents and wall) at 5th day post-infection (F) in OS pre-colonized and non-colonized mice cohorts. Data is representative of N=2, n=7 where N

989 denotes number of biological replicates and n denotes the number of mice per group. Mann
990 Whitney Test was performed to obtain p-values.

991 **G-J**- LM organ loads in Mesenteric lymph Node (MLN) (G), liver (H), spleen (I) and blood
992 (J) at 5th dp. in OS colonized and non-colonized mice cohorts Data is representative of N=2,
993 n=8, where N denotes number of biological replicates and n denotes the number of mice per
994 group. Mann Whitney Test was performed to obtain p-values.

995

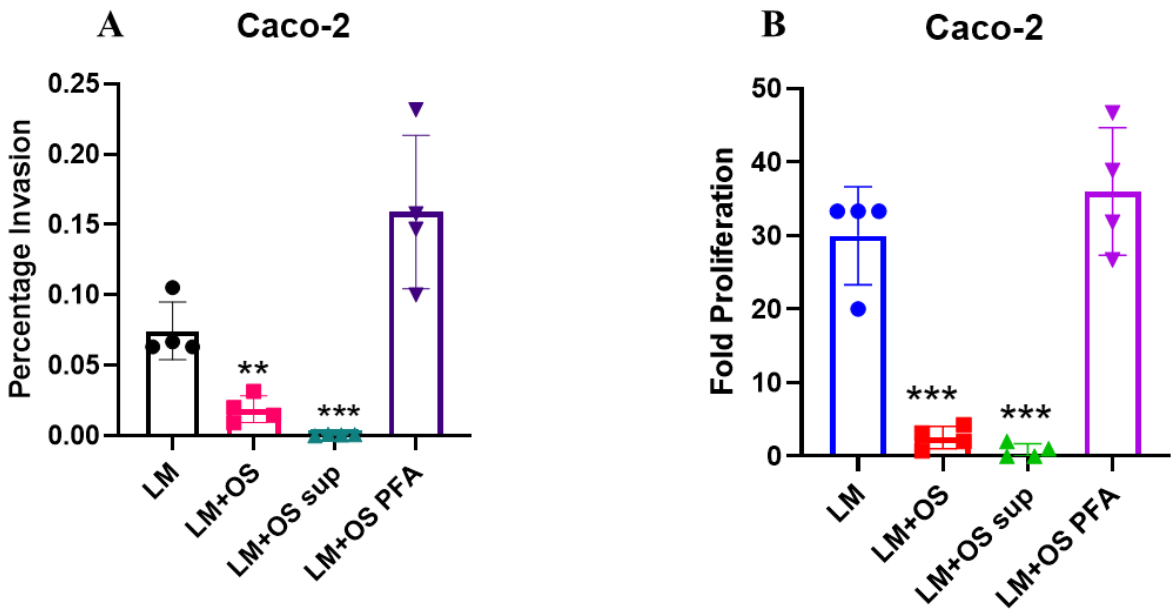

996

997 **Fig. 6 *Odoribacter splanchnicus* and its culture supernatant restricts *Listeria***
998 ***monocytogenes* pathogenesis in human intestinal cells**

999 **A**- Percent invasion of LM in Caco-2 cells in presence or absence of live OS, OS sup, PFA-
1000 fixed-OS. Data is representative of N=3, n=4. One-way ANOVA and Multiple Comparison test
1001 is used to obtain the p-values.

1002 **B**-Intracellular fold proliferation of LM in Caco-2 cells in the presence or absence of live OS,

1003 OS sup, PFA-fixed-OS. Data is representative of N=3, n=4. One-way ANOVA and Multiple

1004 Comparison test is used to obtain the p-values.

1005

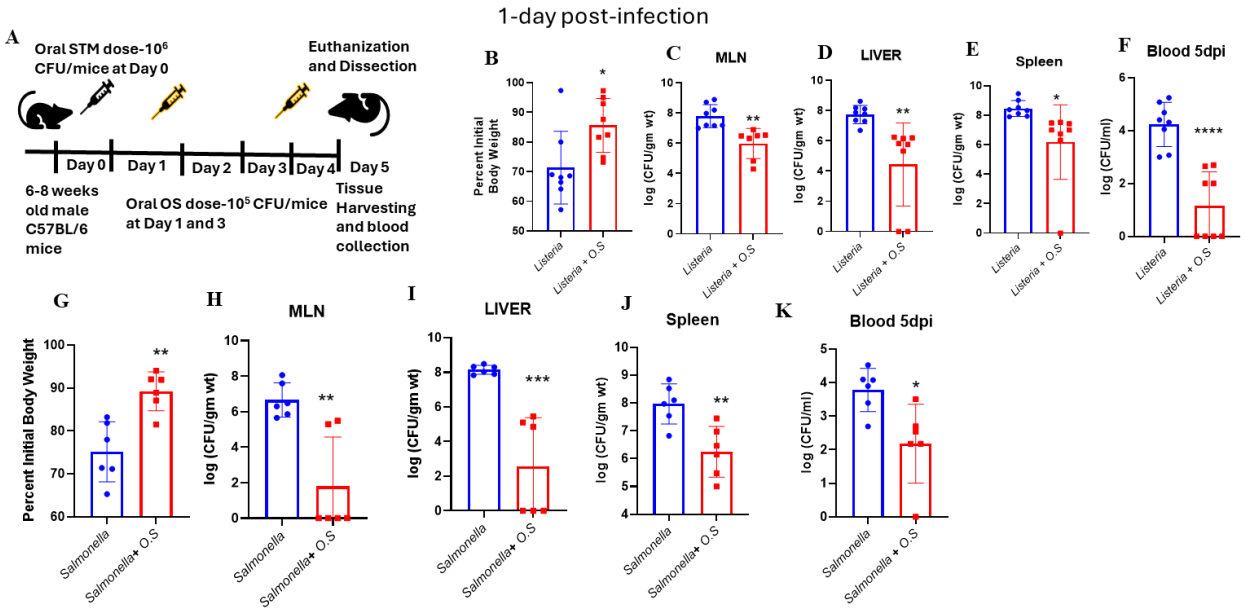

1006

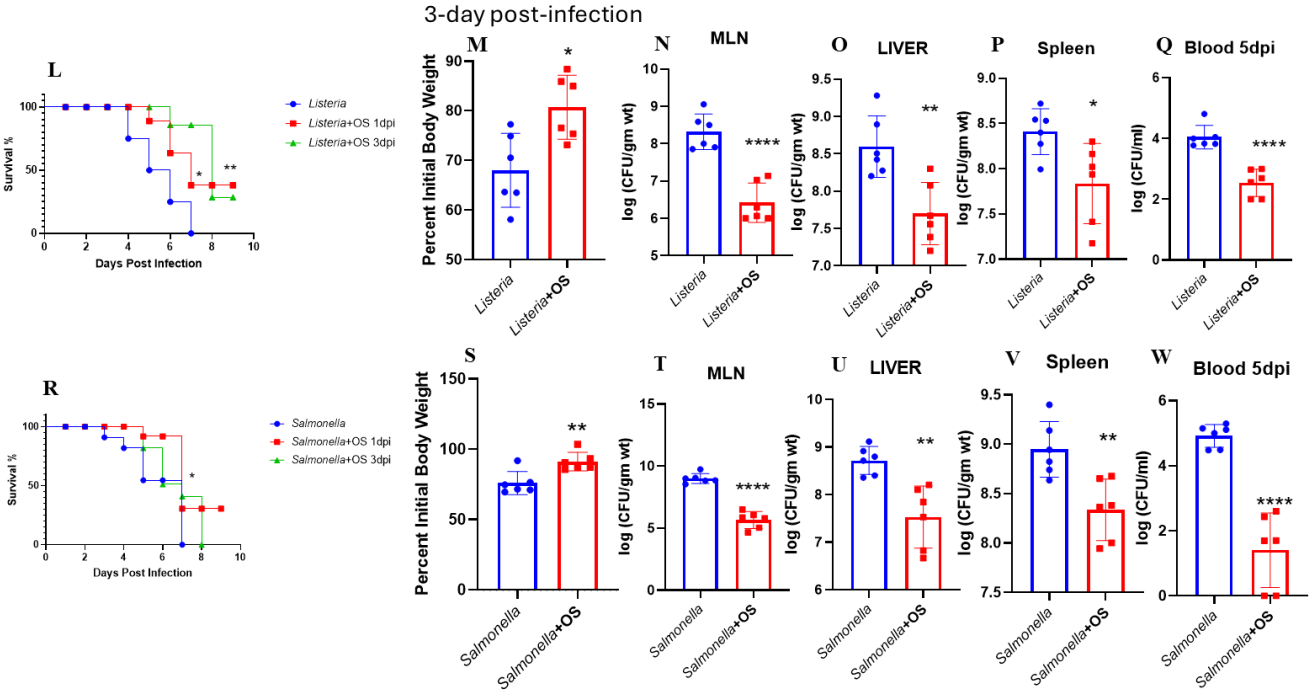

1007

1008

1009

1010 **Fig. 7 *O. splanchnicus* even confers protection against foodborne pathogens when**
1011 **administered post-pathogenic challenge**

1012 **A-** Schematic representation showing the animal experimental strategy of infection.

1013 **B-** Percent of initial weight (at Day 0) exhibited by OS colonized (1-dpi) and non-colonized
1014 mice upon LM infection at 5th dpi. Data is representative of N=2,n=8, where N denotes number
1015 of biological replicates and n denotes the number of mice per group. Mann Whitney Test was
1016 performed to obtain p-values.

1017 **C-F**- LM organ loads in MLN (C), liver (D), spleen (E) and blood (F) at 5th dpi upon OS
1018 administration at 1-dpi. Data is representative of N=2, n=8, where N denotes number of
1019 biological replicates and n denotes the number of mice per group. Mann Whitney Test was
1020 performed to obtain p-values.

1021 **G**- Percent of initial weight (at Day 0) exhibited by OS colonized (1-dpi) and non-colonized
1022 mice upon STM infection at 5th dpi. Data is representative of N=2,n=8, where N denotes
1023 number of biological replicates and n denotes the number of mice per group. Mann Whitney
1024 Test was performed to obtain p-values.

1025 **H-K**- STM organ loads in MLN (H), liver (I), spleen (J) and blood (K) at 5th-dpi upon OS
1026 administration at 1-dpi. Data is representative of N=2, n=8, where N denotes number of
1027 biological replicates and n denotes the number of mice per group. Mann-Whitney Test was
1028 performed to obtain p-values.

1029 **L**- Survival percentage of non-colonized LM-infected mice versus OS-colonized (1 dpi or 3
1030 dpi) *Listeria*-infected mice cohorts. Data is representative of N=2, n=8, where N denotes

1031 number of biological replicates and n denotes the number of mice per group. Mantel Cox or
1032 the log-rank test was used to determine the p values.

1033 **M**- Percent weight loss exhibited by OS colonized (3-dpi) and non-colonized mice upon LM
1034 infection at 5th-day post-infection. Data is representative of N=2,n=8, where N denotes number
1035 of biological replicates and n denotes the number of mice per group.Mann-Whitney Test was
1036 performed to obtain p-values.

1037

1038 **N-Q**- LM organ loads in MLN (N), liver (O), spleen (P) and blood (Q) at 5th-dpi upon OS
1039 administration at 3-dpi. Data is representative of N=2, n=8, , where N denotes number of
1040 biological replicates and n denotes the number of mice per group. Mann-Whitney Test was
1041 performed to obtain p-values.

1042 **R**- Survival percentage of non-colonized *Salmonella*-infected mice versus OS-colonized (1 dpi
1043 or 3 dpi) *Listeria*-infected mice cohorts. Data is represantative of N=2, n=8, where N denotes
1044 number of biological replicates and n denotes the number of mice per group. Mantel Cox or
1045 the log-rank test was used to determine the p values.

1046 **S**- Percent weight loss exhibited by OS-colonized (3-dpi) and non-colonized mice upon STM
1047 infection at 5th-day post-infection. Data is representative of N=2,n=8, where N denotes number
1048 of biological replicates and n denotes the number of mice per group. Mann-Whitney Test was
1049 performed to obtain p-values.

1050 **T-W**-STM organ loads in MLN (T), liver (U), spleen (V), and blood (W) at 5th-dpi upon OS
1051 administration at 3-dpi. Data is representative of N=2, n=8, where N denotes number of
1052 biological replicates and n denotes the number of mice per group. Mann-Whitney Test was
1053 performed to obtain p-values.

1054

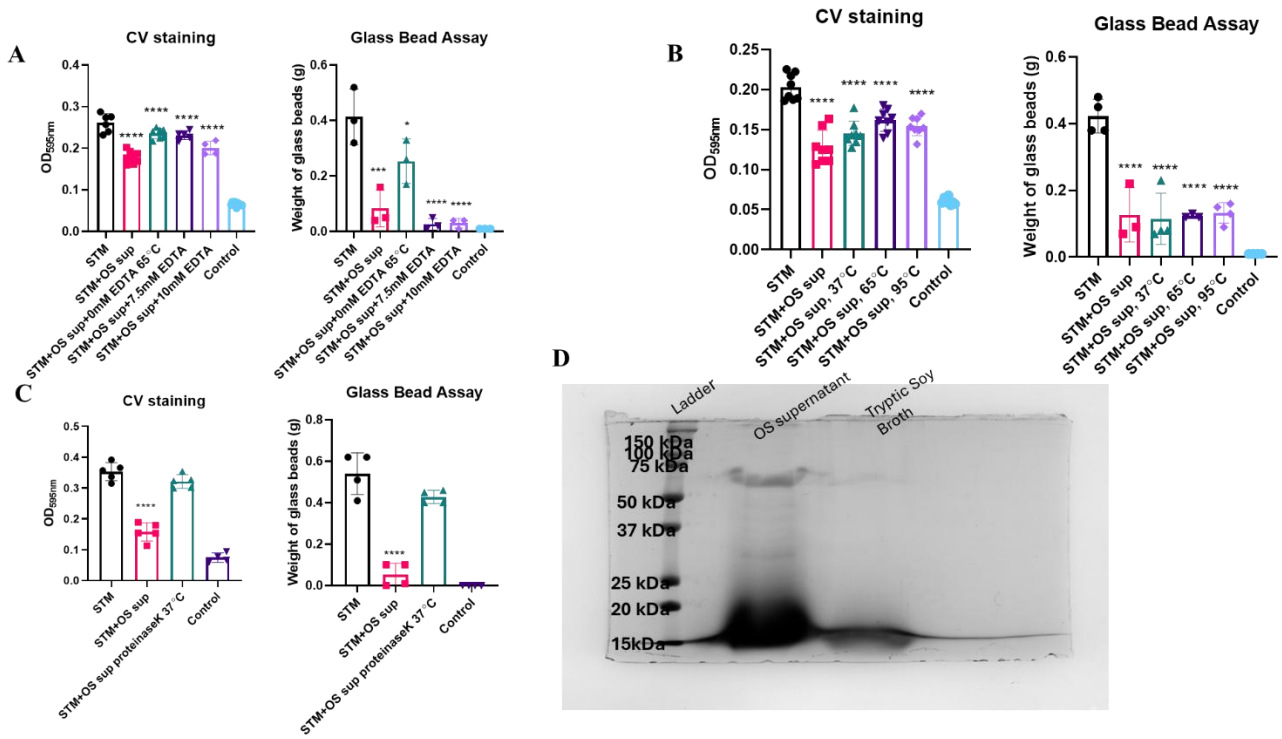

1055

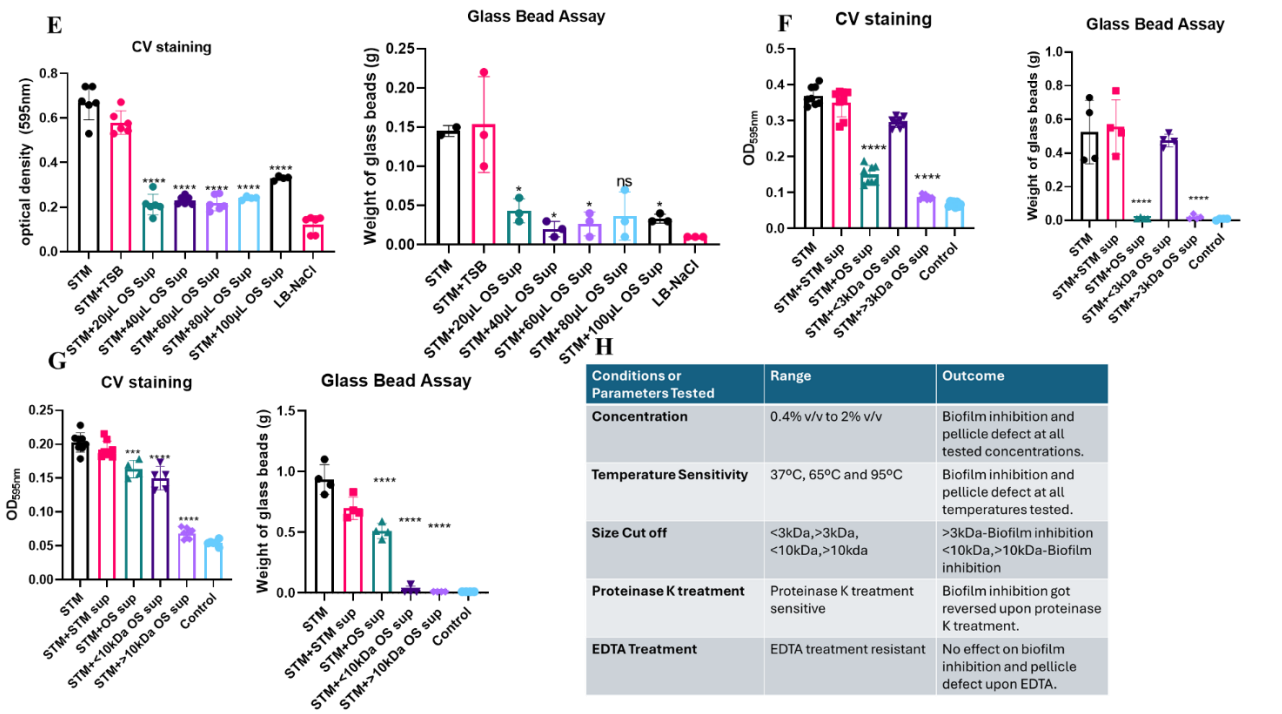

Conditions or Parameters Tested	Range	Outcome
Concentration	0.4% v/v to 2% v/v	Biofilm inhibition and pellicle defect at all tested concentrations.
Temperature Sensitivity	37ºC, 65ºC and 95ºC	Biofilm inhibition and pellicle defect at all temperatures tested.
Size Cut off	<3kDa,>3kDa, <10kDa,>10kda	>3kDa-Biofilm inhibition <10kDa,>10kDa-Biofilm inhibition
Proteinase K treatment	Proteinase K treatment sensitive	Biofilm inhibition got reversed upon proteinase K treatment.
EDTA Treatment	EDTA treatment resistant	No effect on biofilm inhibition and pellicle defect upon EDTA.

1056

1057 **Fig. 8- Characterization of the nature of inhibitory active molecule within *O. splanchnicus***

1058 **culture supernatant**

1059 **A-** Biofilm assay showing the biofilm formation ability of STM after 72h of inoculation in
1060 presence of OS culture supernatant upon EDTA treatment. Data is representative of N=4, n=4.
1061 One-way ANOVA is used to obtain the p-values. Statistical test is performed with respect to
1062 STM.

1063 **B**- Biofilm assay showing the biofilm formation ability of STM after 72h of inoculation in
1064 presence of OS culture supernatant at high temperature conditions. Data is representative of
1065 N=4, n=4. One-way ANOVA is used to obtain the p-values. Statistical test is performed with
1066 respect to STM.

1067 **C-** Biofilm assay showing the biofilm formation ability of STM after 72h of inoculation in
1068 presence of OS culture supernatant under Proteinase K treatment. Data is representative of
1069 N=4, n=4. One-way ANOVA is used to obtain the p-values. Statistical test is performed with
1070 respect to STM.

1071

1072 **D**- Coomassie-stained SDS-PAGE demonstrating the size range of the differential protein
1073 bands present in OS supernatant as opposed to the tryptic soy broth media control.

1074 **E**- Biofilm assay showing the biofilm formation ability of STM after 72h of inoculation in
1075 presence of varying concentration OS culture supernatant. Data is representative of N=4, n=4.
1076 One-way ANOVA is used to obtain the p-values. Statistical test is performed with respect to
1077 STM.

1078 **F**- Biofilm assay showing the biofilm formation ability of STM after 72h of inoculation in
1079 presence of OS culture supernatant fractions fractionated using 3kDa Amicon filter. Data is
1080 representative of N=4, n=4. One-way ANOVA is used to obtain the p-values. Statistical test is
1081 performed with respect to STM.

1082 **G**- Biofilm assay showing the biofilm formation ability of STM after 72h of inoculation in

1083 presence of OS culture supernatant fractions fractionated using 10kDa Amicon filter. Data is

1084 representative of N=4, n=4. One-way ANOVA is used to obtain the p-values. Statistical test is

1085 performed with respect to STM.

1086 **H**- Summary table demonstrating the conditions tested for active molecule characterization and

1087 their effective outcome.

1088

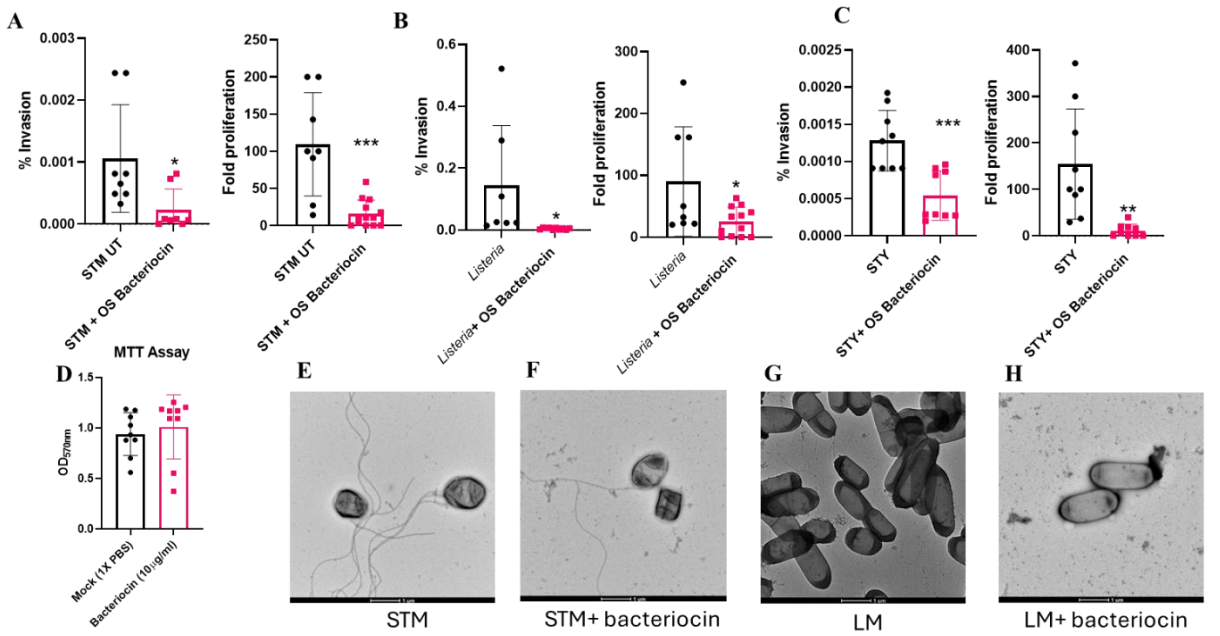

1089

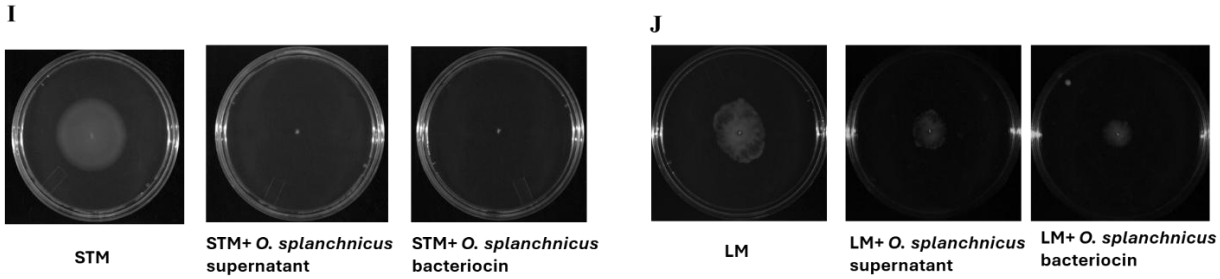

1090

1091 **Fig. 9- *O. splanchnicus* bacteriocin restricts both *Salmonella* and *Listeria* pathogenesis *in***

1092 ***vitro***

1093 **A**- Percent invasion and intracellular fold proliferation of STM in Caco-2 cells under OS
1094 bacteriocin (10µg/ml) treatment. Data is representative of N=2, n=3. Unpaired t-test is used to
1095 obtain the p-values.

1096 **B**- Percent invasion and intracellular fold proliferation of LM in Caco-2 cells under OS
1097 bacteriocin (10µg/ml) treatment. Data is representative of N=2, n=3. Unpaired t-test is used to
1098 obtain the p-values.

1099 **C**- Percent invasion and intracellular fold proliferation of STY in Caco-2 cells under OS
1100 bacteriocin (10µg/ml) treatment. Data is representative of N=2, n=3. Unpaired t-test is used to
1101 obtain the p-values.

1102 **D**-MTT assay evaluating the viability of Caco-2 cells upon 16h of mock or bacteriocin
1103 (10µg/ml) treatment. Data is representative of N=2, n=4.

1104 **E-F**-TEM images of STM under untreated (D) or bacteriocin (10µg/ml) (E) treatment to assess
1105 the possession of flagella.

1106 **G-H**- TEM images of LM under untreated (D) or bacteriocin (10µg/ml) (E) treatment to assess
1107 the possession of flagella.

1108 **I-** Swimming motility assay of STM under OS supernatant or bacteriocin treatment.

1109 **J**- Swimming motility assay of LM under OS supernatant or bacteriocin treatment.

1110

GRAPHICAL ABSTRACT

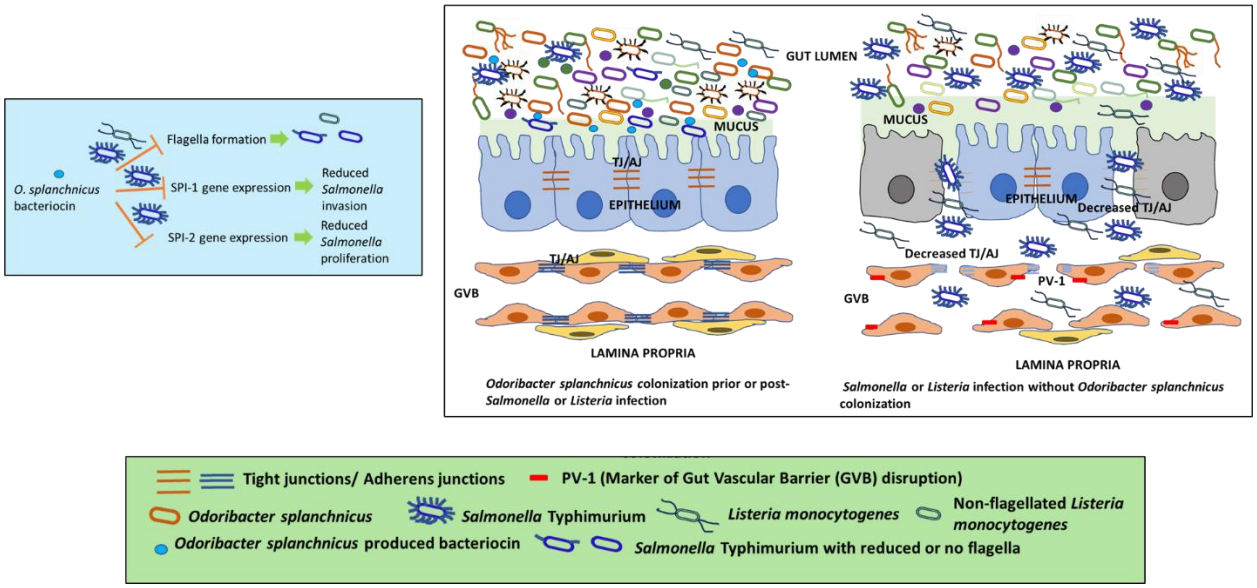

1125 **SUPPLEMENTARY FIGURES AND LEGENDS**

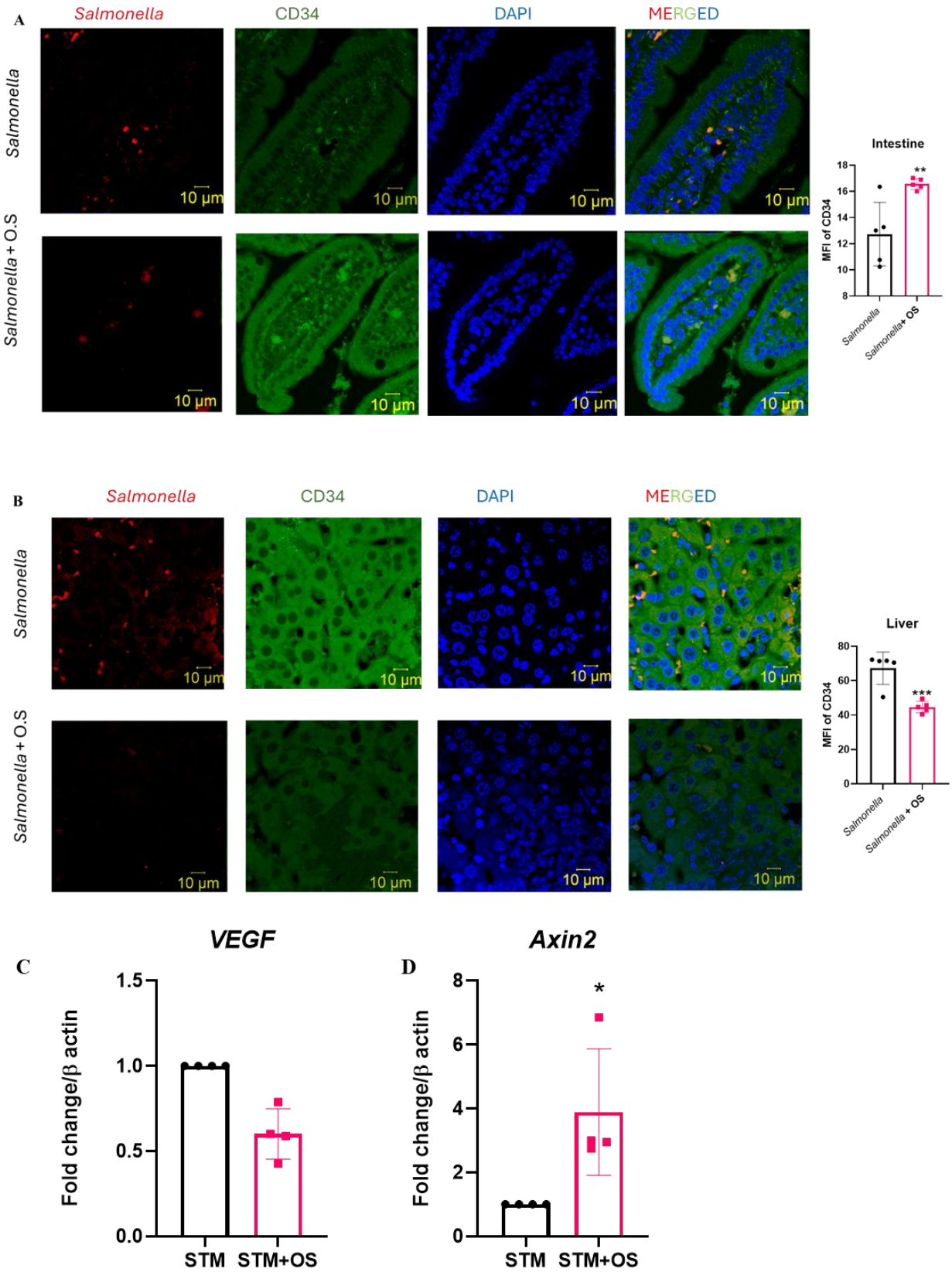

1126

1127 **Fig S1. *O. splanchnicus* gut colonization prevents *Salmonella* dissemination by restricting**

1128 **intestinal GVB damage and angiogenesis**

1129 **A-B** Immunofluorescence image representing CD34 (an endothelial marker of vasculature)

1130 protein expression in intestinal (ileal) (A) and liver (B) tissues of OS non-colonized and

1131 colonized mice cohorts upon STM infection. Data is representative of N=2, n=5 (tissue

1132 samples). Un-paired t-test was used to obtain the p-values.

1133 **C**- qPCR mediated gene expression of pro-angiogenic marker *Vegf* in STM-infected mice liver

1134 tissues in presence or absence of OS pre-colonization. Data is representative of N=2, n=4. Un-

1135 paired t-test was used to obtain the p-values.

1136 **D**- qPCR mediated gene expression of *Axin2* in STM-infected mice intestinal tissues in the

1137 presence or absence of OS pre-colonization. Data is representative of N=2, n=4. Un-paired t-

1138 test was used to obtain the p-values.

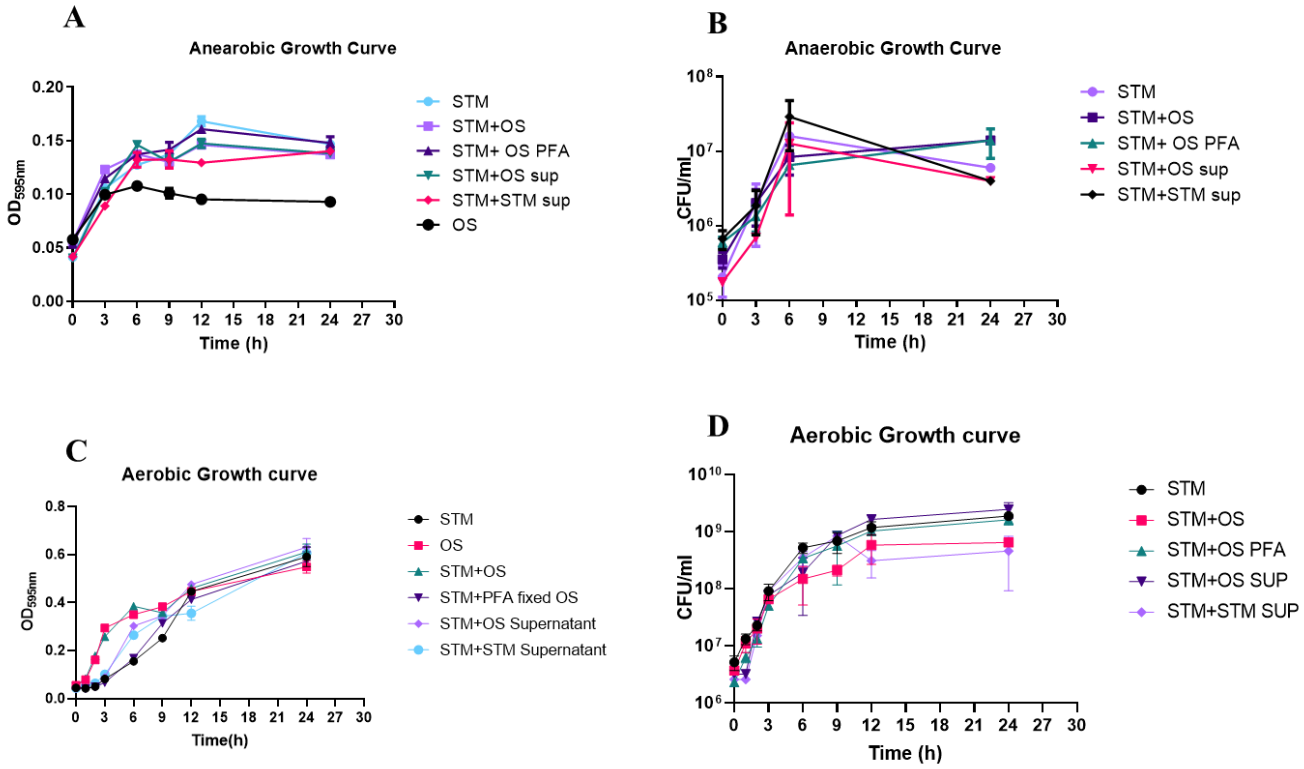

1139

1140 **Fig. S2 In vitro growth kinetics of *Salmonella* Typhimurium in presence of live or dead**

1141 ***O. splanchnicus* or its culture supernatant**

1142 **A-B** Growth kinetics of STM-WT, OS, STM-WT in presence of OS, STM-WT in presence of

1143 STM or OS culture supernatant and STM-WT in presence of PFA-fixed OS in LB under

1144 anaerobic growth conditions.

1145 **C-D**- Growth kinetics of STM-WT, OS, STM-WT in presence of OS, STM-WT in presence of

1146 STM or OS culture supernatant, STM-WT supernatant, and STM-WT in presence of PFA-fixed

1147 OS in LB under aerobic growth conditions.

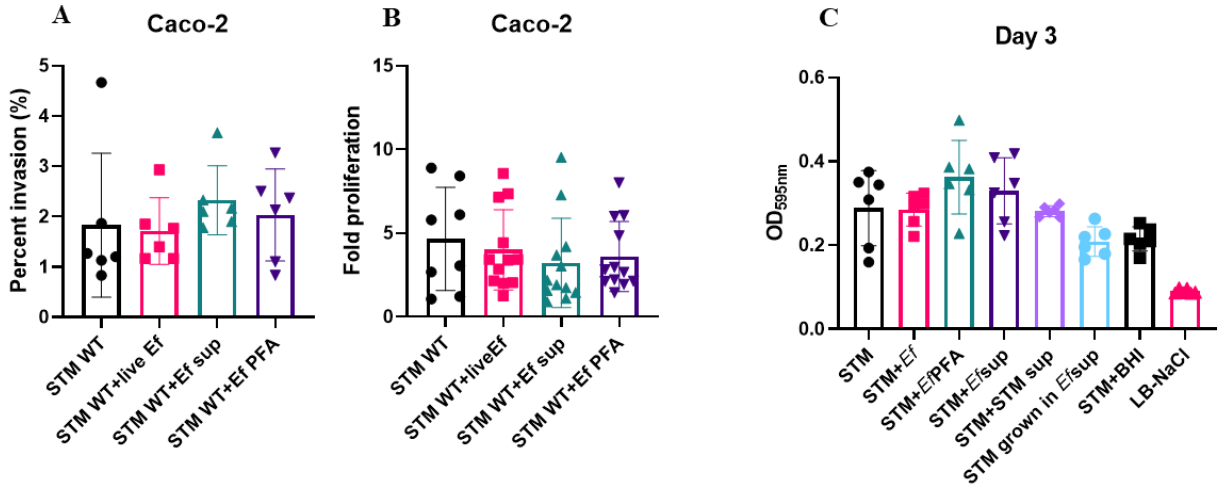

1148

1149 **Fig S3. Unlike *O. splanchnicus, E. faecalis* fail to exert any inhibitory effect on *Salmonella***

1150 ***in vitro* biofilm formation or *Salmonella* invasion and intracellular replication in human**

1151 **intestinal cells**

1152 **A**-Percent invasion of STM in Caco-2 cells in presence or absence of live *E. faecalis* (Ef), Ef

1153 culture supernatant, PFA-fixed-Ef. Data is representative of N=3, n=3. One-way ANOVA is

1154 used to obtain the p-values.

1155 **B**-Intracellular proliferation of STM in Caco-2 cells in presence or absence of live Ef, Ef culture
1156 supernatant, PFA-fixed-Ef. Data is representative of N=3, n=3. One-way ANOVA is used to
1157 obtain the p-values.

1158 **C**- Biofilm assay depicting the biofilm formation ability of STM-WT or STM-WT grown in Ef
1159 supernatant after 72h of inoculation in presence or absence of live Ef, Ef or STM culture
1160 supernatant, PFA-fixed. Crystal-violet staining was performed to assess the biofilm formation
1161 on the solid-liquid interphase and the $[OD]_{595}$ absorbance reading was recorded. Data is
1162 representative of N=3, n=3. One-way Anova is used to obtain the p-values.

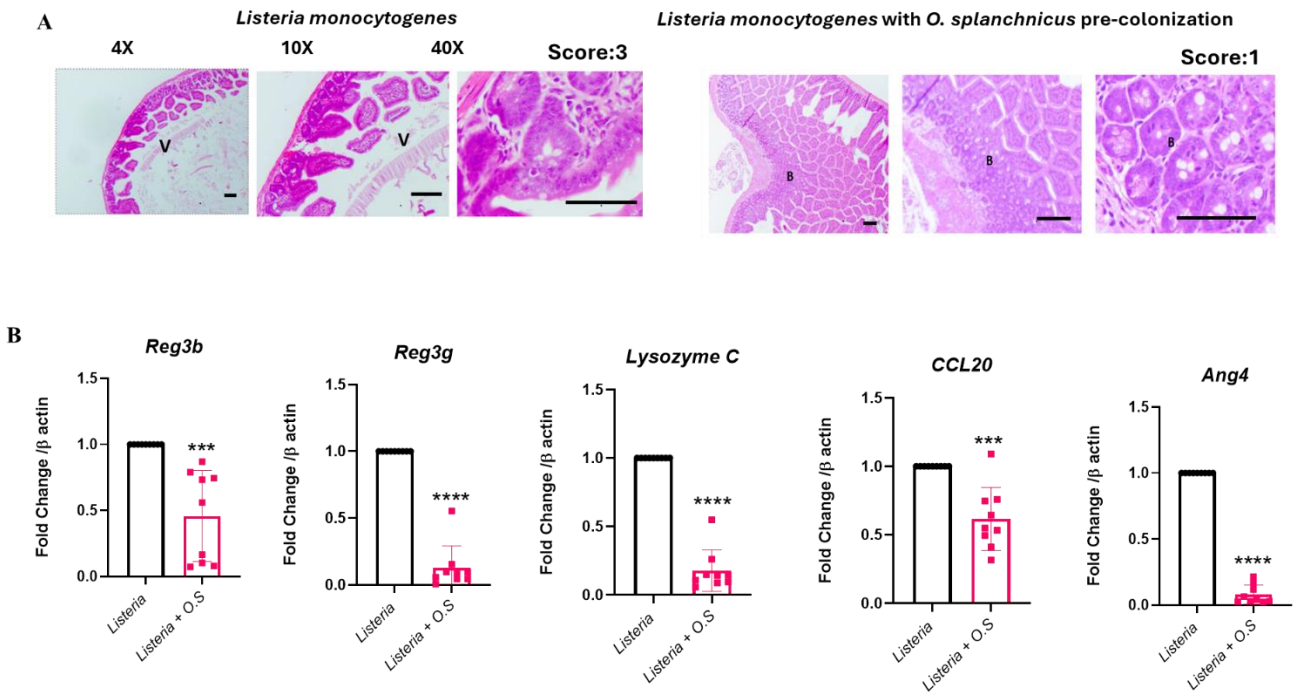

1163

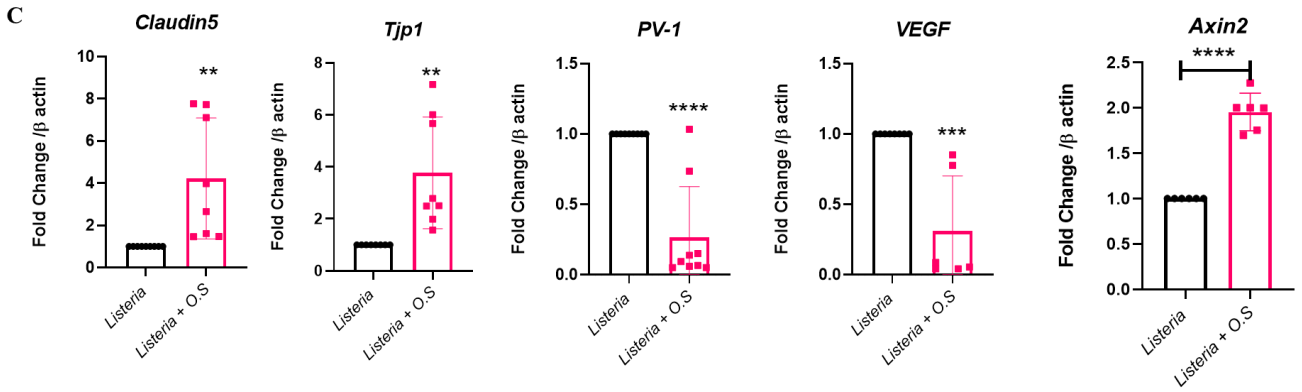

1164

1165

1166

1167

1168

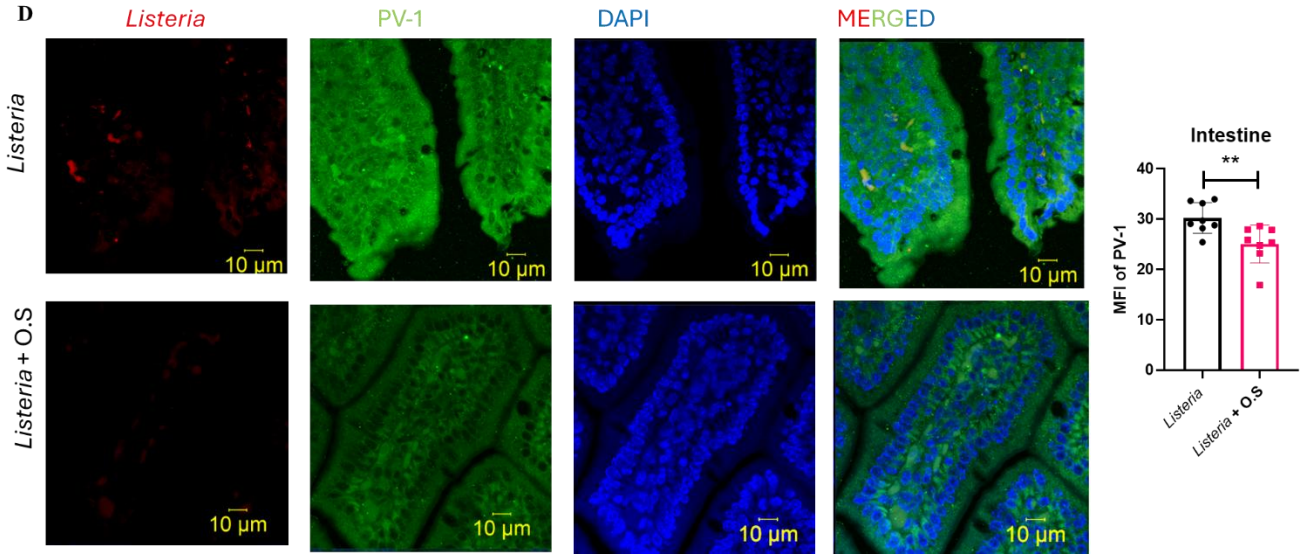

1169

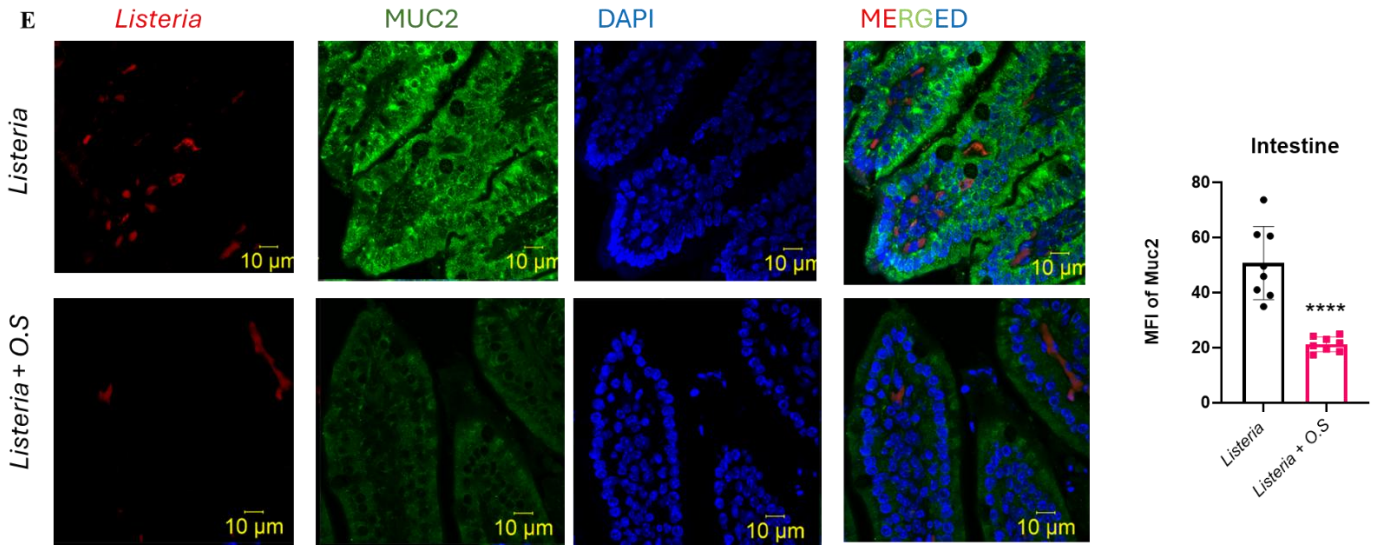

1170

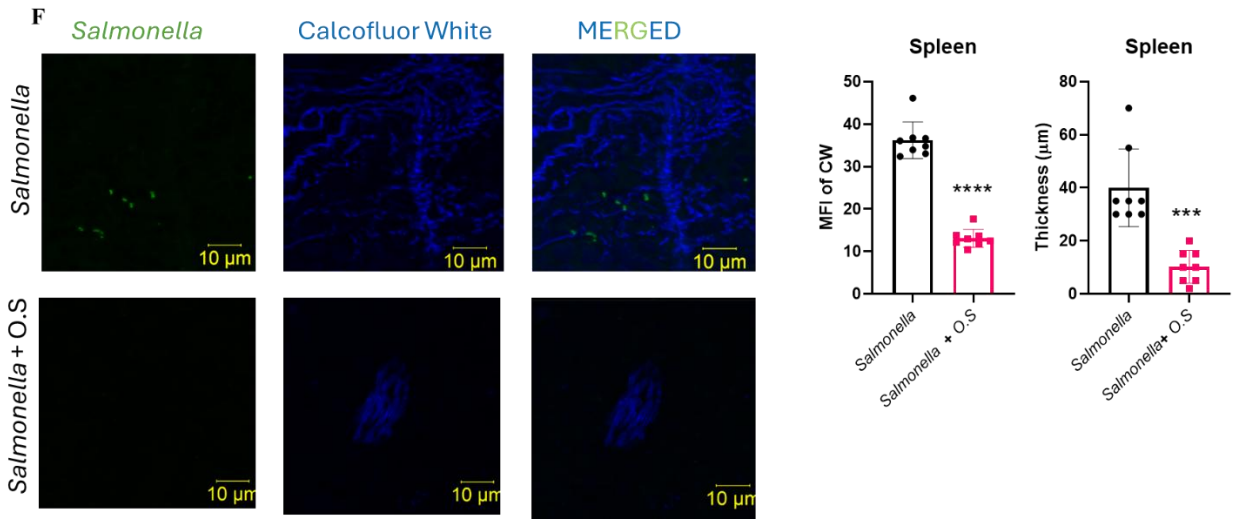

1171

1172

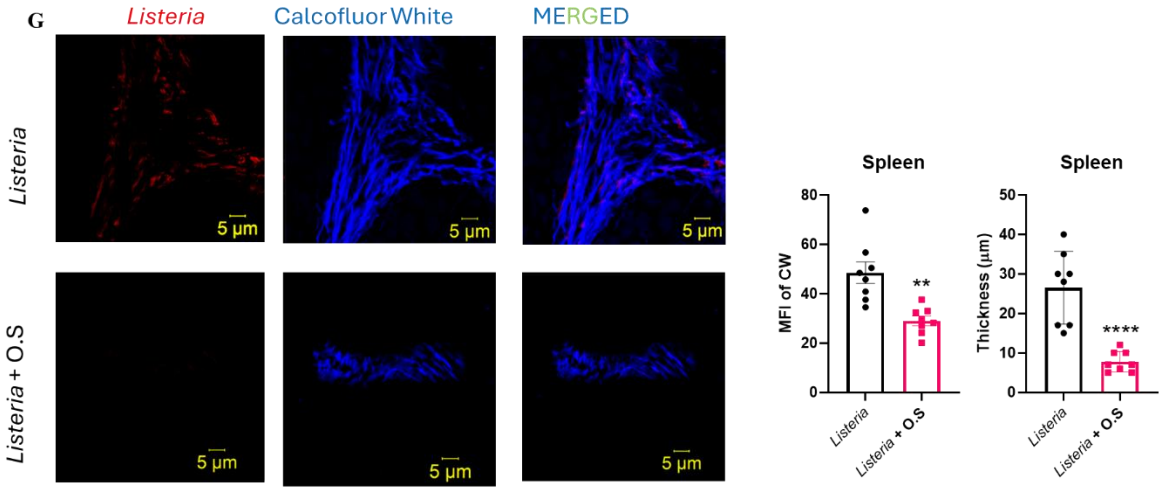

1173

H

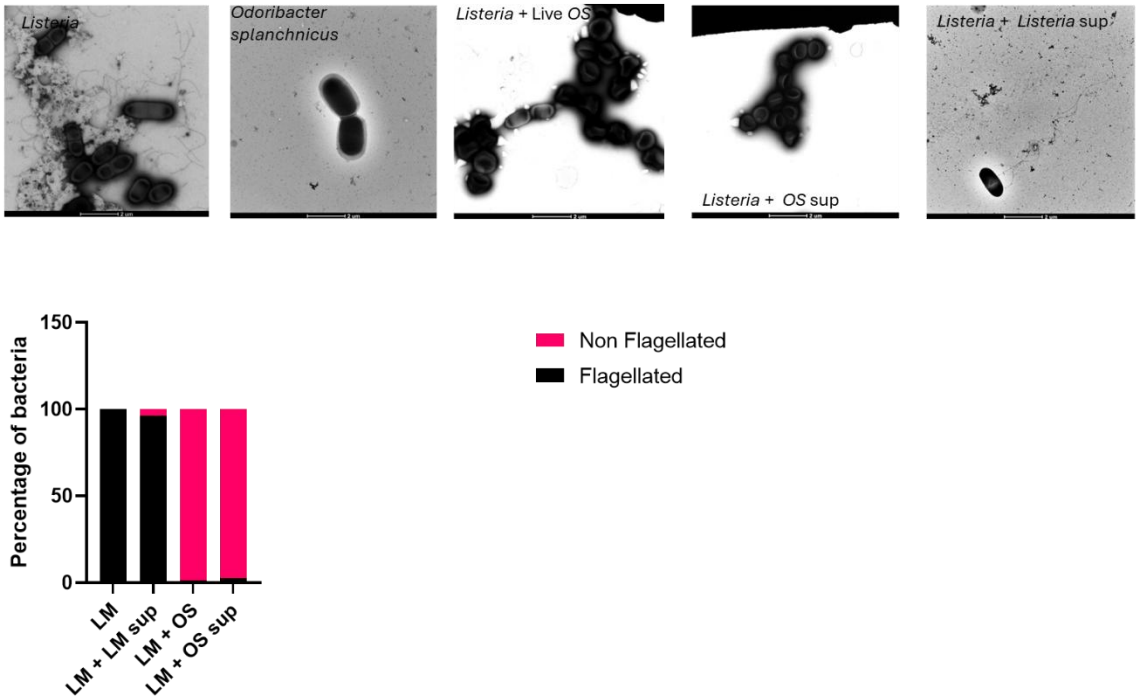

1174

I

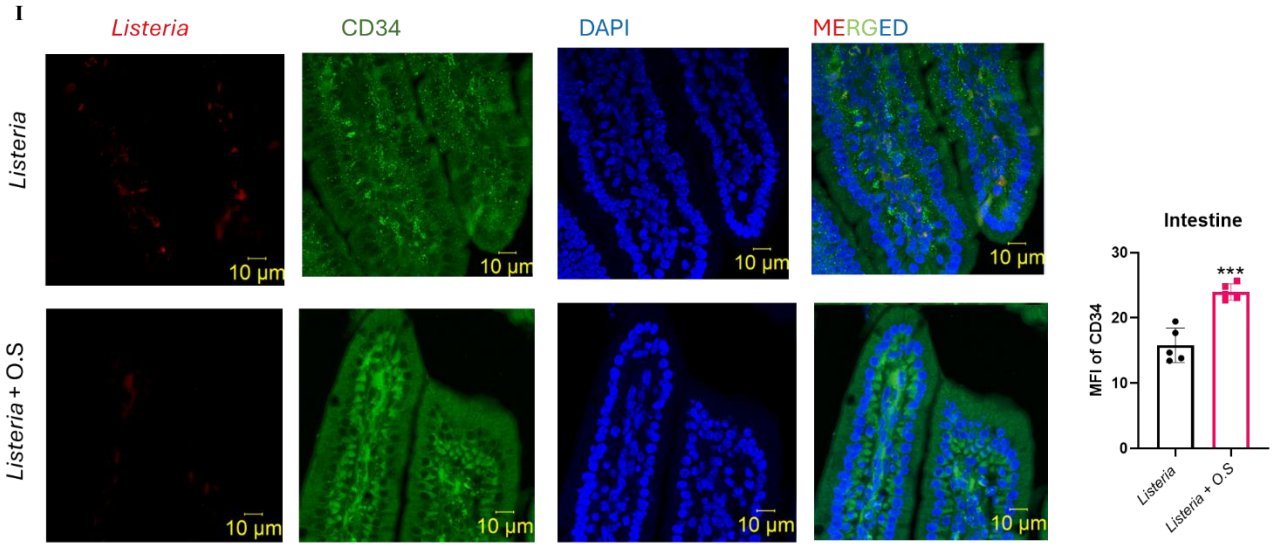

1175

1176

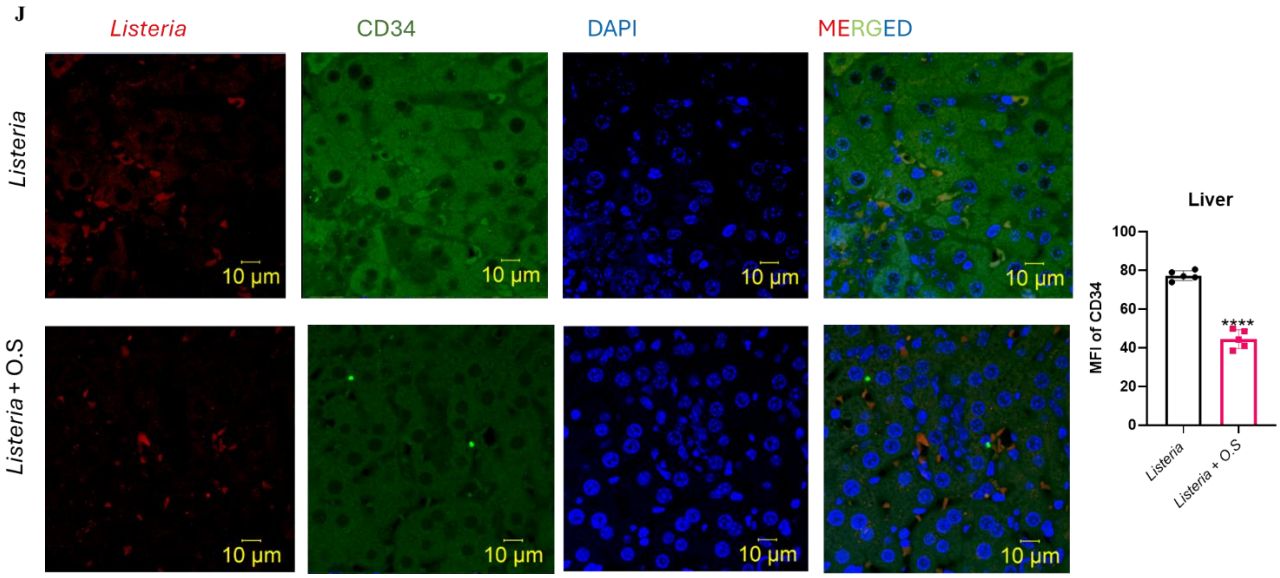

1177

1178

1179 **Fig. S4. *Odoribacter splanchnicus* gut colonization protects mice against *Listeria***

1180 ***monocytogenes* pathogenesis similar to *Salmonella* infection**

1181 **A**-Haematoxylin-eosin-stained intestinal sections harvested from OS non-colonized or

1182 colonized mice cohorts at 5th-day-post-LM-infection. 0-represents normal pathology, 1-

1183 represents- mild pathology, 2-3-represents severe pathology.

1184 **B**-Quantitative gene expression data of several antimicrobial peptides (AMPs) precursor genes

1185 in LM-infected mice intestinal tissues harvested at 5th day post-infection from OS colonized or

1186 non-colonized cohorts. Unpaired Student's t-test is performed to obtain the p-values. Data is

1187 representative of N=2, n=9.

1188 **C**- Quantitative gene expression study of tight junction protein genes *Tjp1*, *Claudin5*, GVB

1189 damage marker *PV-1*, angiogenesis marker-*Vegf,* and *Axin2* in LM- infected mice intestinal

1190 tissues harvested at 5th-dpi from OS colonized or non-colonized cohorts. Unpaired Student's

1191 t-test is performed to obtain the p-values. Data is representative of N=2, n=5.

1192 **D-E**- Immunofluorescence images representing PV-1 protein expression (D) and Muc2 (E) in
1193 intestinal (ileal) tissues of OS-non-colonized and colonized mice cohorts at 5th day post LM
1194 infection. Data is representative of N=2, n=8 (tissue samples). Un-paired t-test was used to
1195 obtain the p-values.

1196 **F**- Representative Calcofluor white (CW) staining of STM-infected mice spleen tissues at 5th-
1197 dpi. Data is representative of N=2, n=8 (tissue samples). Un-paired t-test was used to obtain
1198 the p-values.

1199 **G**- Representative CW staining of LM-infected mice spleen tissues at 5th-dpi. Data is
1200 representative of N=2, n=8 (tissue samples). Un-paired t-test was used to obtain the p-values.

1201 **H**- Transmission Electron Microscopic (TEM) images of LM in presence or absence of LM
1202 supernatant, OS and its supernatant to assess the possession of flagella. The quantification plot
1203 exhibits the percentage of bacterial flagellated or non-flagellated cells (number of cells
1204 quantified $n \geq 100$)

1205 **I-J**- Immunofluorescence images representing CD34 (an endothelial marker of vasculature)
1206 protein expression in intestinal (N) and liver (O) tissues of OS non-colonized and colonized
1207 mice cohorts upon LM infection. Data is representative of N=2, n=5 (tissue samples). Un-
1208 paired t-test was used to obtain the p-values.

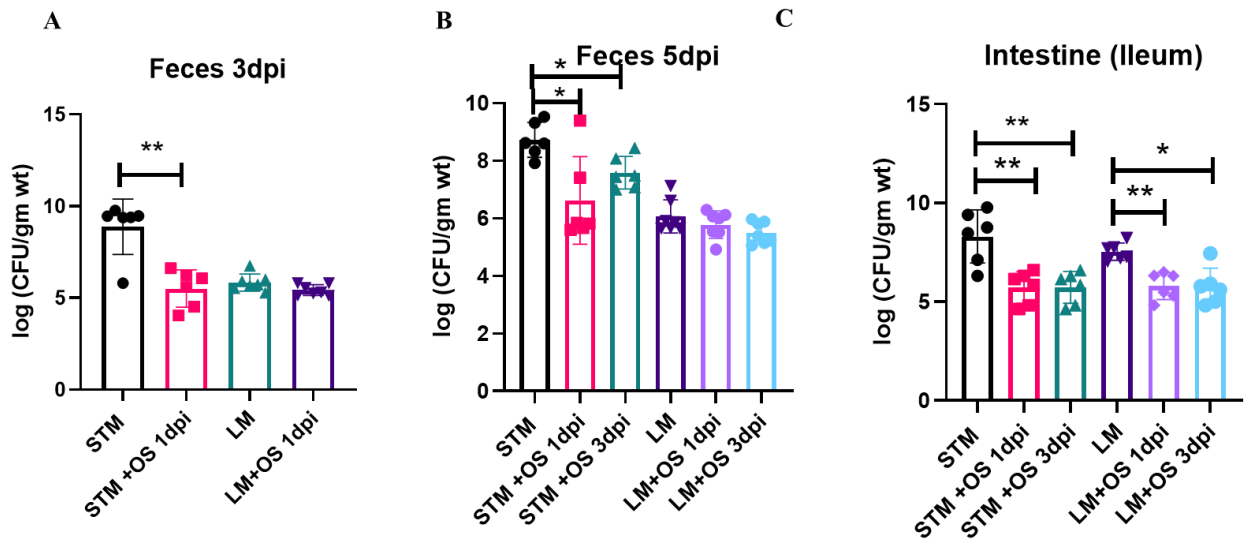

1209

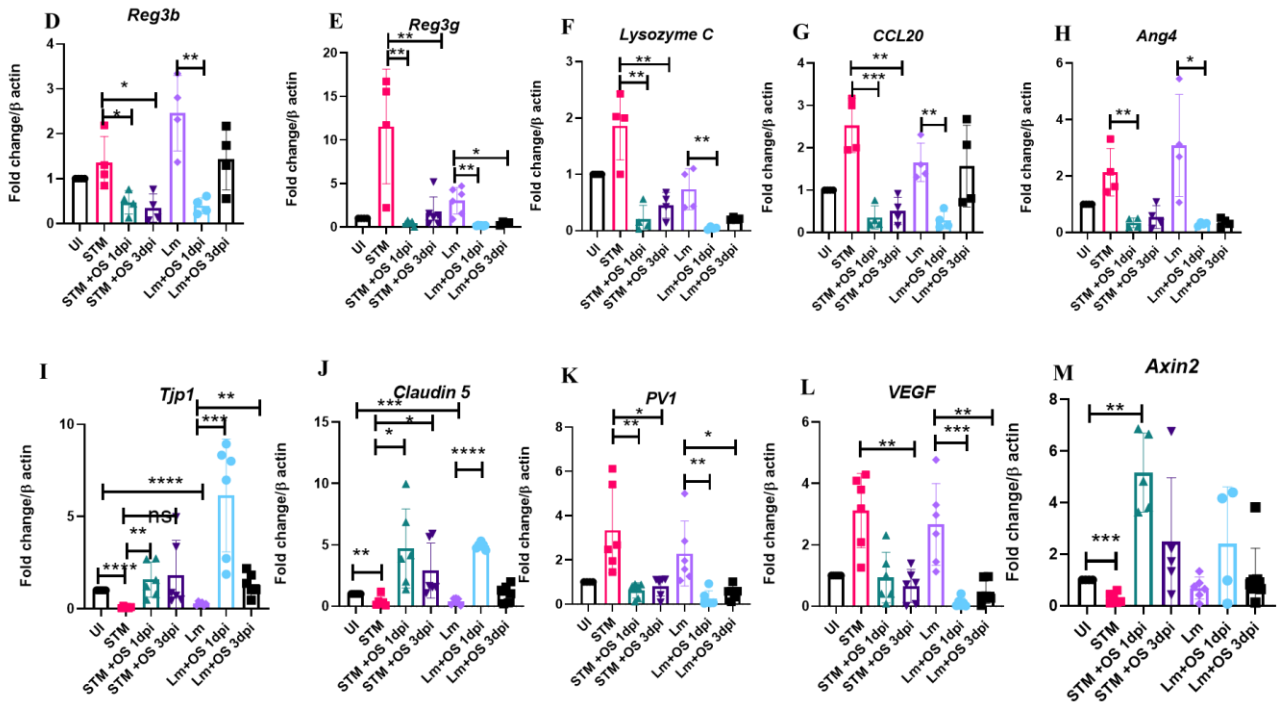

1210

1211

1212

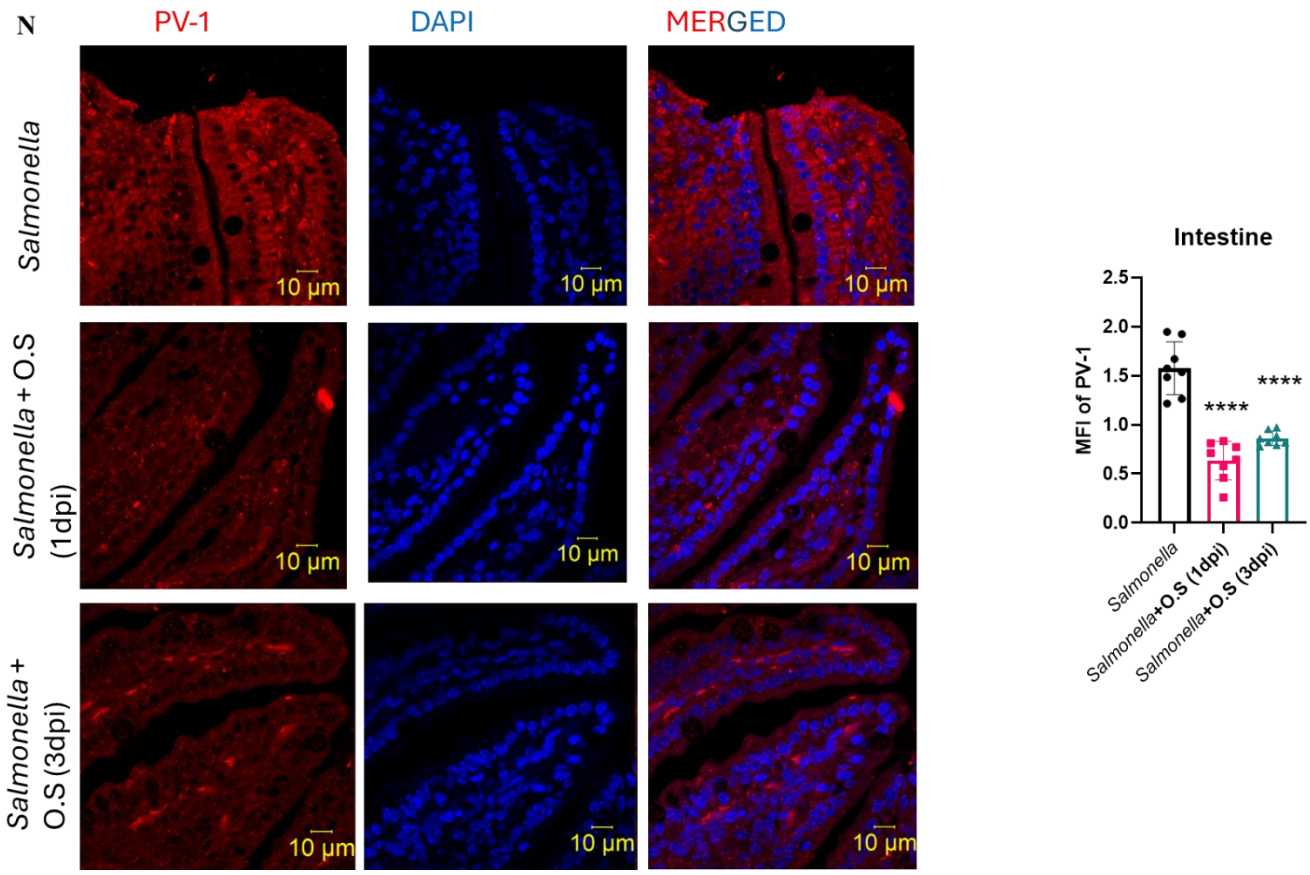
N
PV-1
DAPI
MERGED
Salmonella
Salmonella + O.S (1dpi)
Salmonella + O.S (3dpi)
10 µm
Intestine
MFI of PV-1
2.5
2.0
1.5
1.0
0.5
0.0
****
****
Salmonella
Salmonella+O.S (1dpi)
Salmonella+O.S (3dpi)

1213

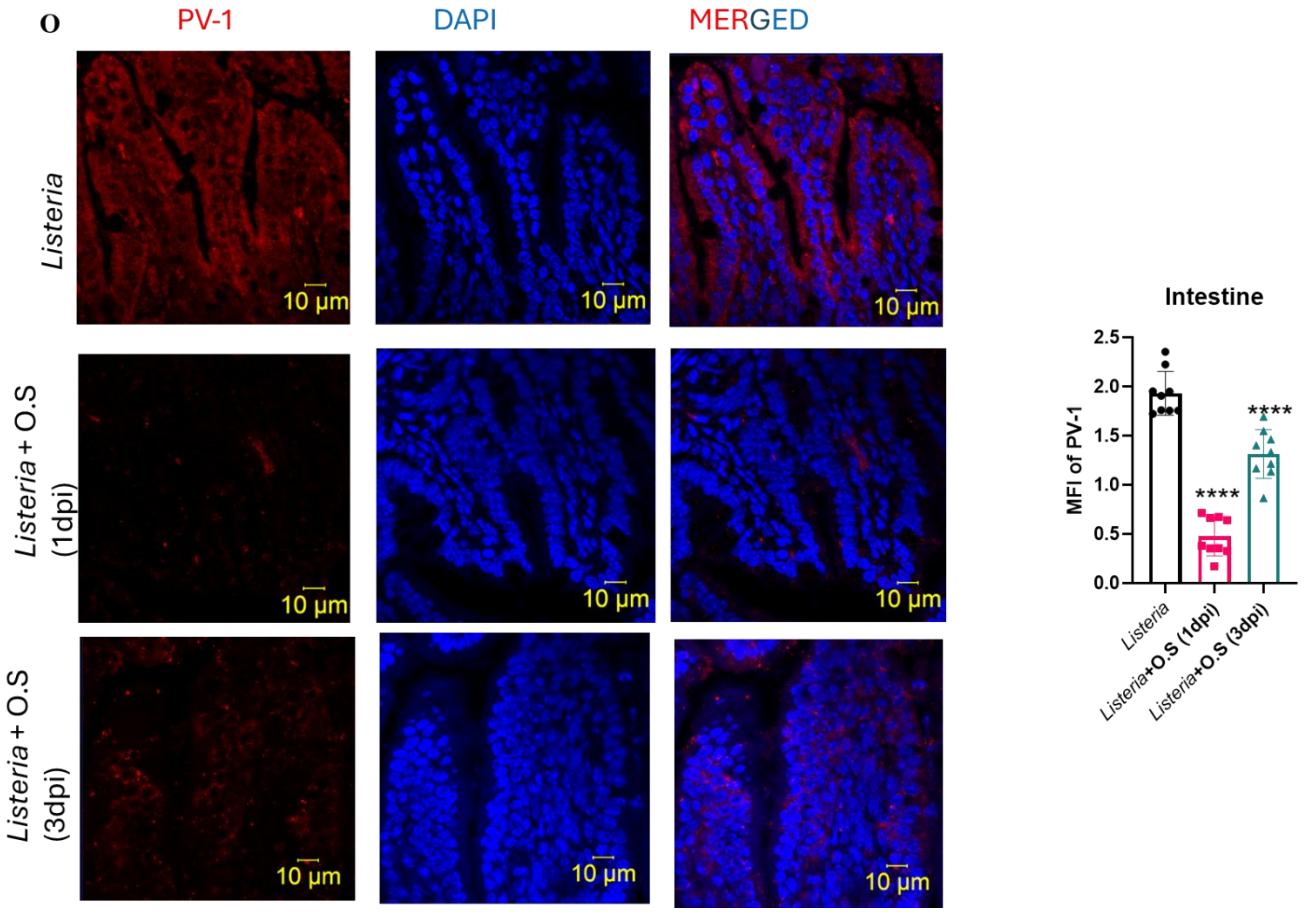
O
PV-1
DAPI
MERGED
Listeria
Listeria + O.S (1dpi)
Listeria + O.S (3dpi)
10 µm
Intestine
MFI of PV-1
2.5
2.0
1.5
1.0
0.5
0.0
****
****
Listeria
Listeria+O.S (1dpi)
Listeria+O.S (3dpi)

1214

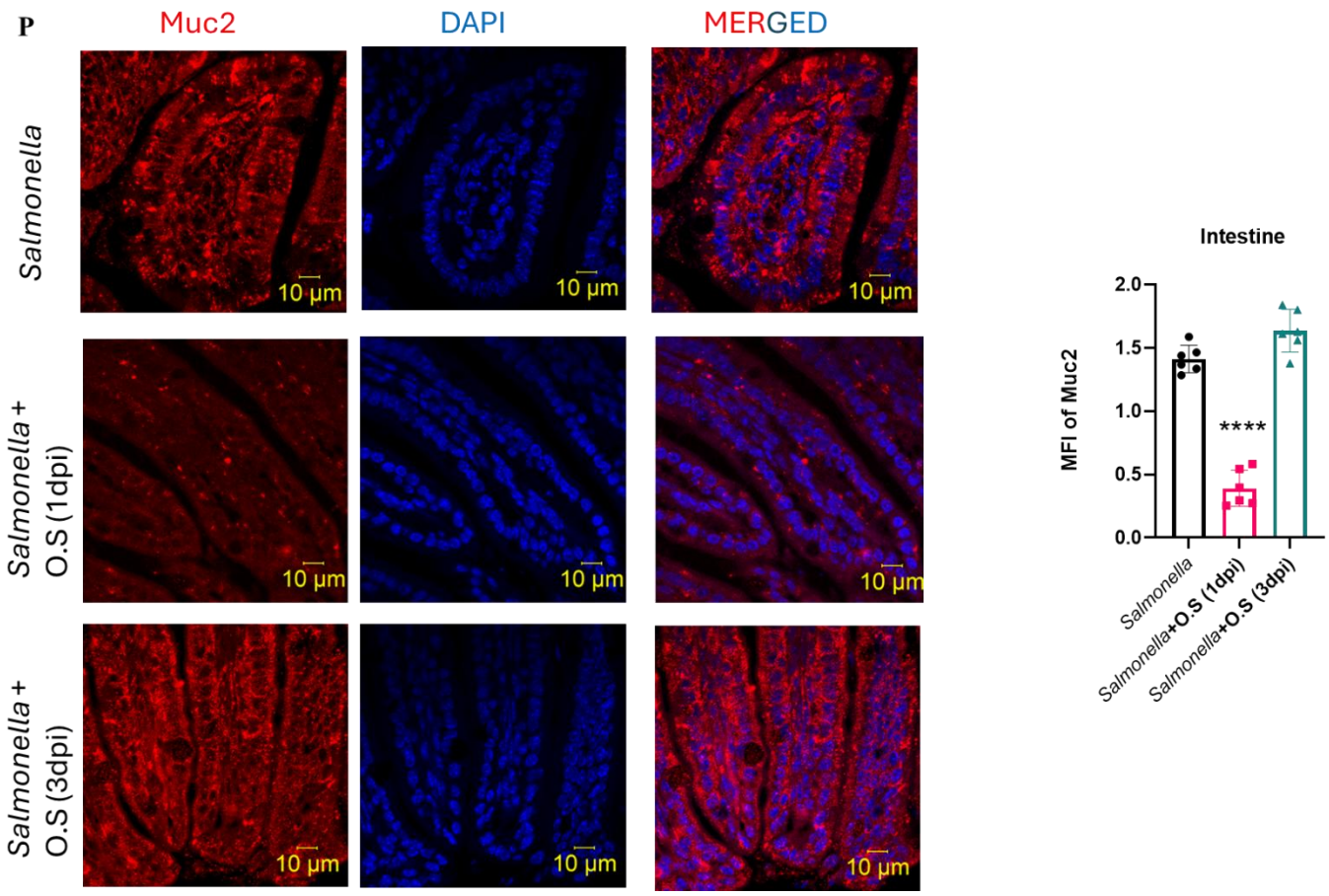
P
Muc2
DAPI
MERGED
Salmonella
Salmonella + O.S (1dpi)
Salmonella + O.S (3dpi)
10 µm
Intestine
MFI of Muc2
2.0
1.5
1.0
0.5
0.0
****
Salmonella
Salmonella+O.S (1dpi)
Salmonella+O.S (3dpi)

1215

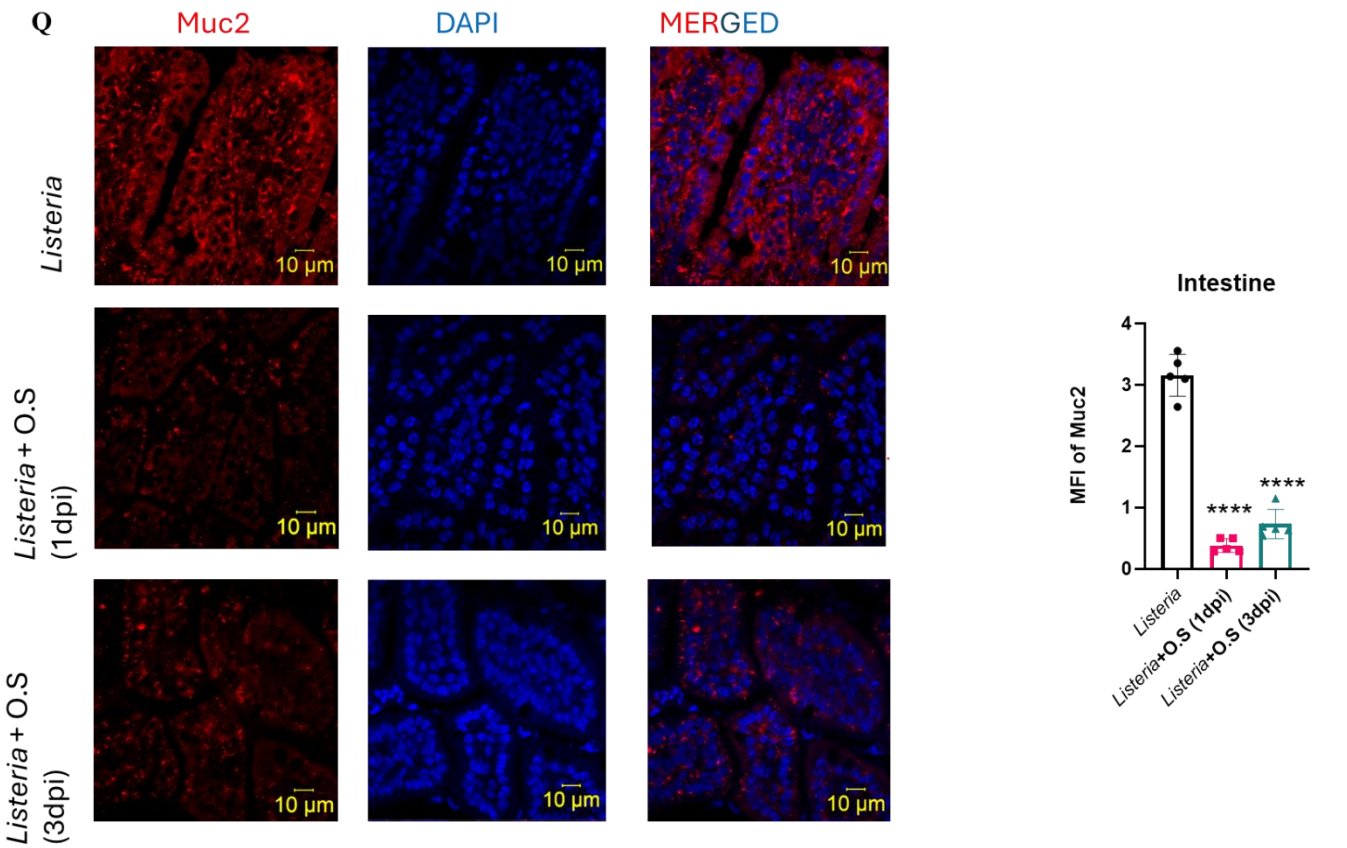
Q
Muc2
DAPI
MERGED
Listeria
Listeria + O.S (1dpi)
Listeria + O.S (3dpi)
10 µm
Intestine
MFI of Muc2
4
3
2
1
0
****
****
Listeria
Listeria+O.S (1dpi)
Listeria+O.S (3dpi)

1216

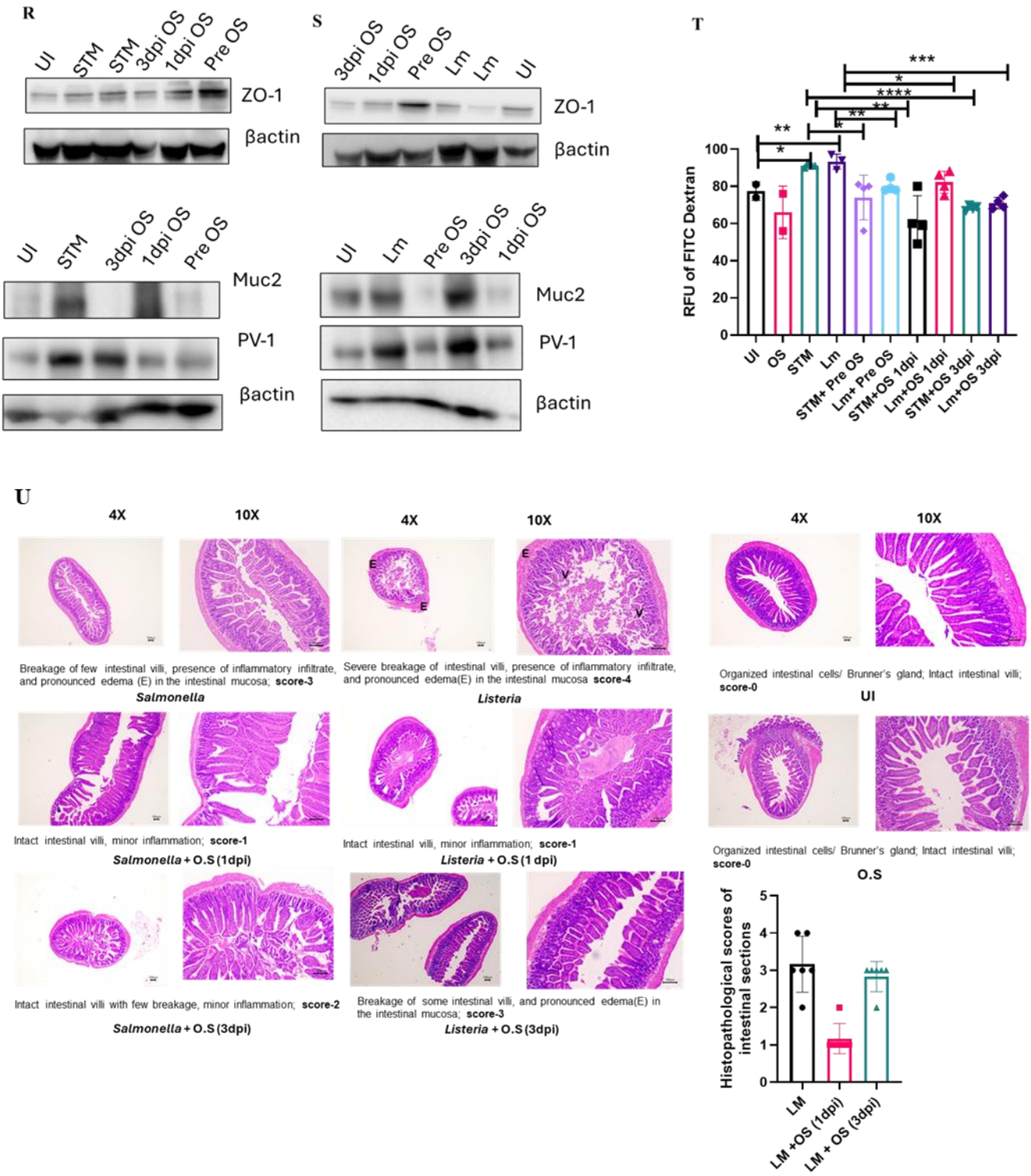
R
UI
STM
STM
3dpi OS
1dpi OS
Pre OS
ZO-1
βactin
UI
STM
3dpi OS
1dpi OS
Pre OS
Muc2
PV-1
βactin
S
3dpi OS
1dpi OS
Pre OS
Lm
Lm
UI
ZO-1
βactin
UI
Lm
Pre OS
3dpi OS
1dpi OS
Muc2
PV-1
βactin
T
RFU of FITC Dextran
UI
OS
STM
Lm
STM+ Pre OS
Lm+ Pre OS
STM+OS 1dpi
Lm+OS 1dpi
STM+OS 3dpi
Lm+OS 3dpi
U
4X
10X
Breakage of few intestinal villi, presence of inflammatory infiltrate, and pronounced edema (E) in the intestinal mucosa; score-3
Salmonella
Severe breakage of intestinal villi, presence of inflammatory infiltrate, and pronounced edema(E) in the intestinal mucosa score-4
Listeria
Organized intestinal cells/ Brunner's gland; Intact intestinal villi; score-0
UI
Intact intestinal villi, minor inflammation; score-1
Salmonella + O.S (1dpi)
Intact intestinal villi, minor inflammation; score-1
Listeria + O.S (1 dpi)
Organized intestinal cells/ Brunner's gland; Intact intestinal villi; score-0
O.S
Intact intestinal villi with few breakage, minor inflammation; score-2
Salmonella + O.S (3dpi)
Breakage of some intestinal villi, and pronounced edema(E) in the intestinal mucosa; score-3
Listeria + O.S (3dpi)
Histopathological scores of intestinal sections
LM
LM +OS (1dpi)
LM + OS (3dpi)

1217

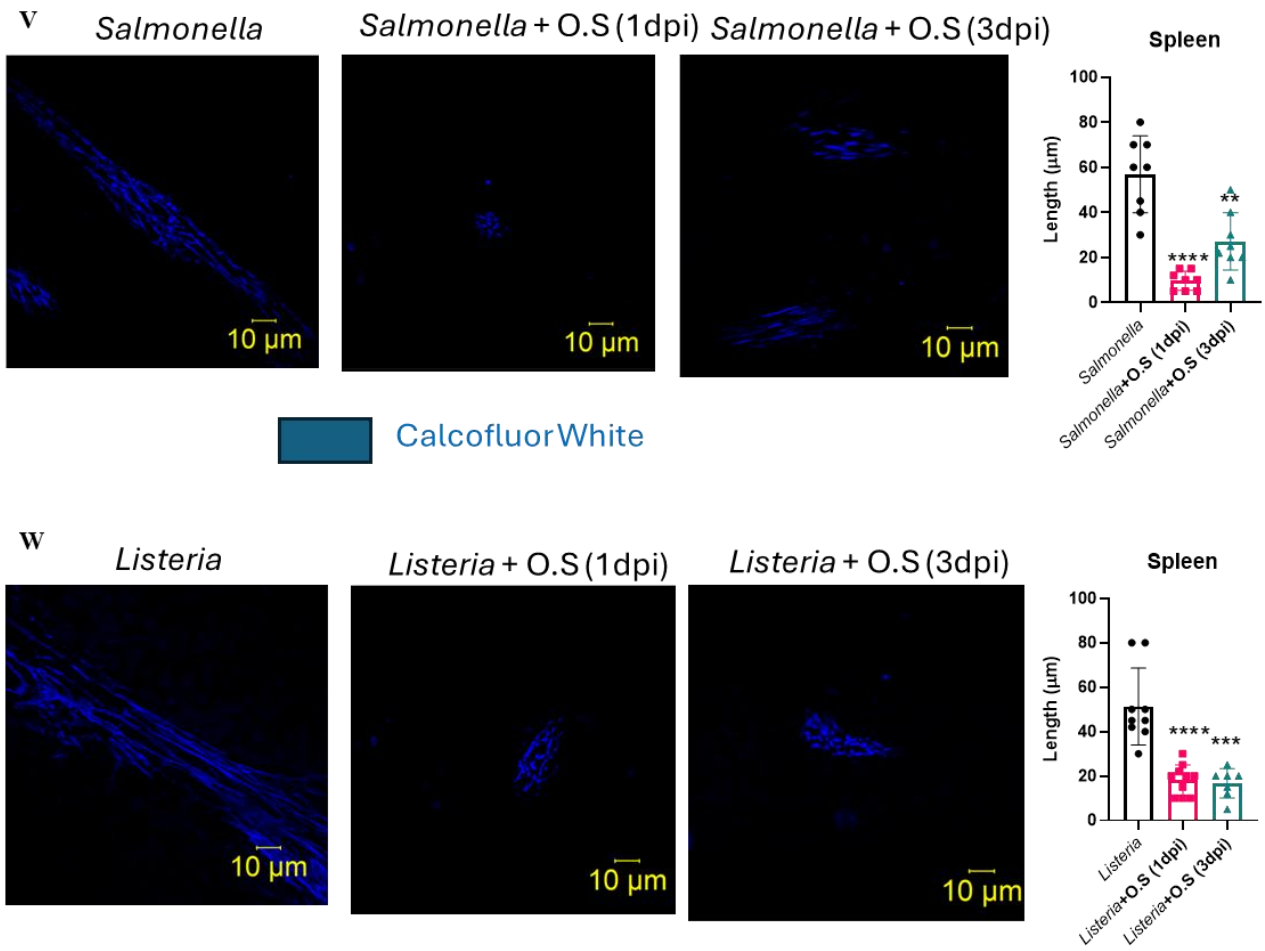

Fig. S5 *Odoribacter splanchnicus* administration post-establishment of infection protected mice against *Listeria monocytogenes* and *Salmonella* Typhimurium

A-C- STM and LM organ loads in feces at 3rd day post-infection (A), 5th post-infection (B) and in ileal tissues (contents and wall) at 5th day post-infection (C) upon OS administration at 1-dpi or 3-dpi. Data is representative of N=2, n=6 where N denotes number of biological replicates and n denotes the number of mice per group. Mann-Whitney Test was performed to obtain p-values.

D-H-Quantitative gene expression data of several antimicrobial peptides (AMPs) precursor genes in LM and STM-infected mice intestinal tissues harvested at 5th dpi upon OS colonization

1228 at 1-dpi or 3-dpi. Unpaired Student's t-test is performed to obtain the p-values. Data is
1229 representative of N=2, n=4.

1230 **I-M**- Quantitative gene expression study of tight junction protein genes *Tjp1*, *Claudin5*, GVB
1231 damage marker *PV-1*, angiogenesis marker-*Vegf,* and *Axin2* in LM and STM-infected mice
1232 intestinal tissues harvested at 5th-dpi upon OS colonization at 1-dpi or 3-dpi. Unpaired
1233 Student's t-test is performed to obtain the p-values. Data is representative of N=2, n=6.

1234 **N-O**- Intestinal (ileal) immunofluorescence images representing PV-1 protein expression in
1235 *Salmonella* (N) or *Listeria* (O)-infected mice harvested on 5th-dpi with or without OS
1236 administration at 1-dpi or 3-dpi. Unpaired Student's t-test is performed to obtain the p-values.
1237 Data is representative of N=2, n=8 (or 9).

1238 **P-Q**- Intestinal (ileal) immunofluorescence images representing Muc2 protein expression in
1239 *Salmonella* (M) or *Listeria* (N)-infected mice harvested on the 5th dpi with or without OS
1240 administration at 1-dpi or 3-dpi. Unpaired Student's t-test is performed to obtain the p-values.
1241 Data is representative of N=2, n=6 (or 5).

1242 **R-S**- Immunoblotting representing the protein expression profile of Muc2, ZO-1, and PV-1 in
1243 *Salmonella* (O) or *Listeria* (P)-infected mice intestinal tissue harvested on 5th-dpi with or
1244 without OS pre-or post-colonization (1-dpi or 3-dpi). Data is representative of N=3.

1245 **T**- Estimation of FITC fluorescence in mice plasma via gut permeability assay in *Salmonella*
1246 or *Listeria*-infected mice cohorts with or without OS pre-or post-colonization (1dpi or 3dpi)
1247 upon oral administration of FITC Dextran (25mg/kg) 4h before euthanization at 5th-dpi.
1248 Unpaired Student's t-test is performed to obtain the p-values. Data is representative of N=2,
1249 n=4 (UI and OS, n=2).

1250 **U-** Haematoxylin-eosin-stained intestinal sections harvested at 5th-dpi from Uninfected (UI) or
1251 *Salmonella* or *Listeria*-infected mice cohorts having non-administered or administered OS (at

1252 1st or 3rd dpi). 0-represents normal pathology, 1- represents- mild pathology, 2-3-represents
1253 severe pathology. Data is representative of N=2, n=6.

1254 **V**- Representative Calcofluor white (CW) staining of STM-infected mice spleen tissues at 5th-
1255 day post-infection with or without OS administration at 1st or 3rd dpi depicting the
1256 quantification of the length of the fibril architecture of CW-stained sections. One-way ANOVA
1257 and multiple comparison test were used to obtain the p-values.

1258 **W**- Representative CW staining of LM-infected mice spleen tissues at 5th-dpi with or without
1259 OS administration at 1st or 3rd dpi depicting the quantification of the length of the fibril
1260 architecture of CW-stained sections. One-way ANOVA and multiple comparison test were used
1261 to obtain the p-values.

1262

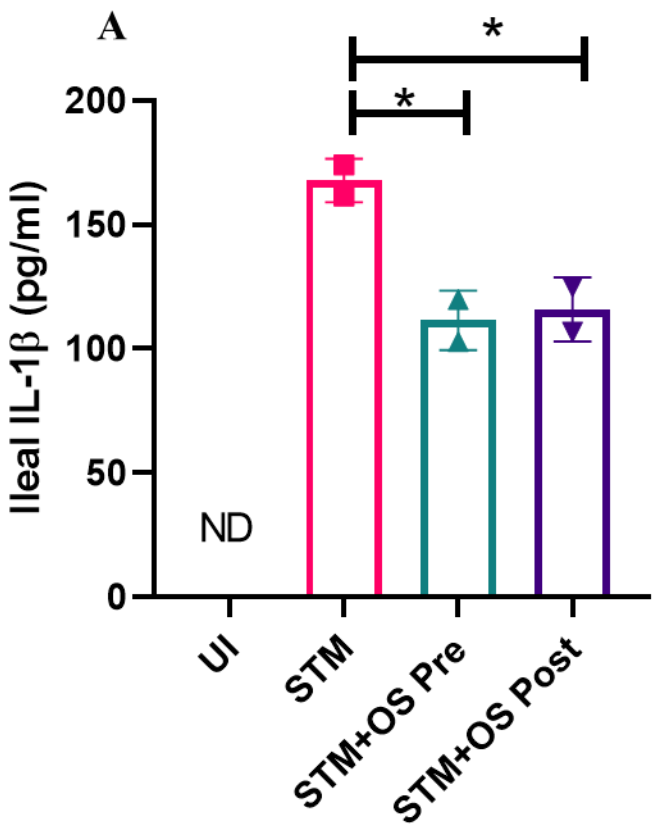

1263

1264 **Fig. S6 *Odoribacter splanchnicus* alleviates *Salmonella*-induced intestinal inflammation in**

1265 **mice both during pre and post-treatment**

1266 **A-** Estimation of IL-1β in the ileal sections of UI or *Salmonell*a-infected mice tissues harvested

1267 at 5th dpi with or without OS pre-or post-colonization (1dpi). Unpaired Student's t-test is

1268 performed to obtain the p-values. Data is representative of N=2, n=4 (UI and OS, n=2).

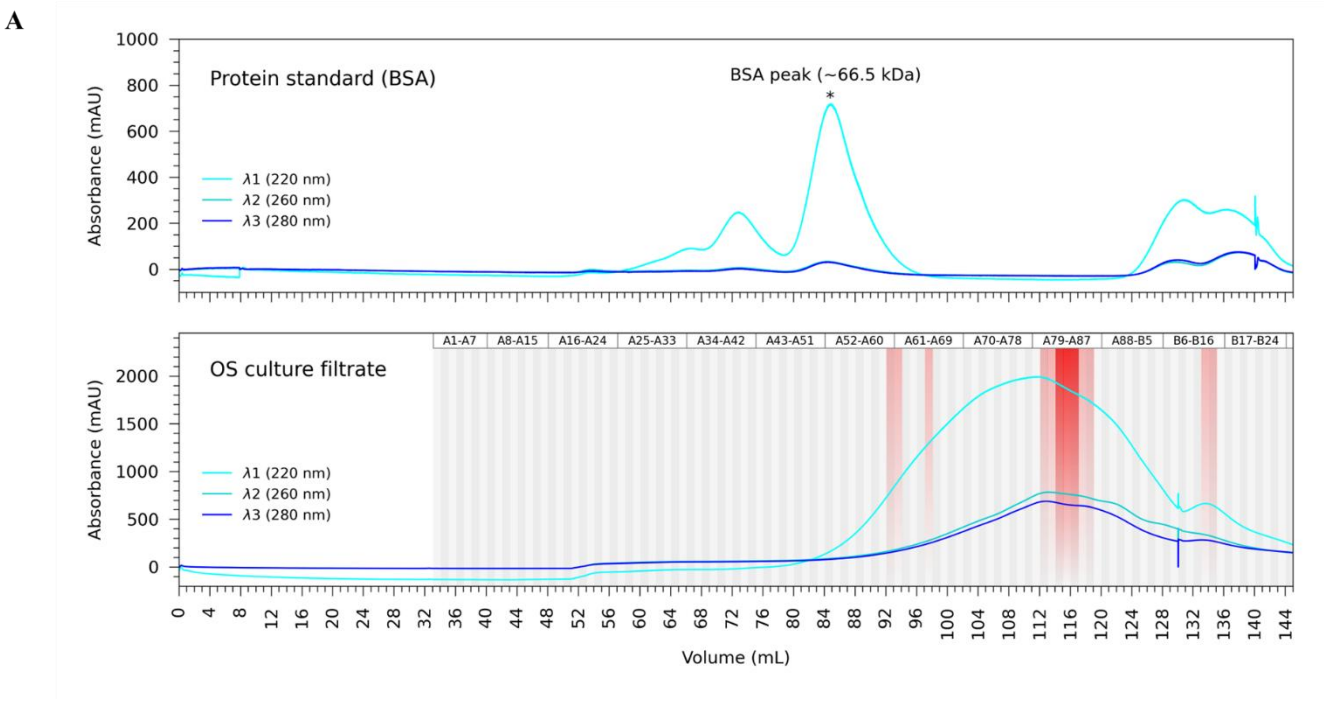

1269

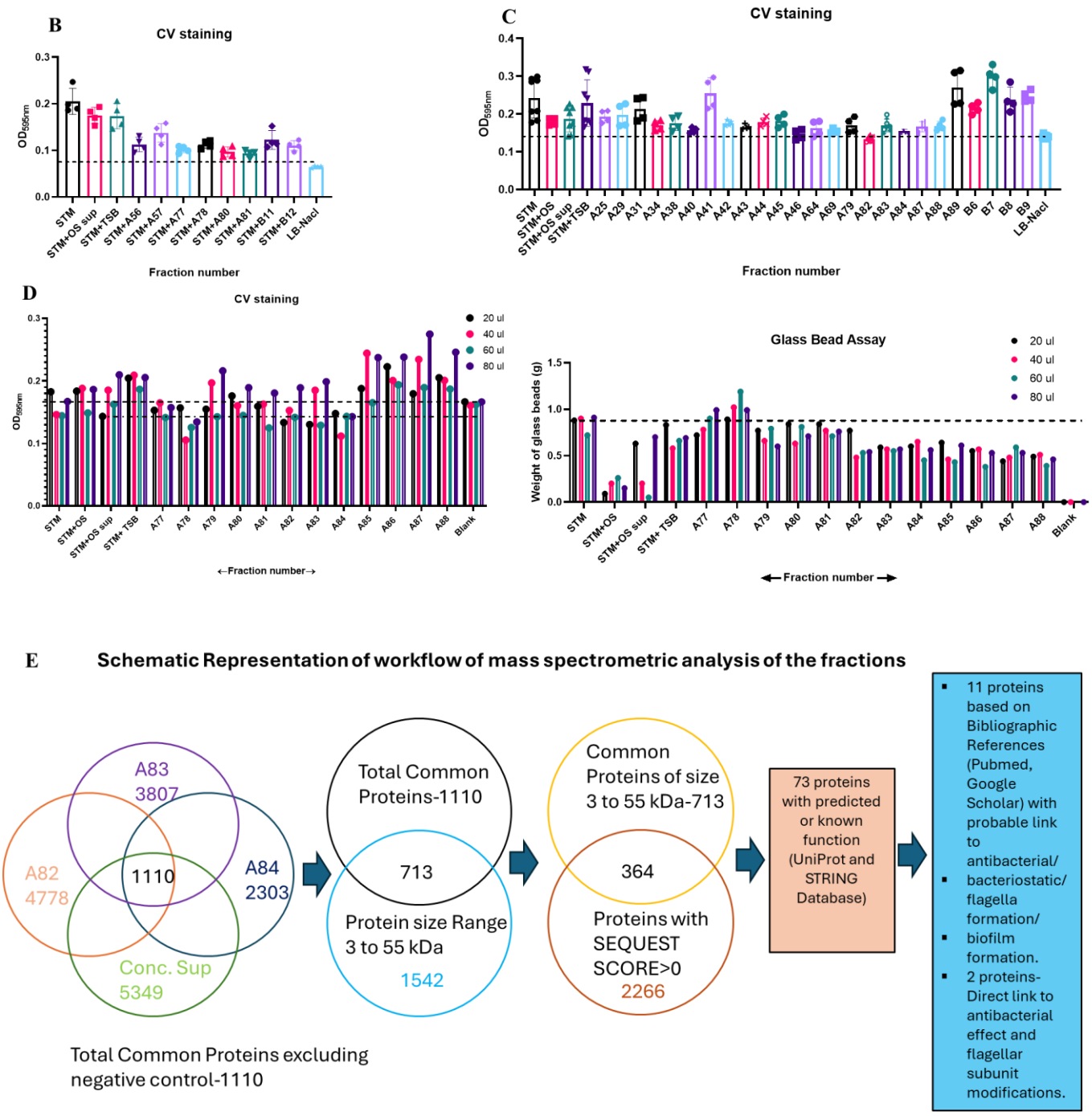

Fig. S7 Characterization of the inhibitory active molecule within *O. splanchnicus* culture supernatant

A-Gel filtration chromatogram of protein standards and the OS culture supernatant. Red shaded region shows the fractions with biofilm inhibitory activity. The dark shaded region indicates the fractions with the highest inhibitory activity.

1277 **B-C**- Biofilm assay showing the biofilm formation ability of STM after 72h of inoculation in
1278 presence of OS supernatant gel filtration fractions. Data is representative of N=2, n=2. One-
1279 way ANOVA is used to obtain the p-values.

1280 **D**- Biofilm assay showing the biofilm formation ability of STM after 72h of inoculation in
1281 presence of varying concentration of OS supernatant biofilm inhibitory gel filtration fractions.
1282 Data is representative of N=2, n=1.

1283 **E**-Schematic representation of the workflow of mass spectrometric analysis of the gel filtration
1284 fractions (A82, A83, A84 and Concentrated supernatant).

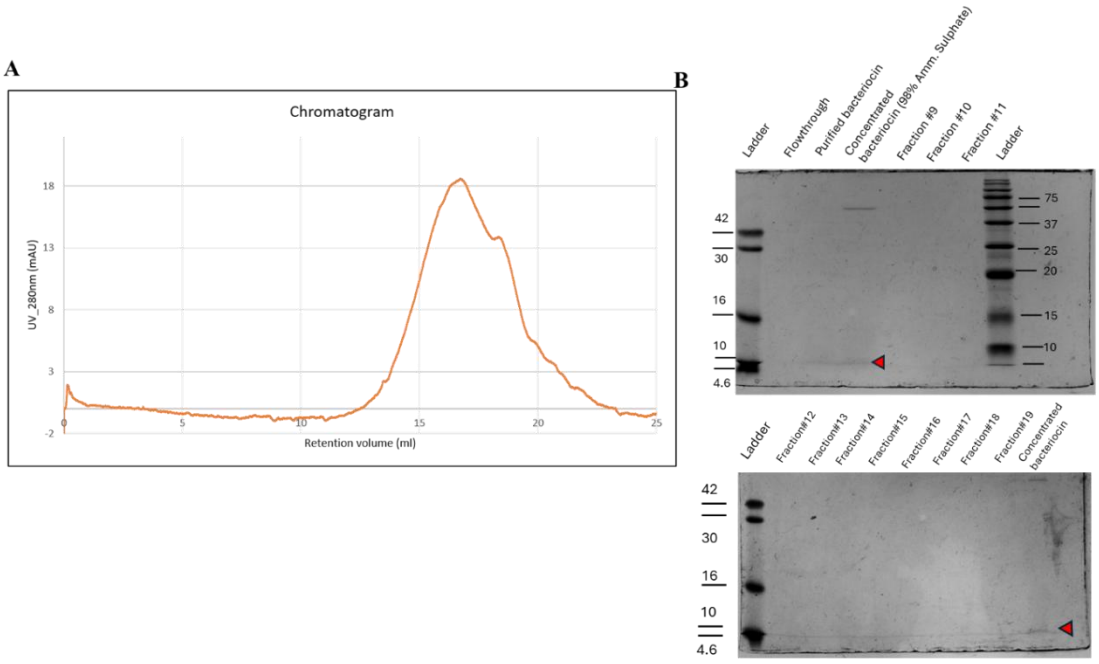

1285

1286 **Fig. S8 Purification procedure of *O. splanchnicus* produced bacteriocin via ammonium**
1287 **sulphate precipitation method followed by Fast Performance Liquid Chromatography**

1288 **A**-Size exclusion chromatogram of OS-produced bacteriocin fractions post 95-98%
1289 ammonium sulphate precipitation.

1290 **B**- Coomassie-stained SDS PAGE showing the purified and concentrated OS bacteriocin.

1291

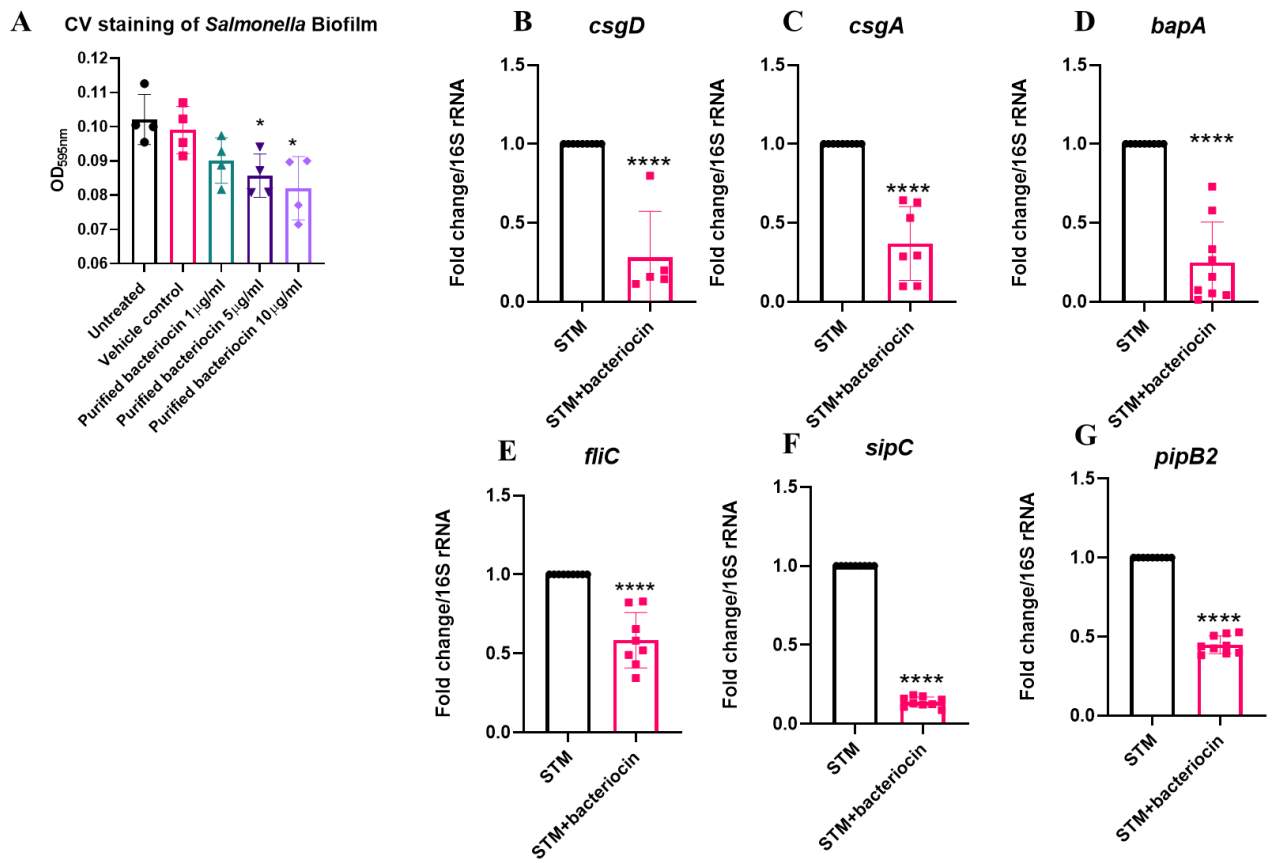

1292

1293 **Fig. S9 *O. splanchnicus* bacteriocin attenuates *Salmonella* pathogenesis *in vitro***

1294 **A**- Biofilm assay showing the biofilm formation ability of STM after 72h of inoculation under

1295 varying concentration of OS bacteriocin. Data is representative of N=2, n=2. Unpaired t-test is

1296 used to obtain the p-values.

1297 **B-G**- RT-qPCR mediated gene expression of STM biofilm regulatory genes *csgD* (B),

1298 *csgA*(C), *bap* (D), along with flagellar gene *fliC*(E), SPI-1-*sipC* (F) and SPI-2-*pipB2*(G) in

1299 presence or absence of OS bacteriocin treatment. Data is representative of N=2, n≥5. Unpaired

1300 Student's t-test was used to obtain the p-values.

1301

1302

1303

1304 **Table S1- Selected List of 11 proteins from Mass Spectrometric Analysis based on**

1305 **bibliographic search**

Accession ID	Protein Name and	Referenced Function
A0A412WBT8	Immunity protein Imm5 domain-containing protein	Uncharacterized
F9Z8G5	Peptidase	Modulate biofilm formation and host defense.
R6F650	Carboxyl-terminal protease	Critical for post-translational processing and associated with regulation of gene expression, stress response, maintenance of cell envelope integrity and bacterial virulence.
A0A412TJE3	ATP-dependent Clp protease proteolytic subunit	Influence virulence and infectivity of pathogenic bacteria. ClpP enhance biofilm formation in *Enterococcus faecalis*.
F9Z604	Peptidase C39 bacteriocin processing	The cysteine peptidase cleave the double glycine leader peptides from the precursors of bacteriocin
A0A412TJV3	UDP-2,4-diacetamido-2,4, 6-trideoxy-beta-L-altropyranose hydrolase	It catalyzes the third step in the biosynthesis of pseudaminic acid. Pseudaminic acid is a sialic-like sugar that modifies flagellin.
A0A412WSU3	Bacteriocin	Antimicrobial peptides that can kill or inhibit closely related or unrelated bacterial strains.
A0A413I832	Serine Protease	Extracellular proteases regulate biofilm formation and growth of competitors.
A0A412W3J2	Glutamate dehydrogenase	Involved in bacterial response to stress adaptation and virulence.
A0A412WSS0	Bacteriocin	Antimicrobial peptides that can kill or inhibit closely related or unrelated bacterial strains.
F9ZBU9	Peptidylprolyl isomerase	Promote biofilm formation in *Mycobacterium tuberculosis.*

1306

1307 **Table S2-List of primers**

Primer Name	Sequence (5'---3')
O. splanchnicus 16S rRNA FP	ATGTAATGATGAGCACTCTAACGG
O. splanchnicus 16S rRNA RP	GGCTTTTGAGATTGGCATCC
PV-1 FP	CGAACTGGAGGCGCGTAA
PV-1 RP	GCAGCGACTTGGCCTTGAC
Claudin5 FP	CCCAGTTAAGGCACGGGTAG
Claudin5 RP	GGCACCGTCGGATCATAGAA

βactin FP	CAGCAAGCAGGAGTACGATG
βactin RP	GCAGCTCAGTAACAGTCCG
Vegf FP	GCAGCGACAAGGCAGACTAT
Vegf RP	AACCTCCTCAAACCGTTGGC
Tjp1 FP	TCTTGCAAAGTATCCCTTCTGT
Tjp1 RP	CAGAAATCGTGCTGATGTGCC
Reg3b FP	GCTTGTCAAGAGCTTCTGGATTTC
Reg3b RP	TGTCCCTTGTCCATGATGCTC
Reg3g FP	CGCTGAAGCTTCCTTCCTGT
Reg3g RP	GGGTTCATAGCCCAGTGTCG
Lysozyme C FP	GGTCTACAATCGTTGTGAGTTG
Lysozyme C RP	TGAGCTAAACACACCCAGTCA
CCL 20 FP	GCAACTACGACTGTTGCCTC
CCL20 RP	TTCTTGACTCTTAGGCTGAGGA
Ang4 FP	TGGTTGTGATTCCTCCAACTCT
Ang4 RP	TGTTGACATCTTTGCAAGGCG
fliC FP	CTAAACAAACTGGGTGGCGC
fliC RP	GCACCCAGGTCAGAACGTAA
bapA FP	ACGGTGACTACGCCTAAAAC
bapA RP	CTTCCGCCTCAGTCACTTTT
csgD FP	ACGATTATCCCTACCGTGAA
csgD RP	GCGGACTCGGTGCTGTTGTA
Salmonella 16S rRNA FP	GTGAGGTAACGGCTCACCAA
Salmonella 16S rRNA RP	TAACCGCAACACCTTCCTCC

sipC FP	GCAGTACGCCGCTACTCAGG
sipC RP	AGCGCGAATATTGCCTGCGA
pipB2 FP	TGGCGCCAATTTACAACACGC
pipB2 RP	CTCGCCTTTCGCAGGTTTGC
csgA FP	TCGCAGCAATCGTAGTT
csgA RP	CGGAACCGTACTGATAA

1308

1309 **Table S3-List of Antibodies**

Antibody Name	**Catalogue Number**	**Source**
PV-1	**A15906-20ul (Abclonal)**	**Rabbit**
CD34	**A19015-20ul (Abclonal)**	**Rabbit**
Muc2	**A4767 (Abclonal)**	**Rabbit**
ZO-1	**R26.4C DHSB, CRL 1597**	**Mouse**
β actin	**A3854 (Sigma), Clone AC-15**	**Mouse**

1310

1311